Physics Library
QC
1
I42

Registered No. M. 3121

PROCEEDINGS

OF THE

INDIAN ACADEMY

OF SCIENCES

VOL. XII] *SECTION A* [No. 1

JULY, 1940

Price Rs. 2 or 3 Sh. *Annual Subscription Rs. 18*

PRINTED AT THE BANGALORE PRESS, BANGALORE CITY, BY G. SRINIVASA RAO,
SUPERINTENDENT, AND PUBLISHED BY THE INDIAN ACADEMY OF SCIENCES,
HEBBAL, BANGALORE.

Physics Lib.
Calc
Indian academy
10-18-43
47604
v.12, no.1-6

EXPERIMENTS ON THE SYNTHESIS OF COMPOUNDS RELATED TO CINCHONINE AND QUININE*

By B. K. Nandi

(*From the Department of Applied Chemistry, College of Technology, Manchester*)
and
(*The Department of Pharmacology, Haffkine Institute, Parel, Bombay*)

Received May 2, 1940

(Communicated by Lt.-Col. S. S. Sokhey, M.D., I.M.S.)

Recent attempts to prepare compounds having anti-malarial action seem to be based largely on Kaufmann's (1912) original views that anti-malarial action is a property of the grouping,

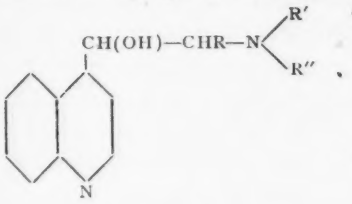

(I)

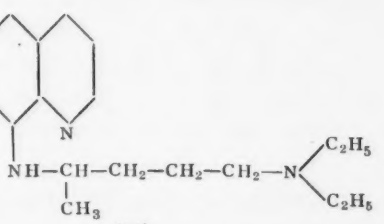

(II)

since the compounds are mainly quinoline derivatives, but the secondary alcohol group is apparently not regarded as essential nor is the 4-position in the quinoline nucleus strictly adhered to. Generally speaking the newer anti-malarials are derivatives of either amino-ethylquinoline or ethyl-amino-quinoline, *i.e.*, the groupings,

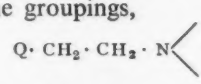

and Q· NH· CH_2· CH_2—

are usually to be found.

The most effective gametocidal drug of all the synthetic anti-malarials is plasmoquine (II) which is 6-methoxy-8-(α-methyl-δ-diethylaminobutyl)-amino quinoline, synthesised by Schulemann and others (1932).

The success of plasmoquine as a most efficient gametocidal drug in malaria led others to synthesise various compounds on a similar line and since then much work has been done in this line by Robinson (1929, 1930, 1931, 1933, 1934, 1935) in England, Forneau (1931, 1933) in France and Magidson

* The latter part of the work was carried out in the Haffkine Institute under the auspices of the Indian Research Fund Association.

(1933, 1934, 1935) in Russia and others elsewhere as a result of which there is now an overwhelming accumulation of data in the line provided by the pioneers in Germany.

Baldwin (1929) has prepared several amino-alkyl amino-quinolines of the structure similar to plasmoquine. Seshadri (1929) also has made some aminoalkylquinolinium salts which have proved of some value in medicine. Kermack and Smith (1930) have prepared piperidine and piperazine derivatives of quinoline which, however, have not been found to be of much value.

(Mrs.) G. M. Robinson (1929) has described pyrrolo-quinolines of the type (III) having similarity in structure with harmine and harmaline which are, according to Gunn and Marshall (1920), reputed anti-malarials, though inferior to quinine.

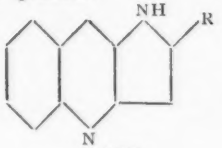

(III)

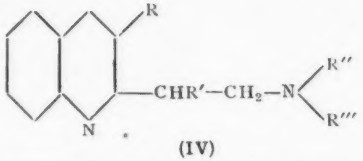

(IV)

Kermack and Muir (1931) have also obtained 2-β-amino-ethylquinolines of the type (IV), and their derivatives and have studied the chemotherapeutic activities of these compounds.

Later Kermack and Smith (1931) have obtained quinoline compounds having in the 4-position a side-chain containing two or more N atoms of the type (V) and (VI).

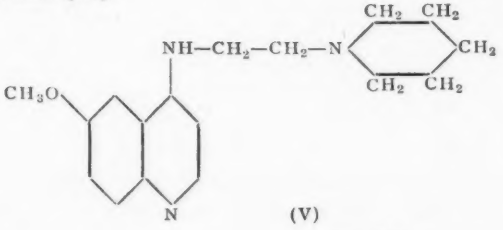

(V)

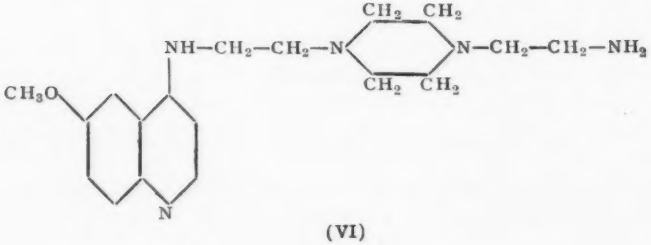

(VI)

Narang and Ray (1931) have obtained glyoxalino-quinolines of the type (VII) which are actively toxic to paramæcia, although Chatterjee's (1929) preparation of β-benziminazolyl-ethylamine derivatives (VIII), whose constitution presents some points of analogy with histamine, have proved to be physiologically inert.

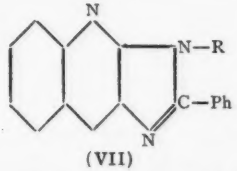

(VII)

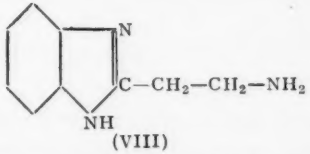

(VIII)

Aggarwal *et al.* (1932) had prepared some α-pyrrylindoles which were found to possess some anti-malarial properties.

Of the several compounds prepared by Robinson and colleagues (*loc. cit.*) some have been found to possess quite satisfactory anti-malarial properties. All of these compounds are quinoline derivatives more or less similar in structure to plasmoquine.

The latest success in the attempts towards this problem is the synthesis of atebrin (IX) synthesised by Mietzsch and Mauss (1933) with the co-operation of Kikuth (1932) for the biological work. This substance is an acridine derivative and is a dye and is regarded as the first synthetic schizonticidal drug in the cure for malaria.

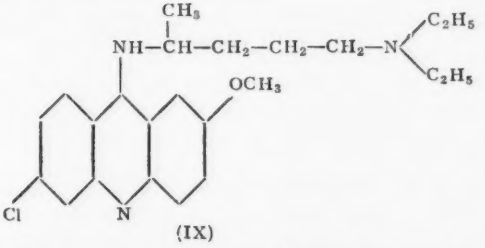

(IX)

It seems, therefore, that all the effective current anti-malarial drugs may be considered as containing a quinoline nucleus, if acridine in the case of atebrin can be regarded as quinoline with a benzene ring fused on it. Although other nuclei have been of some promise it is apparent that quinoline appears to be the most useful so far found, thus confirming Kaufmann's original theory in a modified form. There is undoubtedly considerable room for speculation in the synthesis of compounds on the lines of plasmoquine and atebrin, although one must remember that a modification in the side-chain or a change of position of the quinoline nucleus results in the most

unexpected compounds either with very little or no anti-malarial value. Thus Slotta and Behnisch (1935) have found that when the hydroxyl group of dihydrocupreine is alkylated with dialkyl-aminoalkyl side-chains of the type of plasmoquine, the anti-malarial activity diminishes and finally disappears as the weight of the side-chain increases. On the other hand, Bovet (1933) has found that the insertion of the chain

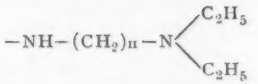

at 8-position in 6-methoxy quinoline yields a product in which activity is not diminished but, strangely enough, is changed by gaining schizonticidal action (as in atebrin) at the expense of some gametocidal activity (as in plasmoquine). Hence it can be not unreasonably assumed that the real effective parasiticidal portion of each of these structures is the quinoline nucleus and the rest of the molecule in respect of their position and configuration just exercise a balanced play of some types of physical and chemical characters on the biological system which are yet unknown.

Following a modification of Kaufmann's theory an attempt was made in the present work to introduce the grouping –CH (OH)–CH–N< into 3-position of the quinoline instead of the 4-, with the ultimate object of ascertaining if compounds of the type (X) would also exhibit physiological activity as in Kaufmann's (1913) and Rabe's (1913, 1917) compounds.

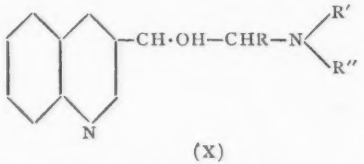

(X)

The starting material for this investigation was ethyl quinoline-3-carboxylate (XI) which was condensed with pure, freshly distilled ethylacetate in presence of alcohol-free sodium ethylate to give ethyl 3-quinoloyl acetate (XII), which was hydrolysed by sulphuric acid to 3-quinolyl methyl ketone (XIII). Bromination of the ketone yielded 3-quinolyl bromomethyl ketone (XIV).

The bromomethyl ketone was then condensed with different secondary amines, such as piperidine, diethylamine and dimethylamine to prepare the aminoketones which were then reduced catalytically to the aminoalcohols of the general formula (X). Thus 3-quinolyl bromomethyl ketone with piperidine gave 3-quinolyl piperidinomethyl ketone, which on catalytic reduction gave β-piperidine-α-hydroxy-α-(3-quinolyl)-ethane. Similarly, 3-quinolyl

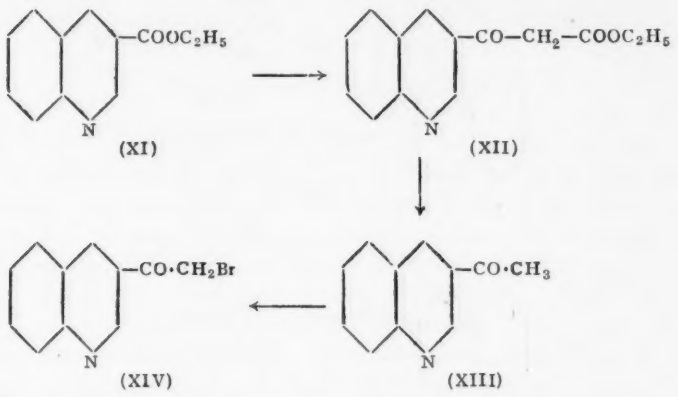

bromomethyl ketone with diethylamine and dimethylamine gave respectively the amino-alcohols β-diethylamino-α-hydroxy-α-(3-quinolyl)-ethane and β-dimethylamino-α-hydroxy-α-(3-quinolyl)-ethane.

Rabe (1931) in his recent remarkable total synthesis of the cinchona alkaloids has been able to effect a synthesis of N-benzoyl homocincholoipon ester, thereby completing the total synthesis of cinchona alkaloids containing the ethyl group in the 3-position of the quinuclidine ring. In the present case, to accomplish the object of closing the quinuclidine ring, N-benzoyl homocincholoipon ester was obtained from cinchonine by reduction according to Heidelberger and Jacobs (1919) and subsequent oxidation according to Kaufmann (1918). Ethyl quinoline-3-carboxylate was thus condensed with N-benzoyl homocincholoipon ester in presence of alcohol-free sodium ethylate and the ethyl ester of α-(3-quinoloyl)-β-4-(3-ethyl-1-benzoylpiperidyl)-propionic acid (XV) was obtained. The condensation product was hydrolysed to 3-quinolyl-4-(3-ethyl piperidyl)-ethyl ketone (XVI), the analogue of dihydrocinchotoxine. It was then brominated by sodium hypobromite to 3-quinolyl-4-(3-ethyl-1-bromopiperidyl)-ethyl ketone (XVII). The bromoderivative was neutral to litmus and did not give rise to a methiodide showing the addition of bromine to the N-atom. This, on treatment with sodium ethylate in alcoholic solution passed into 3′-quinolyl-8-(3-ethyl quinuclidyl)-ketone (XVIII), which on catalytic reduction with palladium black formed the secondary alcohol 3′-quinolyl-8-(3-ethyl quinuclidyl)-methanol† (XIX), the isomeric analogue of dihydrocinchonine.

† Numbering of carbon atoms has been done according to Rabe (1922), who has taken Ruban, the parent substance of the cinchona alkaloids, as a basis of nomenclature.

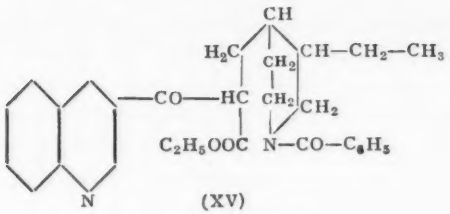

(XV)

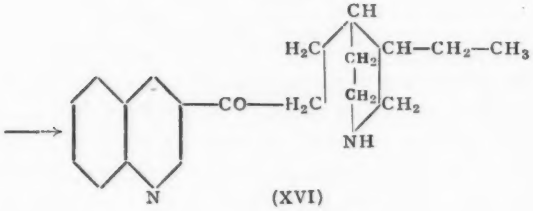

(XVI)

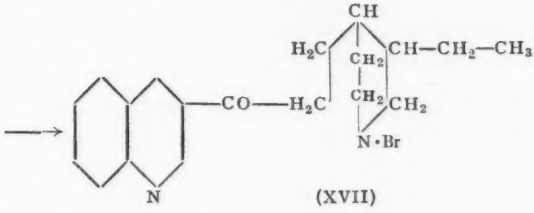

(XVII)

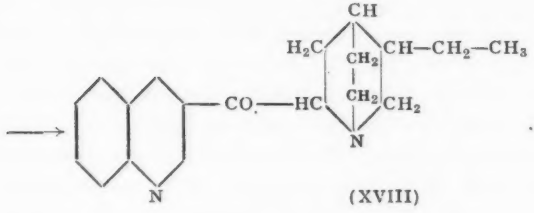

(XVIII)

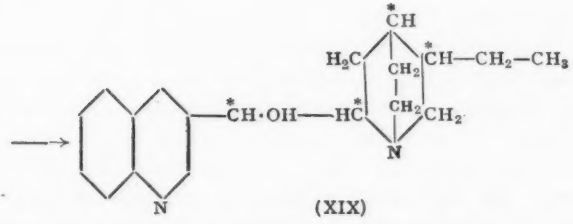

(XIX)

In a second series ethyl 2-methoxy quinoline-3-carboxylate (XX) was taken as the starting material and converted, similarly as in the previous series, into 2-methoxy-3-quinolyl-bromomethyl ketone (XXI).

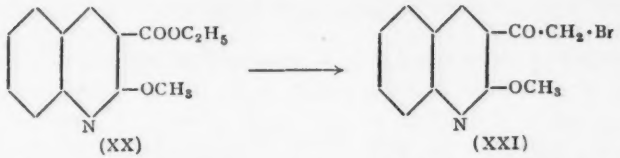

(XX) (XXI)

The bromomethyl ketone was then condensed as before with piperidine, diethylamine and dimethylamine and reduced respectively to β-piperidino-α-hydroxy-α-(2-methoxy-3-quinolyl)-ethane, β-diethylamino-α-hydroxy-α-(2-methoxy-3-quinolyl)-ethane and β-dimethylamino-α-hydroxy-α-(2-methoxy-3-quinolyl)-ethane. To effect a synthesis of the isomeric analogue of dihydroquinine, ethyl 2-methoxy quinoline-3-carboxylate was condensed with N-benzoyl homocincholoipon ethyl ester, and through the series of reactions as shown in the case of the synthesis of the isomeric analogue of dihydrocinchonine, the final product 2′-methoxy-3′-quinolyl-8-(3-ethyl quinuclidyl)-methanol (XXII), the isomeric analogue of dihydroquinine, was obtained.

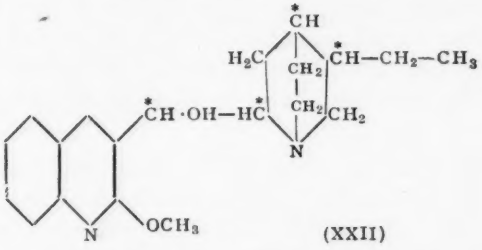

(XXII)

It is to be expected that like dihydrocinchonine and dihydroquinine there will be four optical isomers of each of the compounds (XIX) and (XXII) due to the asterisked asymmetric carbon atoms. Recently Rabe (1932) has been able to isolate all the sixteen possible optical isomers of quinine, hydroquinine, cinchonine and hydrocinchonine and has classified them by following the methods used by King and Palmer (1922) in deducing the sign of the contribution made by the various asymmetric centres in these alkaloids. The resolution of the racemic mixture that has been obtained in the present work is to form the subject of a future investigation.

All of the 3-quinolyl substituted bases of the first series (cinchonine-related) were examined for anti-malarial property by courtesy of the Medical Research Council, London, and were found to be ineffective against avian malaria.

The compounds, however, still retain some parasiticidal activity as has been found by their effect against paramæcia.

Experimental

Ethyl-3-quinoloyl Acetate.—5 gm. of alcohol-free sodium ethylate (1·5 mol.) were made in a flask and a mixture of 10 gm. of ethyl quinoline-3-carboxylate (1 mol.) and 6·5 gm. of pure ethyl acetate (1·5 mol.) dissolved in 10 c.c. of dry benzene were added in it and refluxed on water-bath for 12 hours. A brown solid mass was formed at the end of the reaction, to which was added crushed ice and then 20 c.c. of 10% caustic soda. When everything dissolved, the aqueous solution after being shaken with 80 c.c. of ether to remove any unreacted substances, was rendered acid to congo-red by dilute sulphuric acid.

The oily product which separated, was taken up in ether, the ethereal solution dried over anhydrous sodium sulphate and the ether distilled. A brown oil was left behind which could not be distilled unchanged. Yield 80% of the theoretical.

Copper Salt of Ethyl-3-quinoloyl Acetate.—On dissolving the oil in ether and adding a saturated solution of copper acetate, a pale blue crystalline copper salt separated out on scratching. It crystallises well from ligroin in small needles, m.p. 202–03° C., and is soluble in chloroform, ether and ligroin. (Found: N, 5·08; Cu, 11·61%; $C_{14}H_{12}O_3NCu$ requires N, 5·11; Cu, 11·58%.)

3-Quinolyl Methyl Ketone.—5 gm. of the crude ethyl 3-quinoloyl acetate were heated with 20 c.c. of 25% sulphuric acid on the water-bath for 30–40 minutes until no more CO_2 was evolved. The solution was then cooled, diluted and made alkaline with sodium carbonate, when the ketone came out as an oil, which soon solidified on scratching. Yield 3 gm.

3-Quinolyl methyl ketone is highly soluble in alcohol and sparingly so in benzene and ligroin. It crystallises in colourless plates from ligroin, m.p. 98° C. (Found: C, 77·31; H, 5·14; N, 8·20%. $C_{11}H_9ON$ requires C, 77·18; H, 5·26; N, 8·18%.)

Semicarbazone of 3-Quinolyl Methyl Ketone.—When molecular quantities of the ketone and semicarbazide hydrochloride are dissolved in alcohol and heated with excess of fused sodium acetate under reflux on the water-bath for half an hour, the semicarbazone of the ketone is formed and separates out on cooling. It is sparingly soluble in alcohol, benzene and ether, and crystallises from alcohol in silky aggregates of white needles, m.p. 235° C. (Found: N, 24·63%. $C_{12}H_{12}ON_4$ requires N, 24·56%.)

Phenylhydrazone of 3-Quinolyl Methyl Ketone.—When molecular quantities of phenylhydrazine and the ketone are refluxed on a water-bath for one

hour in alcoholic solution with a little glacial acetic acid, the phenylhydrazone of the ketone is formed and it separates out on dilution with water. It crystallises in very pale yellow needles from alcohol, m.p. 202° C. (Found: N, 16·17%. $C_{17}H_{15}N_3$ requires N, 16·09%.)

3-*Quinolyl Bromomethyl Ketone*.—5 gm. of 3-quinolyl methyl ketone (1 mol.) were dissolved in 20 c.c. of 45% hydrobromic acid by heating on a water-bath. Then 4·5 gm. of bromine (2 atoms) in the vapour form were drawn through the hydrobromic acid solution while keeping it hot at 70–75° C., in a hot water-bath. The hydrobromide of the bromo-ketone separated out almost quantitatively on cooling.

3-Quinolyl bromomethyl ketone hydrobromide crystallises well from hot water in yellow needles, m.p. 215° C. (decomp). If, however, the salt is subjected to prolonged heating in water, it decomposes giving off bromine.

To isolate the free-bromoketone, the hydrobromide was dissolved in warm water and a dilute solution of sodium carbonate added till alkaline to litmus, when the free bromoketone separated out. It crystallises from alcohol in long, light yellow needles, m.p. 120° C.

The free bromoketone is not stable in the atmosphere and on keeping, turns brown in colour. (Found: N, 5·61 ; Br, 31·89%. $C_{11}H_8ONBr$ requires N, 5·60; Br, 32·00.)

3-*Quinolyl Piperidinomethyl Ketone*.—3 gm. of piperidine (3 mols.) were dissolved in 25 c.c. of dry benzene and 4 gm. of 3-quinolyl bromomethyl ketone (1 mol.) in fine powder were gradually added with constant shaking at a temperature not exceeding 5° C. On allowing to stand in ice for one hour, a white precipitate of piperidine hydrobromide separated out which was filtered off and washed well with dry benzene. Benzene was distilled off at reduced pressure, leaving behind the reddish brown piperidinomethyl ketone as an oil which was kept in vacuum desiccator containing sulphuric acid and paraffin wax, to absorb any adhering piperidine or benzene.

The oily piperidinomethyl ketone could not be crystallised and was soluble in almost all organic solvents. It distilled at a temperature of 165–68° C./15 mm. pressure, as faintly yellow coloured liquid. (Found: C, 75·37; H, 7·18; N, 11·21%. $C_{16}H_{18}ON_2$ requires C, 75·59; H, 7·08; N, 11·02%.)

Monohydrobromide of 3-*Quinolyl Piperidinomethyl Ketone*.—0·9 gm. of the ketone was dissolved in 10 c.c. of acetone and 0·75 c.c. of 45% hydrobromic acid (calculated as a little less than 1 mol. HBr to 1 mol. of ketone)

in 5 c.c. of acetone added. Crystals of monohydrobromide separated out at once which were filtered off.

For crystallisation, the hydrobromide was dissolved in the least quantity of 99% alcohol and then its own volume of acetone added and the solution left to stand. Soon lustrous light yellow coloured plates separated out, m.p. 245–46° C., turning brown at 230° C.

The monohydrobromide is readily soluble in water and on long exposure to air turns brownish in colour. (Found: N, 8·25; Br, 23·75%; $C_{16}H_{18}ON_2$ HBr requires N, 8·35; Br, 23·88%.)

The *Dipicrate* was obtained by adding excess of alcoholic picric acid solution to an alcoholic solution of the ketone. It crystallises from alcohol in beautiful yellow needles, m.p. 139–41° C.

β-Piperidino-α-Hydroxy-α-(3-Quinolyl)-Ethane.—1 gm. of gum arabic was dissolved in 100 c.c. of water by heating. To this 1 gm. of palladium chloride was dissolved with a few drops of hydrochloric acid to make an one per cent. solution of palladium chloride.

5 c.c. of this hot solution were introduced into the reduction flask, which was then evacuated and then hydrogen gas purified by passing through $KMnO_4$ solution was passed in under the pressure of a column of water about 30 inches in height, with mechanical stirring. A fine suspension of palladium black was thus obtained.

A solution of 4 gm. of the aminoketone in 2 c.c. of strong hydrobromic acid was now quickly introduced into the reduction flask and hydrogen passed in again. Hydrogen was being absorbed slowly at first and afterwards fairly quickly till 360 c.c. was absorbed (theoretical 340 c.c.). The absorption extended over about 3½ hours. The solution was filtered from the metallic palladium and dilute sodium carbonate solution added. A colloidal precipitate was obtained which was extracted with ether, the ethereal solution dried over sodium sulphate and the ether distilled off. A greenish yellow oily product which soon turned brown in the air, was obtained. This oil solidified on cooling and scratching.

Purification of the substance was effected by re-crystallising from acetone when the material separated out in colourless plates on standing, melting at 93–94° C. (Found : C, 75·21 ; H, 7·69 ; N, 10·88% ; $C_{16}H_{20}ON_2$ requires C, 75·00 ; H, 7·81 ; N, 10·93%.)

The *Dipicrate* of the aminoalcohol separates out easily from alcoholic solutions on adding excess of picric acid. It crystallises in yellow needles from alcohol, m.p. 161–63° C. (Found: N, 15·63%; $C_{16}H_{20}ON_2$, 2 $C_6H_3O_7N_3$ requires N, 15·68%.)

3-*Quinolyl Diethylaminomethyl Ketone*.—5 gm. of 3-quinolyl bromomethyl ketone (1 mol.) were dissolved in 25 c.c. of ether and added gradually to a solution of 3·5 gm. of diethylamine (2 mols.) in 40 c.c. of ether. After leaving for 1½ hours, the hydrobromide of the diethylamine separated out. Filtered and the reddish yellow filtrate containing the aminoketone was evaporated off leaving an oily product which could not be crystallised out. The oil is soluble in most of the organic solvents and could not be distilled unchanged.

The *Monohydrobromide* of 3-quinolyl diethylamino-methyl ketone was formed similarly as in the case of the piperidine derivative in acetone solution. It crystallises from a mixture of alcohol and acetone, m.p. 142–45° C. (Found: N, 8·78%. $C_{15}H_{18}ON_2$, HBr requires N, 8·66%.)

The *Dipicrate* of the aminoketone was formed by adding a saturated solution of picric acid in alcohol in excess to the aminoketone dissolved in a little alcohol. The salt comes out on evaporation of alcohol to a little extent and then standing. Recrystallised from alcohol, m.p. 150–51° C. (Found: N, 16·21%. $C_{15}H_{18}ON_2$, 2 $C_6H_3O_7N_3$ requires N, 16·00%.)

β-Diethylamino-α-Hydroxy-α-(3-Quinolyl)-Ethane.—The ketone was reduced with hydrogen in presence of palladium black as catalyst as in the case of 3-quinolyl piperidinomethyl ketone. The base crystallised from acetone in small granular crystals melting at 89–90° C. It is very readily soluble in alcohol and sparingly so in ether and benzene. (Found: C, 73·91; H, 8·00; N, 11·51%. $C_{15}H_{20}ON_2$ requires C, 73·77; H, 8·19; N, 11·47%.)

The *Dipicrate* was formed by adding excess of a saturated picric acid solution to an alcoholic solution of the base. On standing the yellow picrate separated out in needles which crystallised from alcohol, m.p. 139–41° C. (Found: N, 16·06%. $C_{15}H_{20}ON_2$; 2 $C_6H_3O_7N_3$ requires N, 15·95%.)

3-*Quinolyl Dimethylaminomethyl Ketone*.—9 c.c. of aqueous dimethylamine (3 mols.) solution (330 gm./litre) were taken in 75 c.c. of benzene and the solution cooled to 5° C. 6·5 gm. of finely powdered 3-quinolyl bromomethyl ketone hydrobromide (1 mol.) were added gradually with good shaking, as described. The benzene solution was once washed with 10 c.c. of water and dried and the volume of benzene reduced to about 25 c.c. It was then treated with 4% alcoholic hydrochloric acid when the hydrochloride of the base separated out gradually on standing. This was recrystallised from alcohol in colourless needles, m.p. 157–58° C. The hydrochloride is sparingly soluble in alcohol. (Found: C, 54·14; H, 5·42; N, 9·80; Cl, 24·53%. $C_{13}H_{14}ON_2$; 2 HCl requires C, 54·35; H, 5·57; N, 9·75; Cl, 24·73%.)

The free base is an oil when liberated from the hydrochloride by dilute sodium carbonate solution.

The *Dipicrate* formed in the usual manner crystallised from alcohol, m.p. 147–49° C. (decomp.). (Found: N, 16·69%. $C_{13}H_{14}ON_2$; 2 $C_6H_3O_7N_3$ requires N, 16·66%.)

β-Dimethylamino-α-Hydroxy-α-(3-Quinolyl)-Ethane.—3 gm. of the ketone hydrochloride were dissolved in 5 c.c. of 1% palladium chloride solution, and reduced similarly as before. The free base appeared as an oil which was extracted with ether.

On treatment with 4% alcoholic hydrochloric acid, the oil formed a hydrochloride which crystallised from alcohol on addition of ether and allowing to stand. It melts at 171–73° C. (Found: C, 53·79; H, 6·31; N, 9·61%. $C_{13}H_{16}ON_2$, 2 HCl requires C, 53·97; H, 6·22,; N 9·68%.)

The *Acetyl derivative* was formed by heating with acetyl chloride (1 mol.) and caustic soda solution (2 mols.) for a few minutes. The acetyl derivative came out as a solid on adding to water. It crystallised from chloroform in colourless prisms, m.p. 139° C. (Found: N, 10·76%. $C_{15}H_{18}O_2N_2$ requires N, 10·85%.)

Ethyl Ester of α-(3-Quinoloyl)-β-4-(3-Ethyl-1-Benzoyl Piperidyl)-Propionic Acid.—10 gm. of N-benzoyl homocincholoipon ester (1 mol.) and 6·2 gm. of ethyl quinoline-3-carboxylate (1 mol.) were dissolved in 60 c.c. of dry benzene, and added to a flask containing 3·2 gm. of alcohol-free sodium ethylate and the whole refluxed on the water-bath for 12 hours. At the end a solid mass resulted. This was cooled and treated with powdered ice and shaken till everything dissolved. The solution was extracted with 80 c.c. of ether to remove any unreacted substance. The aqueous layer containing the sodium salt of the condensation product was acidified to congo-red paper with dilute sulphuric acid, when an oily product separated out. After extraction with ether and drying over sodium sulphate, ether was distilled off leaving the β-ketonic ester as a dark thick oil which could not be crystallised nor could it be distilled unchanged even at 2 mm. pressure. The yield was about 40% of the theoretical.

The *Copper Salt* was obtained by adding a saturated solution of copper acetate to an ethereal solution of the β-ketonic ester. The salt separated rapidly in crystalline shape and was recrystallised from benzene in small pale blue needles m.p. 251° C., darkening at about 237° C. It is soluble in alcohol and almost insoluble in ether. (Found: N, 5·61; Cu, 6·43%. $C_{29}H_{31}O_4N_2$ Cu requires N, 5·56; Cu, 6·35%.)

3-*Quinolyl*-4-(3-*Ethylpiperidyl*)-*Ethyl Ketone*.—The β-ketonic ester was hydrolysed with about 8–10 times its weight of 17% hydrochloric acid by refluxing for 4 hours over a small flame. On cooling, the benzoic acid crystallised out and filtered off. The filtrate was then treated with caustic soda solution till it was only slightly acidic and extracted with ether. The aqueous solution was made strongly alkaline with caustic soda and the oil separated was taken up with ether, dried over anhydrous potassium carbonate and the ether distilled off. An oil of deep brown colour was obtained; the yield about 70% of the theoretical.

The ketone thus obtained was distilled at 225° C./9 mm. giving an almost colourless, viscous oil. (Found: C, 76·38; H, 8·25; N, 9·49%. $C_{19}H_{24}ON_2$ requires C, 77·02; H, 8·10; N, 9·45%.)

The Phenylhydrazone Dipicrate derivative of the ketone was obtained by treating 3 gm. of the ketone (1 mol.) with 1·2 gm. of phenyl-hydrazene (1 mol.) and 4·7 gm. of picric acid (2 mols.) in alcoholic solution with a little glacial acetic acid. A red coloration was obtained which on scratching deposited a crystalline reddish yellow substance. It crystallised from alcohol in plates, m.p. 195–97° C. (Found: N, 16·603. $C_{25}H_{30}N_4$; $2\,C_6H_3O_7N_3$ requires N, 16·58%.)

3-*Quinolyl*-4-(3-*Ethyl*-1-*Bromo-Piperidyl*)-*Ethyl Ketone*.—The N-bromo derivative of the ketone was obtained according to the following method: 14 gm. of 3-quinolyl-4-(3-ethyl-piperidyl)-ethyl ketone (1 mol.) were dissolved in 50 c.c. of normal hydrochloric acid (1 mol.) and 125 c.c. of ether added to it. Then at ordinary temperature and with mechanical stirring a cold solution of sodium hypobromite prepared from 8 gm. of bromine (1 mol.) and 100 gm. of 6% caustic soda solution (3 mols.) were added drop by drop. After 10 minutes the ethereal layer was removed quickly and dried over sodium sulphate. On standing for 24 hours an oily product separated out and was found to be the unreacted ketone. The ether solution was filtered off and on concentration of ether the N-bromo compound separated out in faintly coloured crystals in a yield of 5 gm.

The bromo-derivative crystallised in lustrous needles from alcohol, m.p. 137–39° C. It is insoluble in water, moderately so in ether and alcohol.

The product is neutral to litmus and does not give rise to a methiodide with methyliodide. (Found: N, 7·41; Br, 21·20%. $C_{19}H_{23}ON_2Br$ requires N, 7·46; Br, 21·33%.)

3′-*Quinolyl*-8-(3-*Ethylquinuclidyl*)-*Ketone*.—6 gm. of 3-quinolyl-4-(3-ethyl-1-bromo-piperidyl)-ethyl ketone were dissolved in 50 c.c. of alcohol on the

water-bath under reflux. 25 c.c. of sodium alcoholate solution containing 1·2 gm. of sodium were added and the whole refluxed for half an hour, the solution assuming a reddish yellow colour. After cooling, the whole was acidified with dilute hydrochloric acid and the alcohol distilled off. On neutralising with sodium carbonate a yellowish solid base came out which was extracted with ether and dried over potassium carbonate. On evaporation of the ether, a yellow coloured crystalline product was left behind which crystallised in needles from alcohol, m.p. 122–24° C. It is soluble in benzene and ligroin. (Found: C, 76·98; H, 7·29; N, 9·59%. $C_{19}H_{22}ON_2$ requires C, 77·55; H, 7·48; N, 9·52%.)

The *Monopicrate* of the ketone was formed by treating the alcoholic solution with one molecular proportion of picric acid in alcohol. On standing the yellow crystals of the picrate separated out and were crystallised in yellow needles from alcohol, m.p. 167–68° C. (Found: N, 13·42%. $C_{19}H_{22}ON_2$; $C_6H_3O_7N_3$ requires N, 13·38%.)

3′-*Quinolyl*-8-(3-*Ethyl Quinuclidyl*)-*Methonol*.—3 gm. of the ketone were dissolved in 25 c.c. of 5% hydrochloric acid and 10 c.c. of 1% palladium chloride added and reduced as described before. The metallic palladium was filtered off and the clear filtrate was made alkaline by dilute caustic soda when the base was precipitated as solid. It was filtered off and it crystallised in colourless needles from alcohol, melting at 225–26° C.

The base is easily soluble in alcohol, sparingly so in ether and almost insoluble in ligroin and benzene. (Found: C. 76·70; H, 7·98; N, 9·51%. $C_{19}H_{24}ON_2$ requires C, 77·02; H, 8·10; N, 9·45%.)

The *Dihydrochloride* of the base was obtained by treating it with 4% alcoholic hydrogen chloride and concentrating. The salt separated on cooling in lustrous colourless needles, m.p. 261–63° C. It can be recrystallised from a mixture of alcohol and water. (Found: N, 7·48; Cl, 18·95%. $C_{19}H_{24}ON_2$, 2 HCl requires N, 7·58; Cl, 19·24%.)

The *Chloroplatinate* was formed by dissolving the substance in 20% hydrochloric acid solution and adding one molecular proportion of platinic chloride solution. The salt came out immediately and crystallised from alcohol in an amorphous form, m.p. 286–89° C. with decomposition. (Found: N, 4·02; Pt, 27·49%. $C_{19}H_{24}ON_2$, H_2PtCl_6 requires N, 3·96; Pt, 27·62%.)

2-*Methoxyl*-3-*Quinolyl Methyl Ketone*.—7 gm. of freshly made alcohol-free sodium ethylate (1·8 mols.) and a mixture of 10 gm. of ethyl 2-methoxy-quinoline-3-carboxylate (1·4 mols.), 5·5 gm. of pure ethyl acetate

(1·5 mols.) and 20 c.c. of dry benzene were refluxed on the water-bath for 10 hours. At the end of the reaction crushed ice was added followed by 25 c.c. of a 10 per cent. caustic soda solution. It was shaken with ether to remove any unreacted substances and was then rendered acid to congo-red paper by dilute sulphuric acid, when brown oil separated. This crude oil, after separation by ether, was directly hydrolysed by 30 c.c. of 25 per cent. sulphuric acid by heating on the water-bath for half an hour. The solution was then cooled, diluted and made alkaline with sodium carbonate. The ketone, which separated out as a solid product, was crystallised in colourless leafy plates from ligroin, m.p. 110–12° C. Yield 2·8 gm. (Found: C, 70·91; H, 5·49; N, 6·77%. $C_{12}H_{11}O_2N$ requires C, 71·14; H, 5·47; N, 6·96%.)

Phenylhydrazone of 2-*Methoxy*-3-*Quinolyl Methyl Ketone.*—On refluxing on the water-bath for 2 hours equimolecular quantities of phenylhydrazine and the ketone in absolute alcohol with a few drops of glacial acetic acid, the phenylhydrazone of the ketone is formed which separates out on dilution with water. It crystallises from alcohol in light yellow plates, m.p. 177° C. (Found: N, 14·57%. $C_{18}H_{17}ON_3$ requires N, 14·43%.)

2-*Methoxy*-3-*Quinolyl Bromomethyl Ketone.*—The bromination of 2-methoxy-3-quinolyl methyl ketone was done as described before. The free bromoketone was isolated by dissolving the hydrobromide in warm water (50° C.) and adding a dilute solution of sodium carbonate till alkaline to litmus. It crystallises from alcohol in long, pale yellow needles, m.p. 126–27° C. (Found: N, 5·20; Br, 27·98%. $C_{12}H_{10}O_2N$ Br requires N, 5·00; Br, 28·57%.)

2-*Methoxy*-3-*Quinolyl Piperidinomethyl Ketone.*—5 gm. of piperidine (3 mols.) were dissolved in 40 c.c. of dry benzene and 7 gm. of 2-methoxy-3-quinolyl bromomethyl ketone hydrobromide (1 mol.) in extremely fine powder were added gradually with constant shaking at ice cold temperature. On allowing to stand in cold for about 2 hours, the precipitate of piperidine hydrobromide was filtered and washed well with dry benzene. Benzene was then distilled off at reduced pressure leaving behind a brown oil, which on keeping in a vacuum desiccator overnight, solidified. It was crystallised from alcohol in very small needles, m.p. 69–71° C. It is soluble in most of the organic solvents. (Found: C, 71·86; H, 6·89; N, 9·96%. $C_{17}H_{20}O_2N_2$ requires C, 71·83; H, 7·04; N, 9·86%.)

The *Monohydrobromide* was obtained by dissolving the base in acetone and adding a molecular proportion of hydrobromide acid. It is crystallised from a mixture of alcohol and acetone as yellow needles melting at 251–56° C. with decomposition.

β-Piperidino-α-Hydroxy-α-(2-Methoxy-3-Quinolyl)-Ethane. — The ketone was reduced to the secondary alcohol with hydrogen in presence of palladium black as catalyst as described before. The free base was extracted with ether on evaporation of which a brown solid was obtained which crystallised easily from alcohol treated with animal charcoal. Colourless needles, m.p. 102–04° C. (Found: C, 70·97; N, 7·59; N, 9·91%. $C_{17}H_{22}O_2N_2$ requires C, 71·32; H, 7·69; N, 9·79%.)

2-*Methoxy*-3-*Quinolyl Diethylaminomethyl Ketone.*—To a solution of 3 gm. of 2-methoxy-3-quinolyl bromomethyl ketone in dry ether (20 c.c.) were added gradually a solution of 1·9 gm. of diethylamine (2 mols.) in 20 c.c. of dry ether while shaking in ice cold water. The monohydrobromide of the aminoketone was prepared in the usual manner from acetone solution. It crystallises in pale yellow leaf from a mixture of acetone and alcohol, m.p. 134–36° C. (Found: N, 7·70; Br, 22·15%. $C_{16}H_{20}O_2N_2$, HBr requires N, 7·93; Br, 22·66%.)

β-Diethylamino-α-Hydroxy-α-(2-Methoxy-3-Quinolyl)-Ethane.— The reduction of the aminoketone to the secondary alcohol was carried out similarly as before. The free base was crystallised in colourless prisms from alcohol, m.p. 78–79° C. (Found: C, 69·82; H, 7·76; N, 10·20%. $C_{16}H_{22}O_2N_2$ requires C, 70·07; H, 8·02; N, 10·21%.)

2-*Methoxy*-3-*Quinolyl Dimethylaminomethyl Ketone.*—4 gm. of finely powdered 2-methoxy-quinolyl bromomethyl ketone hydrobromide (1 mol.) were added gradually to a solution of 6 c.c. of 33% dimethylamine (3 mols.) in 50 c.c. of benzene as described. The benzene solution was washed with a little water and then treated with an alcoholic solution of hydrochloric acid when the hydrochloride of the base separated out on standing. On recrystallisation from alcohol it melts at 177° C. (Found: N, 9·00; Cl, 21·90 %. $C_{14}H_{16}O_2N_2$, 2 HCl requires N, 8·83, Cl, 22·39%.)

β-Dimethylamino-α-Hydroxy-α-(2-Methoxy-3-Quinolyl)-Ethane.—The reduction of the amino ketone to the alcohol was carried out as before. The free base is an oil which in ethereal solution forms crystalline hydrochloride from alcoholic hydrochloric acid. The colourless needles melt at 167–69° C. (Found : N, 8·91; Cl, 22·63%. $C_{14}H_{18}O_2N_2$, 2 HCl requires N, 8·77, Cl, 22·25%.)

The *Dipicrate* was prepared from an alcoholic picric acid solution and an alcoholic solution of the base. It crystallises in yellow groups of needles, m.p. 173–75° C. (Found: N, 15·68%. $C_{14}H_{18}O_2N_2$, 2 $C_6H_3O_7N_3$ requires N, 15·90%.)

2-*Methoxy*-3-*Quoinolyl*-4-(3-*Ethylpiperidyl*)-*Ethyl Ketone*.— 12 gm. of N-benzoyl homocincholoipon ester (1 mol.) and 8·5 gm. of ethyl 2-methoxy-quinoline-3-carboxylate (1 mol.) dissolved in 75 c.c. of dry benzene were subjected, as previously described, to Claisen condensation in presence of 4·5 gm. of alcohol-free sodium ethylate. The crude ethyl ester of α-(2-methoxy-3-quinoloy)-β-4-(3-ethyl-1-benzoyl piperidyl)-propionic acid, was without further purification hydrolysed with large excess of 17% hydrochloric acid by refluxing for 4 hours. On cooling the hydrolysed mass, benzoic acid separated out which was filtered off. The acidity of the filtrate was then considerably reduced by caustic soda and extracted with ether to remove impurities. The aqueous solution was then made strongly alkaline. An oil separated which was taken up by ether, the ethereal solution dried over potassium carbonate and the ether distilled. A brown oil was obtained. The crude ketone thus obtained was distilled at 197–200° C./5 mm. giving 2 gm. of a heavy colourless oil. (Found: C, 73·38,; H, 8·01; N, 8·72%. $C_{20}H_{26}O_2N_2$ requires C, 73·61; H, 7·97; N, 8·58%.)

The *Phenylhydrazone dipicrate* derivative was prepared as described before. The orange-red crystals melt at 188–89° C.

2-*Methoxy*-3-*Quinolyl*-4-(3-*Ethyl*-1-*Bromo-Piperidyl*)-*Ethyl Ketone*.—5 gm. of 2-methoxy-3-quinolyl-4-(3-ethyl-piperidyl)-ethyl ketone (1 mol.) were dissolved in 16 c.c. of normal hydrochloric acid (1 mol.) and 80 c.c. of ether added to it. Then under mechanical stirring a cold solution of sodium hypobromite prepared from 3 gm. of bromine (1 mol.) and 37 gm. of 6% caustic soda solution (3 mols.) were added drop by drop from a funnel with subsequent treatment as described before. The N-bromo derivative was crystallised in colourless needles from alcohol, m.p. 158–62° C. (Found: N, 7·04; Br, 19·55%. $C_{20}H_{25}O_2N_2$ Br, requires N, 6·91; Br, 19·75%.)

2′-*Methoxy*-3′-*Quinolyl*-8-(3-*Ethylquinuclidyl*)-*Ketone*.—5 gm. of the above N-bromo derivative were taken in 50 c.c. of absolute alcohol and mixed with 30 c.c. of freshly made sodium alcoholate solution containing 1·0 gm. of sodium. The whole was refluxed on the water-bath for an hour. Alcohol was then removed under reduced pressure and the residue acidified with hydrochloric acid and the acid solution was treated with decolourising charcoal. On neutralising with sodium carbonate solution a solid product separated out which was extracted with ether. The ketone crystallised in colourless plates from alcohol, m.p. 155–56° C. It is freely soluble in ligroin. (Found: N, 8·58%. $C_{20}H_{24}O_2N_2$ requires N, 8·64 %.)

2′-*Methoxy*-3′-*Quinolyl*-8-(3-*Ethylquinuclidyl*)-*Methanol*.—2·5 gm. of the above ketone were dissolved in 30 c.c. of 5% hydrochloric acid and 10 c.c.

of 1% palladium chloride added. Reduction was done as already described. The base was crystallised in colourless needles from alcohol, m.p. 259–61° C. (Found: C, 73·50; H, 7·81; N, 8·84%. $C_{20}H_{26}O_2N_2$ requires C, 73·61; H, 7·97; N, 8·58%.)

Summary

1. Some quinoline compounds that are structurally related to cinchonine and quinine have been synthesised starting from ethyl quinoline-3-carboxylate and ethyl 2-methoxy quinoline-3-carboxylate respectively.

2. The respective bromomethyl ketones made from ethyl quinoline-3-carboxylate and ethyl 2-methoxy quinoline-3-carboxylate have been condensed with different secondary amines such as, piperidine, diethylamine and dimethylamine to prepare the amino-ketones which have then been reduced catalytically to their respective amino alcohols of the type–CH (OH)–CH–N<. Ethyl quinoline-3-carboxylate and ethyl 2-methoxy quinoline-3-carboxylate have also been condensed with N-benzoyl homocincholoipon ester for the ultimate synthesis of the isomeric analogues of dihydrocinchonine and dihydroquinine respectively. These two new series of compounds differ from cinchonine and quinine in the fact that the linking –CH (OH)–CH–N< is attached to the 3-position of the quinoline nucleus instead of 4-, and in the quinine analogue the position of the methoxyl group is in position 2 instead of 6.

3. Although it has been found that these new series of compounds are effective against paramæcia, the cinchonine-related series have, however, proved ineffective against avian malaria. The quinine-related series still await examination.

My best thanks are due to Prof. J. Kenner, D.Sc., F.R.S., Head of the Department of Applied Chemistry, College of Technology, Manchester, under whose suggestion and guidance the main portion of the work was carried out. My thanks are also due to Dr. B. B. Dikshit for kindly undertaking to examine the compounds of the quinine-related series for any anti-malarial property.

REFERENCES

Aggarwal, J. S., Qureshi, A. V., and Ray, J. N. .. *J. Amer. Chem. Soc.*, 1932, **54**, 3988.

Baldwin, A. W. .. *J. C. S.*, 1929, **295**.

Bovet, D. .. *Ann. Inst. Pasteur.*, 1933, **51**, 528.

Chatterjee, B. .. *J. C. S.*, 1929, 2965.

Fourneau, E. .. *Ann. Inst. Pasteur*, 1931, **45**, 514; 1933, **50**, 731.

Gunn and Marshall .. *Proc. Roy. Soc. Edin.*, 1920, **15**, 145.

Heidelberger, M., and Jacobs, W. J.	*J. Amer. Chem. Soc.*, 1919, **41**, 817.
Kaufmann, A. ..	*Ber.*, 1912, **45**, 3096, 3090; 1913, **46**, 57, 1823, 1833, 2920; 1918, **51**, 116.
Kermack, W. O., and Muir, W.,	*J.C.S.*, 1931, 3089.
———— and Smith, J. F. ..	*Ibid.*, 1930, 1356; 1931, 3096.
Kikuth, W. ..	*Deut. Med. Woch.*, 1932, **58**, 530.
King, H., and Palmer, P.	*J.C.S.*, 1922, 2577.
Magidson, O. Y., *et al.* ..	*Arch. Pharm.*, 1933, **271**, 359, 569; 1934, **272**, 74; 1935, **273**, 320.
Mietzsch, F., and Mauss, H. ..	*Klin., Woch.*, 1933, **12**, 1276.
Narang, K. S., and Ray, J. N. ..	*J.C.S.*, 1931, 976.
Rabe, P. ..	*Ber.*, 1913, **46**, 1032, 1917, **50**, 144; 1922, **55**, 522; 1931, **64**, 2487.
———— (*Idem.*) ..	*Annalen.*, 1932, **492**, 242.
Robinson, G. M. (Mrs.) ..	*J.C.S.*, 1929, 2948.
Robinson, R., *et al.* ..	*Ibid.*, 1929, 2947, 2952, 2959, 2965; 1930, 1356; 1931, 3089, 3096; 1933, 1467; 1934, 1264, 1267, 1322, 1520, 1524; 1935, 1143, 1421.
Schulemann, W., Schonhofer, F., and Wingler, A.	*Klin. Woch.*, 1932, **381**, No. 9.
Seshadri, T. R. ..	*J.C.S.*, 1929, 2952.
Slotta, K. H., and Behnisch, R.	*Ber.*, 1935, **68**, 754.

ON DECIMALS OF IRRATIONAL NUMBERS

By T. Vijayaraghavan

Received May 25, 1940

Let $a_0 \cdot a_1 a_2 \ldots$ represent a number θ in the scale of m,

$$\theta_n = \cdot a_n a_{n+1} \ldots \ldots \qquad (n = 1, 2, 3 \ldots .)$$

and L be the set of limit points of $\theta_1, \theta_2, \ldots .$

Theorem. *If θ is irrational then L contains an infinity of points.*

Suppose to the contrary that L consists of a finite number of points only. Let them be $\alpha_1 \alpha_2, \ldots \alpha_k$, where we suppose that if a member of L has two representations in the scale of m then that member has been counted twice, say, as α_p and α_q, corresponding to the two representations. Take r so large that the first r digits of no two of the α's are the same, and denote by β_n that one of the α's the first r digits of which are the same as those of θ_n. Since the number of α's is finite it is seen that β_n is defined uniquely for all large values of n, say, for $n > M$. Take $N > M$, and further let N be so large that β_n and θ_n have the same first $r + 1$ digits whenever $n > N$. It then follows that to every $x\,(1 \leqslant x \leqslant k)$ there corresponds one and only one $y\,(1 \leqslant y \leqslant k)$ such that if $n > N$, and $\beta_n = \alpha_x$ then $\beta_{n+1} = \alpha_y$. Hence we deduce that the 'decimal' is a recurring one which is contrary to the hypothesis that θ is irrational.

The converse of the result is true and is completely trivial. That the set L may be enumerable is also trivial as is seen by considering the case in which $a_n = 0$ if and only if n is not a square number.

A Corollary. *Suppose that $\theta = \sqrt[q]{m}$, and is irrational; the fractional part of θ^{an+1} $(n = 1, 2, 3, \ldots .)$ is plainly θ_{n+1}, and we see that the set of the limit points of the fractional parts of the powers of θ contains an infinity of points.*

The property noticed in the above corollary is not one that belongs to every irrational number greater than unity as is seen from the following known examples. From the bionomial theorem we see that $(2+\sqrt{2})^n + (2-\sqrt{2})^n$ is an integer for $n = 1, 2, 3, \ldots$ Hence the fractional parts of powers of $2+\sqrt{2}$ have only one limit point, *viz.*, 1. Similarly, the fractional parts of the powers of $1+\sqrt{2}$ have only two limit points, *viz.*, 0 and 1.

THE KINETICS OF MUTAROTATION OF OXYMETHYLENE-*d*-CAMPHOR—PART II*

By Bawa Kartar Singh and M. K. Srinivasan
(*From the Chemical Laboratories, Science College, Patna*)

Received May 2, 1940

In a previous paper[1] it was stated that the temperature coefficient of the velocity constant of mutarotation of oxymethylenecamphor in benzene solution ($k_{45°}/k_{35°} = 29{\cdot}3$) was 10 to 15 times as large as that found for an ordinary chemical reaction, the value of k at 35° being $1{\cdot}927 \times 10^{-4}$ and that at 45° being $56{\cdot}55 \times 10^{-4}$. The velocity of the change at 45° was so high that the equilibrium was attained within 15 minutes of the preparation of the solution. Such high values of temperature-coefficient are not met with in homogeneous reactions taking place in a liquid solvent. They are to be found in those regions of gaseous reactions which border on explosions.

It was thus apparent that some catalyst had been introduced into the system at 45° C., which was responsible for the abnormal increase in the velocity of mutarotation. After a careful consideration of the different factors entering into the problem, it was considered probable that moisture in traces might bring about the observed result: the reason for this supposition lay in the circumstance that oxymethylenecamphor was purified by steam distillation. A dry sample of oxymethylenecamphor, having $k_{35°} = 1{\cdot}850$ (Table I) was steam distilled and the velocity constants of mutarotation were redetermined at 25° and 45° after drying it for varying periods. The value of $k_{25°}$ after 48 hours' drying was found to be 5·552 (Table II), which is much higher than that at 35° C. It was dried further for another 48 hours and the value of k fell to 4·436 (Table III). The sample was then allowed to remain in the vacuum desiccator for 20 days, when the value of k fell to 0·98 (Table IV). The mutarotation of this sample of oxymethylenecamphor dried over such a long period was determined at 45° and the value of k was constant (Table V) and about twice that found at 35°C. (compare Table I). These experiments give the values of temperature-coefficient of mutarotation

* Section (*b*) of an earlier paper (Singh and Bhaduri, *J. Ind. Chem. Soc.*, 1930, **7**, 779) may be taken as Part I of this Series (B. K. S.).

[1] Singh and Bhaduri, *J. Ind. Chem. Soc.*, 1930, **7**, 779.

which are normal, namely, $k_{45°}/k_{35°} = \frac{3 \cdot 492}{1 \cdot 89} = 1 \cdot 89$ and $k_{35°}/k_{25°} = \frac{1 \cdot 85}{0 \cdot 98} = 1 \cdot 89$. According to Arrhenius, the effect of temperature on reaction velocity amounts at the ordinary temperature to an increase of 10 to 15 per cent. for one degree rise.[2] The observed values of temperature-coefficient thus fall within the range postulated by Arrhenius for ordinary reactions.

Another series of experiments, showing the influence of progressive drying on the value of k were made at 35°. The value of $k_{35°}$, determined for a sample which was examined soon after its being steam distilled, was found to be very fluctuating. After 24 hours' drying in vacuum, the value of k ranged from 3·991 to 2·734 (Table VI). After 3 days' drying, it fell to 2·127 (Table VII), after 4 days' drying to 1·867 (Table VIII) and on further drying it remained constant. It is, therefore, concluded that traces of moisture accelerate the chemical change involved in mutarotation catalytically. This is further borne out by the different times of drying observed with samples of varying amount. When the quantity of sample taken was about 30 grams, the value of velocity constant was still high after 4 days' drying in vacuum (Tables II, III and IV), whereas in the case of another sample weighing only 10 grams, it reached the normal value in that period (Tables VI, VII and VIII).

Arrhenius Equation for the Variation of Velocity of Mutarotation of Oxymethylenecamphor with Temperature

In a balanced reaction, the variation with temperature of the equilibrium constant K, which equals k_1/k_2, is given by the Van't Hoff isochore

$$\frac{d \log K}{dT} = \frac{Q}{RT^2},$$

where k_1 and k_2 are the velocity constants of the direct and reverse reactions respectively and Q is the heat of reaction.

Arrhenius found empirically that the variation of the velocity constant, k, with temperature can be expressed in a satisfactory manner by the simplified equation,

$$\frac{d \log k}{dT} = \frac{A}{RT^2} \quad \text{or} \quad \log k = C - \frac{A}{RT}.$$

This equation may be tested by plotting the logarithm of velocity constant against the reciprocal of the absolute temperature: the Arrhenius equation holds good if a straight line is obtained. The values of k, determined at 25°, 35° and 45° are given below:

[2] Arrhenius Memorial Lecture, *J.C.S.*, 1928, 1934.

Absolute temperature	$k \times 10^{-4}$ time in seconds and conc. in gm. per 100 c.c.
298°	0·98
308	1·85
318	3·492

The $\log k/\frac{1}{T}$ plot (Fig. 1) is a straight line. This indicates that the chemical reaction involved in the mutarotation of oxymethylenecamphor is a simple and not a composite one.

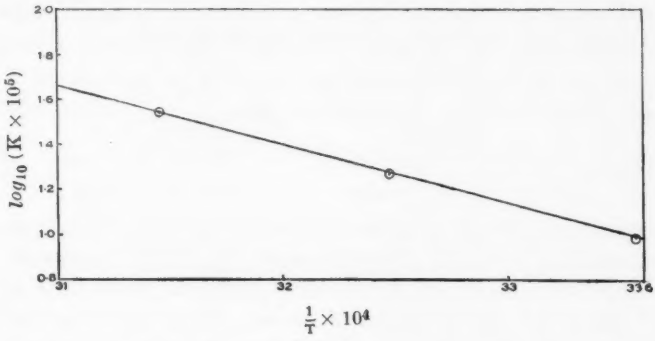

FIG. 1

Influence of temperature on the velocity constant of mutarotation of oxymethylene-*d*-camphor

Claisen put forward the *three* following fomulæ for oxymethylenecamphor :

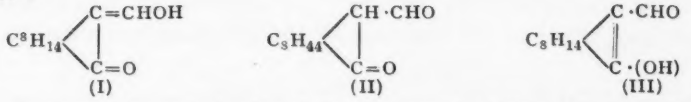

The prototropic changes involved in the mutarotation of oxymethylenecamphor are reversible in character and may be represented by the following scheme:

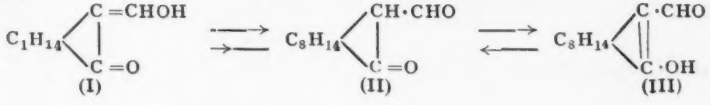

In benzene, which is found to be an enolising solvent in this case,[3] the mutarotation of oxymethylenecamphor may be represented by II → I or II → III. Since the curve log $k/\frac{1}{T}$ is a straight line (Fig. 1) only one of these two reactions takes place, unless the temperature coefficient of both is the same. If on the other hand, the observed reaction were a composite one made up of two concurrent reactions II → I and II → III, differently influenced by temperature, the plot of log k against $\frac{1}{T}$ would not have been a straight line.

The Structure of Oxymethylenecamphor and the Chemical Changes Involved in its Mutarotation

It follows from what has been said above that the mutarotation of oxymethylenecamphor must be represented by either of the two reactions II → I or II → III. Oxymethylenecamphor undergoes condensation with primary and secondary amines and the products of its condensation with a primary amine may be represented by any of the following formulæ IV, V and VI:

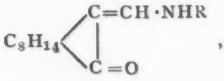

(IV)

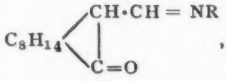

(V)

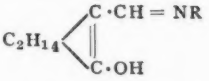

(VI)

Whereas oxymethylenecamphor gives with ferric chloride violet colouration, the above-mentioned products of condensation do not give any such colour reaction. This indicates absence of (OH) group in their formulæ, and, therefore, formula VI cannot represent them. They must be represented by formulæ IV and V. It may be concluded that oxymethylenecamphor reacts with aromatic primary amines in the ketonic form II and the enolic form I. The absence of the enolic form III of oxymethylenecamphor is indicated by the negative colour reaction of ferric chloride with the above-mentioned products of condensation (IV and V). The mutarotation of oxymethylenecamphor may, therefore, be indicated by the following reversible change:

Oxymethylenecamphor in solution is, therefore, an equilibrium mixture of the two isodynamic forms represented by I and II.

---

[3] Singh and Bhaduri, *loc. cit.*

Experimental

The solution was prepared by dissolving the given weight of oxymethylenecamphor in benzene, which had been previously kept in the thermostat at the required temperature. The thermostat was heated electrically and its temperature was controlled by means of a toluene regulator. The temperature was read with a Beckmann thermometer, which was correct to within $\frac{1}{50}$th of a degree centigrade. The rotatory power was determined in a 2-dcm. jacketted tube, through which water was circulated by means of an Albany pump from the thermostat. The polarimeter was of the Adam Hilger triple field type, which carried a D. V. spectroscope in the eyepiece. A vertical slit was used as a source of light at the polariser end, which was illuminated with a mercury arc.

The value of k, the velocity constant, is calculated from the monomolecular formula, $k = \frac{2 \cdot 303}{t_y - t_x} \cdot \log \frac{[\alpha]_x - [\alpha]_\infty}{[\alpha]_y - [\alpha]_\infty}$, the time being expressed in seconds.

TABLE I

Temperature 35° C. Concentration (g/100 c.c.) = 1·0008

Time in minutes	$[\alpha]_{Hg_{5461}}$	$k \times 10^{-4}$
5	186·8°	..
25	169·6	1·850
38	160·3	1·851
65	144·3	1·881
105	128·9	1·801
146	118·4	1·867
∞ (after 48 hours)	100·4	..
		Mean 1·850

TABLE II

Quantity of substance taken for drying = 30 *grams*
Duration of drying 48 *hours*

Temperature 25° C. Concentration (g/100 c.c.) = 1·000

Time in minutes	$[\alpha]_{Hg_{5461}}$	$k \times 10^{-4}$
6	167·8°	..
19	143·0	5·676
40	121·5	5·502
66	109·0	5·582
112	102·0	5·450
∞ (after 24 hours)	100·0	..
		Mean 5·552

TABLE III

Quantity of substance taken for drying about 30 *grams*
Duration of drying 96 *hours*

Temperature 25° C. Concentration (g/100 c.c.) = 1·000

Time in minutes	$[\alpha]_{Hg_{5461}}$	$k \times 10^{-4}$
0	175°	..
18	146	4·480
38	127	4·452
58	116	4·377
∞ (after 24 hours)	100	..
		Mean 4·436

TABLE IV

Quantity of substance taken for drying about 30 *grams*
Duration of drying 20 *days*

Temperature 25° C. Concentration (g/100 c.c.) = 1·0016

Time in minutes	$[\alpha]_{Hg_{5461}}$	$k \times 10^{-4}$
5	195·10°	..
27	187·70	0·982
52	174·72	0·951
80	164·73	0·990
115	154·25	1·005
155	145·01	0·970
∞ (after 48 hours)	109·8	..
		Mean 0·98

TABLE V

This is the same sample as that given in Table IV.

Temperature 45° C. Concentration (g/100 c.c.) = 1·000

Time in minutes	$[\alpha]_{Hg_{5461}}$	$k \times 10^{-4}$
0	196·5°	..
15½	169·5	3·484
30	151·0	3·492
44⅓	137·5	3·500
83′–21″	116·0	3·492
∞ (after 24 hours)	99·0	..
		Mean 3·492

TABLE VI

Quantity of substance taken for drying about 10 *grams*
Duration of drying 24 *hours*

Temperature 35° C. Concentration (g/100 c.c.) = 1·000

Time in minutes	$[\alpha]_{Hg_{5461}}$	$k \times 10^{-4}$
0	182·0°	..
19	152·0	3·991
34	137·5	3·630
54	127·0	2·734
∞ (after 48 hours)	100·0	..

TABLE VII

Quantity of substance kept for drying 10 *grams*
Duration of drying 72 *hours*

Temperature 35° C. Concentration (g/100 c.c.) = 1·000

Time in minutes	$[\alpha]_{Hg_{5461}}$	$k \times 10^{-4}$
0	185·0°	..
10	174·5	2·184
26	161·0	2·084
50	145·0	2·111
79	131·0	2·130
∞ (after 48 hours)	100·0	..
		Mean 2·127

TABLE VIII

Quantity of substance taken for drying 10 *grams*
Duration of drying 96 *hours*

Temperature 35° C. Concentration (g/100 c.c.) = 1·000

Time in minutes	$[\alpha]_{Hg_{5461}}$	$k \times 10^{-4}$
0	195·0°	..
21·5	175·0	1·842
40·0	161·0	1·872
51·0	154·0	1·861
84·0	137·5	1·861
110·0	128·0	1·899
∞ (after 48 hours)	100·5	..
		Mean 1·867

The initial time of reading, given in the tables, from the commencement of solution, was not the same, but varied in the different experiments. These experiments were completed in 1935–36 and further work with this compound and its *lævo* enantiomeride is in progress.

ON WARING'S PROBLEM $g(6) = 73$

By S. S. Pillai

Received January 3, 1940
(Communicated by Prof. B. S. Madhava Rao)

In the Conference of the Indian Mathematical Society held at Lucknow in 1938, I announced that I proved that $g(6) = 73$. But later on, I found a mistake and only after great deal of trouble I succeeded in proving the result. When I was about to write down the proof, by a curious and happy chance, I came across a paper by Van der Corput, with the help of which I can dispense with the major portion of an extensive table of R. C. Shook and a laborious calculation for $d_5(N)$ when log N is about 25000, which were essential for my first proof. Further, it can be shown that $g(5) \leqslant 41$ and $g(4) \leqslant 27$. The best known results about these functions are that $g(5) \leqslant 54$ and $g(4) \leqslant 35$, which are due to L. E. Dickson. But I postpone the proofs for these two results to another occasion.

Notations

k and s are fixed positive integers.

$$\nu = 1/k. \qquad \mathrm{E}\{x\} = e^x. \qquad \mathrm{P} = \mathrm{N}^{\nu}.$$

$$\mathrm{S}_{a,q} = \sum_{r=0}^{q-1} \mathrm{E}\{2\pi i a r^k/q\}.$$

$$\mathrm{A}_q(n) = \sum_a q^{-s}\, \mathrm{S}_{a,q}^s\, \mathrm{E}\{-2\pi i a n/q\},\ (a, q) = 1,\ a \leqslant q.$$

$$\mathfrak{S} = \mathfrak{S}(n) = \sum_{q=1}^{\infty} \mathrm{A}_q(n).$$

$$b_1(x) = x - [x] - \tfrac{1}{2};\ b_i(x+1) = b_i(x).$$

$$\int_0^x b_i(y)\, dy = b_{i+1}(x) - b_{i+1}(0).$$

$$\mathrm{T} = \mathrm{T}(\alpha) = \sum_{\mu=1}^{\mathrm{P}} \mathrm{E}\{2\pi i \mu^k \alpha\}.$$

$$\mathrm{S} = \mathrm{S}(\alpha) = \sum_u \mathrm{E}\{2\pi i u \alpha\},$$

where u runs through the integers $\leqslant \frac{1}{4}\mathrm{P}^k$, which can be expressed as the sum of at most l kth powers.

X = the number of u's $\leqslant P^k/4$.

$$I = I(\beta) = \int_0^P E\{2\pi i \beta v^k\}\, dv.$$

We divide the interval (0, 1) in the usual manner according to the Farey fractions a/q, where $1 \leqslant q \leqslant P^{k-\rho}$, $(a, q) = 1$, $1 \leqslant a \leqslant q$.

Further we divide the intervals into three classes M_1, M_2, M_3, where

(1) in M_1, $1 \leqslant q \leqslant M^k P^{k(1-\rho)}$

(2) in M_2, $M^k P^{k(1-\rho)} < q \leqslant P^\rho$

(3) in M_3, $P^\rho < q \leqslant P^{k-\rho}$,

where M is a number to be determined later.

In any case, the interval has the form

$$\alpha = \frac{a}{q} + \beta, \quad -\theta_1 q^{-1} P^{\rho-k} \leqslant \beta \leqslant \theta_2 q^{-1} P^{\rho-k},$$

$\frac{1}{2} \leqslant \theta_1 \leqslant 1$ and $\frac{1}{2} \leqslant \theta_2 \leqslant 1$.

$f(x) = \theta\{\psi(x)\}$ means that $|f(x)| \leqslant \psi(x)$.

$\phi = (1 - \nu)^l$; $K = 2^{k-1}$.

$$A = \frac{\Gamma^s(1 + \nu)}{\Gamma(s\nu)}; \quad A_1 = (2\pi k)^r; \quad L = M^k P^{k(1-\rho)}$$

$$Q = A \mathfrak{S} P^{s-k}/2^{sv-1}$$

$$U = U(\alpha) = |T^s - q^{-s} S^s_{a,q} I^s|.$$

$$t = \{(k-1)^i - 1\}/i.$$

$$H = \tfrac{1}{2}\{(P^\rho/6)^{1-1/i} \times (\log P + 1)^{-t}\}^{1/K}$$

$$d = (p - 1, k)$$

$$j = 1 + \frac{2}{\pi k} + \frac{2}{M}.$$

$$f = r(1 - \rho)$$

$c(n)$ means condition No. n.

Conditions

(1) $k \geqslant 4$; $s \geqslant 2k + 2$.

(2) $q \leqslant \dfrac{P^\rho \pi k \log 2}{r(r-1)(k-1)}$.

(3) $|b_l(x)| \leqslant 1$, for $1 \leqslant l \leqslant r$.

(4) $S_{a,\,q} = \theta(M\,q^{1-\nu})$.

(5) $P^{1-(r+k)(1-\rho)} \geqslant 9 . M^k/A_1$.

(6) $P^{f-\rho\nu} \geqslant A_1$.

(7) $P^f \geqslant 40\, sA_1\, 2^{s\nu}\,(k+1)\,(jM)^{s-1}/(A\mathfrak{Z})$.

(8) $P^{(s-2k)(1-\rho)} \geqslant 10\, kM^{2k}/\mathfrak{Z}$.

(9) $P^{\rho(s-k+s\nu-1)-(s-k)} \geqslant 10 \times 4^{s\nu}\, M^{s-k}/A$.

(10) $H^s\, P^{-k\phi} \geqslant 2^{s\nu+2}\, k^k/(A\mathfrak{Z})$.

(11) $P^{s(1-\rho)-k\phi} \geqslant 7^s \cdot 2^{s\nu} \cdot 20 \cdot k^k/(A\mathfrak{Z})$.

(12) $P^k > n \geqslant P^k/2$.

(13) $\mathfrak{Z} > 0$.

Up to the end of lemma (18), it is assumed that all these conditions are satisfied.

Preliminary Lemmas

Lemma 1. $\sum\limits_{\substack{m \\ a \leqslant m+t < b}} f(m+t) = \int\limits_a^b f(x)\,dx + \sum\limits_{l=0}^{r-1} \Big\{ f^l(b)\, b_{l+1}(t-b) - f^l(a)\, b_{l+1}(t-a) \Big\} - \int\limits_a^b f^r(x)\, b_r(t-x)\,dx.$

R (2)

Lemma 2. $1 + T(\alpha) = q^{-1} S_{a,\,q}\, I + \sum\limits_{l=0}^{r-1} \{\phi^l(P/q)\, a_l(P/q) - \phi^l(0)\, a_l(0)\} - R,$

where $\phi(x) = E\{2\pi i \beta x^k q^k\}$,

$$a_l(t) = \sum_{v=1}^{q} E\{2\pi i a v^k/q\}\, b_{l+1}(-t+v/q),$$

and $$R = \sum_{v=1}^{q} E\{2\pi i a v^k/q\} \int_0^{P/q} \phi^r(x)\, b_r(-x+v/q)\,dx.$$

This follows as in R (2) .....

Lemma 3. When $|x| \leqslant P/q$, and $q \leqslant \dfrac{P^\rho \pi k \log 2}{r(r-1)(k-1)}$,

$$|\phi^r(x)| \leqslant \sqrt{2} \cdot A_1 \cdot P^f.$$

Let $B = 2\pi k i \cdot \beta q^k$.

It is obvious that

$$\phi^r(x) = \phi(x)\,\{f_r(x)\},$$

where $f_r(x)$ is a polynomial of degree $r(k-1)$. Then

$$\phi^{r+1}(x) = \phi(x)\{f_r(x)\,\mathrm{B}\,x^{k-1} + f_r'(x)\}.$$

Let the sum of the modulii of the terms in $f_r(x) \leqslant \mathrm{F}_r$, when $|x| \leqslant \mathrm{P}/q$.
Then the sum of the modulii of the terms in

$$f_r'(x) \leqslant r(k-1)\,\mathrm{F}_r \cdot q/\mathrm{P} = \psi\,\mathrm{F}_r, \text{ where } \psi = r(k-1)\,q/\mathrm{P}.$$

Let $$\mathrm{F} = 2\pi k\,\mathrm{P}^{\rho-1}.$$

Then when $$|x| \leqslant \mathrm{P}/q,$$

$$|\mathrm{B}\,x^{k-1}| \leqslant 2\pi k q^k\, q^{-1}\,\mathrm{P}^{\rho-k}\,(\mathrm{P}/q)^{k-1} = \mathrm{F}.$$

$$|\mathrm{F}_1| \leqslant \mathrm{F}; \quad |\mathrm{F}_2| \leqslant \mathrm{F}^2 + \psi\,\mathrm{F} = \mathrm{F}(\mathrm{F}+\psi).$$

$$|\mathrm{F}_3| \leqslant \mathrm{F}^2(\mathrm{F}+\psi) + \mathrm{F}\,\psi\,(\mathrm{F}+\psi) = \mathrm{F}(\mathrm{F}+\psi)^2.$$

So by induction, $$|\mathrm{F}_r| \leqslant \mathrm{F}(\mathrm{F}+\psi)^{r-1}.$$

Hence $$|\phi^r(x)| \leqslant \mathrm{F}(\mathrm{F}+\psi)^{r-1} \leqslant \mathrm{F}^r(1+\psi/\mathrm{F})^{r-1} \leqslant \sqrt{2}.\mathrm{F}^r,$$

in virtue of C (2).

Lemma 4. $$\mathrm{T}(\alpha) = q^{-1}\mathrm{S}_{a,q}\,\mathrm{I} + \theta\{\sqrt{2}.\mathrm{A}_1\,\mathrm{P}^{1-f} + 4.5\,q\}.$$

When $r \geqslant 1$, $f_r(0) = 0$ and, for all r, $a_r(t) = \theta(q)$. So from lemmas (2) and (3),

$$|\mathrm{T}(\alpha) - q^{-1}\mathrm{S}_{a,q}\,\mathrm{I}| \leqslant 1 + q + q + \sqrt{2}.q \sum_{l=2}^{r-1} (2\pi k \mathrm{P}^{\rho-1})^l + \sqrt{2}\,(2\pi k \mathrm{P}^{\rho-1})^r\,\mathrm{P} + q\,(2\pi k)\,\mathrm{P}^{\rho-1}$$

$$= \theta(\sqrt{2}.\mathrm{A}_1\,\mathrm{P}^{1-f} + 4.5\,q\}, \text{ by C (7)}.$$

On M_1

$$1 \leqslant q \leqslant \mathrm{L}.$$

We assume that $r \geqslant 2$.

Lemma 5. $$\mathrm{I} = \theta\left(1 + \frac{2}{\pi k}\right)|\beta|^{-\nu}$$

In I, put $\beta v^k = y^k$.

Then $$\mathrm{I} = |\beta|^{-\nu} \int_0^{|\beta|^\nu \mathrm{P}} e^{\pm 2\pi i y^k}\,dy.$$

$$= |\beta|^{-\nu} \left\{\int_0^1 + \int_1^{|\beta|^\nu \mathrm{P}}\right\} e^{\pm 2\pi i y^k}\,dy.$$

$$= |\beta|^{-\nu} \left\{\theta(1) + \int_1^{|\beta|^\nu \mathrm{P}} e^{\pm 2\pi i y^k}\,dy\right\}, \text{ putting } y^k = x,$$

$$= |\beta|^{-\nu} \left\{\theta(1) + \nu \int_{1}^{|\beta| P^k} (e^{\pm 2\pi i x}/x^{1-\nu})\, dx\right\}.$$

$$= |\beta|^{-\nu} \left\{\theta(1) + \theta\left(\nu \times \frac{4}{2\pi}\right)\right\}, \text{ by the mean value theorem}$$

$$= \theta\left(1 + \frac{2}{\pi k}\right) |\beta|^{-\nu}.$$

Lemma 6. $\sum_{M_1} \int_{M_1} U\, d\alpha = \theta(Q/10)$.

From C (5), $4.5\, q \leqslant (2 - \sqrt{2})\, A_1 P^{1-f}$.

So from lemma (4),

$$T(\alpha) = q^{-1} S_{a,q} I + \theta(2 A_1 P^{1-f}). \tag{1}$$

From C (7), $2 A_1 P^{1-f} \leqslant 2 MPq^{-\nu}/(\pi k)$.

So $T(\alpha) = \theta(jM P q^{-\nu})$.

Again from C (6), $Mq^{-\nu} |\beta|^{-\nu} \geqslant M A_1 P^{1-f}$. (2)

Therefore, from lemmas (4) and (5),

$$T(\alpha) = \theta(M q^{-\nu} |\beta|^{-\nu}) \left(1 + \frac{2}{\pi k} + \frac{2}{M}\right) = \theta(jM q^{-\nu} |\beta|^{-\nu}). \tag{3}$$

From (2) and (3),

$U = \theta(A_1 P^{1-f}) (jMP)^{s-1} s q^{-\nu(s-1)}$, and

$U = \theta(A_1 P^{1-f}) (jM)^{s-1} s q^{-\nu(s-1)} |\beta|^{-\nu(s-1)}$.

So

$$\int_{M_1} U d\alpha = \theta(2) \left(\int_{0}^{P^{-k}} + \int_{P^{-k}}^{q^{-1} P\rho^{-k}}\right) |U|\, d\beta.$$

$$= \theta(2 A_1 P^{1-f})\, s\, (jM)^{s-1} q^{-\nu(s-1)} \{P^{s-1} \int_{0}^{P^{-k}} d\beta + \int_{P^{-k}}^{q^{-1} P\rho^{-k}} |\beta|^{-\nu(s-1)}\, d\beta\}.$$

$$= \theta(2 A_1 P^{s-k-f})\, s\, (jM)^{s-1} q^{-\nu(s-1)} \left\{1 + \frac{1}{\nu(s-1) - 1}\right\}$$

$$= \theta(4 s A_1 P^{s-k-f}) (jM)^{s-1} q^{-\nu(s-1)}$$

Hence $\sum_{M_1} \int_{M_1} U d\alpha = \theta(4 s A_1 P^{s-k-f}) (jM)^{s-1} \sum_{q \leqslant L} \frac{1}{q^{\nu(s-1)-1}}$

$$= \theta\{4 s A_1 P^{s-k-f} (jM)^{s-1} (k+1)\}$$

$$= \theta(Q/10), \text{ from C (7)}.$$

Lemma 7. If $B_1 = \sum_{M_1} q^{-s} S_{a,q}^{s} e^{-2\pi i n a/q}$,

then $\mathrm{B}_1 \geqslant 9\,\mathfrak{S}/10.$

$$\mathrm{B}_1 = \mathfrak{S} + \theta\{\sum_{q>\mathrm{L}} \mathrm{M}^s q^{1-\nu s}\}$$

$$= \mathfrak{S} + \theta(\mathrm{M}^s)\int_{\mathrm{L}}^{\infty} x^{1-\nu s}\,dx = \mathfrak{S} + \theta(\mathrm{M}^s)(k/\mathrm{L}^{s\nu-2})$$

$$= \mathfrak{S} + \theta(k\mathrm{M}^{2k}\,\mathrm{P}^{(\rho-1)(s-2k)}) = \mathfrak{S} + \theta(\mathfrak{S}/10), \text{ from C (8)}$$

$$\geqslant 9\,\mathfrak{S}/10.$$

Lemma 8. $\int_{-\infty}^{\infty} e^{-2\pi i n\beta}\,\mathrm{I}^s\,d\beta = \mathrm{A}.n^{s\nu-1}.$

(Landau, *M. Z.*, 31 : 1929.)

Lemma 9.

$$\int_{\mathrm{M}_1} e^{-2\pi i n\beta}\mathrm{I}^s\,d\beta \geqslant \tfrac{9}{10}\,\mathrm{A}\,\mathrm{P}^{s-k}/2^{s\nu-1}.$$

From lemma (5),

$$\int_{\beta \text{ not on } \mathrm{M}_1} \mathrm{I}^s\,d\beta = \theta(4)\int_{\frac{1}{2}q^{-1}\mathrm{P}^{\rho-k}} |\beta|^{-s\nu}\,d\beta = \theta\left\{\frac{4k}{s-k}\,(2^{-1}q^{-1}\,\mathrm{P}^{\rho-k})^{1-s\nu}\right\}$$

$$= \theta(2\cdot 2^{s\nu}\,\mathrm{P}^{s-k-\rho(s\nu-1)}\,q^{s\nu-1}) = \theta(\cdot 1\,\mathrm{A}\,\mathrm{P}^{s-k}\cdot 2^{1-s\nu}), \text{ from C (9).}$$

From this and lemma (8), the present one follows :

Lemma 10. If $\mathrm{B}_2 = \sum_{\mathrm{M}_1}\int_{\mathrm{M}_1} \mathrm{E}\{-2\pi i n\alpha\}\,\mathrm{T}^s\,d\alpha,$

then $\mathrm{B}_2 \geqslant 7\,\mathrm{Q}/10.$

$$\mathrm{B}_2 = \sum_{\mathrm{M}_1}\int_{\mathrm{M}_1} \{q^{-s}\,\mathrm{S}^s_{a,q}\,e^{-2\pi i n\alpha}\,\mathrm{I}^s + \theta(\mathrm{U})\}\,d\alpha$$

$$= \sum_{\mathrm{M}_1} q^{-s}\,\mathrm{S}^s_{a,q}\,e^{-2\pi i n a/q}\int_{\mathrm{M}_1} e^{-2\pi i n\beta}\,\mathrm{I}^s\,d\beta + \theta(\mathrm{Q}/10),$$

from lemma (6),

$$\geqslant \sum_{\mathrm{M}_1} q^{-s}\,\mathrm{S}^s_{a,q}\,e^{-2\pi i n a/q} \times \frac{9}{10}\,\mathrm{A}\,\mathrm{P}^{s-k}/2^{s\nu-1} + \theta(\mathrm{Q}/10),$$

from lemma (9),

$$\geqslant \frac{81}{100}\,\mathrm{Q} + \theta(\mathrm{Q}/10), \text{ from lemma (7).}$$

$$> 7\,\mathrm{Q}/10.$$

Lemma 11. If $\mathrm{B}_3 = \mathrm{R}\sum_{\mathrm{M}_1\,\mathrm{M}_1}\int e^{-2\pi i \mathrm{N}\alpha}\,\mathrm{T}^s\,S^2 d\alpha,$

then $B_3 > 7\,QX^2/10.$

$$B_3 = R \sum_{u_1 \leqslant P^k/4} \sum_{u_2 \leqslant P^k/4} \sum \int_{M_1} e^{-2\pi i (N-u_1-u_2)\alpha}\, T^s\, d\alpha$$

$\geqslant 7\,QX^2/10$, from lemma (10) and C (12).

$$\text{On } M_2 \qquad L < q \leqslant P^\rho.$$

Lemma 12. If $B_4 = \sum \int_{M_2} |T^s|\,|S^2|\,d\alpha,$

then $B_4 = \theta\,(7^s\,P^{\rho s}\,X).$

Put $r = 2$. Then C (2) is satisfied. So from lemma (4),

$$T(\alpha) = \theta\,\{M\,P\,q^{-\nu} + \sqrt{2}\,(2\pi k)^2\,P^{1-2(1-\rho)} + 4\cdot 5q\} \tag{4}$$

Since $q > L$, $MP\,q^{-\nu} \leqslant P^\rho$ (5)

From C (7), $\sqrt{2}\,(2\pi k)^2\,P^{1-2(1-\rho)} \leqslant \sqrt{2}\,.P^\rho$ (6)

From (4) to (6), when α is on M_2,

$$T(\alpha) = \theta\,\{P^\rho + \sqrt{2}\cdot P^\rho + 4\cdot 5\,P^\rho\} = \theta\,(7\cdot P^\rho)$$

Hence $B_4 \leqslant \underset{\text{on } M_2}{\text{Max.}}\,|T^s| \sum \int_{M_2} |S|^2\,d\alpha$

$$\leqslant \text{Max.}\,|T^s| \int_0^1 |S|^2\,d\alpha = \theta\,(7^s\,P^{\rho s}\,X).$$

$$\text{On } M_3 \qquad P^\rho < q \leqslant P^{k-\rho}.$$

Lemma 13. When $\alpha = \dfrac{a}{q} + \dfrac{\theta}{q^2}$, where $|\theta| \leqslant 1$,

$$|T(\alpha)/P|^K \leqslant 2^K\,[k\cdot P^{-1} + (\log P + 1)^t\,\{(2 + P^{-1}q)\,2\,(q^{-1} + P^{1-k})\}^{1-1/t}]$$

In Satz 265 (Landau's *Zahlentheorie*), it can be easily verified that $|S|^\kappa \leqslant 2^\kappa\,(k\cdot m^{\kappa-1} + m^{\kappa-k}\,\Sigma \text{ min.})$, where S stands for the sum given there.

The rest of the proof follows as in R (1).

Lemma 14. $T(\alpha) = \theta\,(P/H).$

$$\beta = \alpha - \frac{a}{q} = \theta\,(q^{-1}\,P^{\rho-k}) = \theta\,(q^{-2}\cdot q\cdot P^{\rho-k}) = \theta\,(q^{-2}).$$

So lemma (13) can be applied.

Hence $|T(\alpha)/P|^\kappa < 2^\kappa \left\{k\,P^{-1} + 2^{1-1/t}\,(\log P + 1)^t \left(\dfrac{2}{q} + \dfrac{2}{P^{k-1}} + \dfrac{1}{P} + \dfrac{q}{P^k}\right)^{1-1/t}\right\}$

$$\leqslant 2^\kappa\,(\log P + 1)^t\,(6\,P^{-\rho})^{1-1/t}$$

From this, the lemma follows.

Lemma 15. If $B_5 = \sum_{M_3} \int_{M_3} |T^s| \, |S^2| d\alpha,$

then $B_5 = \theta (P/H)^s X.$

From lemma (14),

$$B_5 \leqslant \underset{\text{on } M_3}{\text{Max.}} |T^s| \sum_{M_3} \int_{M_3} |S|^2 \, d\alpha$$

$$\leqslant \underset{\text{on } M_3}{\text{Max.}} |T^s| \int_0^1 |S|^2 \, d\alpha = \theta (P/H)^s X.$$

The Fundamental Lemma

Lemma 16. $X \geqslant P^{k-k\phi}/(4k^k).$

From a well-known result

$$X \geqslant (P^k/4)^{1-\phi}/k^k > P^{k-k\phi}/(4\, k^k).$$

Lemma 17. $\int_0^1 e^{-2\pi i N\alpha} T^s (\alpha) S^2 (\alpha) \, d\alpha > 0.$

From lemmas (12) and (16), and C (11),

$$B_4 = \theta (7^s P^{\rho s} X) = \theta (Q X^2/10) \tag{7}$$

From lemmas (15) and (16), and C (10),

$$B_5 = \theta (P/H)^s X = \theta (\tfrac{1}{2} QX^2) \tag{8}$$

So the real part of the Integral $= R \sum_{M} \int_{M} e^{-2\pi i N\alpha} T^s S^2 \, d\alpha$

[Here M stands for a typical subinterval but not the constant in C (4).]

$$= R \sum_{u_1 \leqslant N/4} \sum_{u_2 \leqslant N/4} \sum_{M} \int_{M} e^{-2\pi i (N-u_1-u_2)\alpha} T^s \, d\alpha$$

$$= X^2 R \sum_{M} \int_{M} e^{-2\pi i (N-u_1-u_2)\alpha} T^s \, d\alpha$$

$\geqslant \{7 QX^2/10 + \theta (QX^2/10) + \theta (\frac{1}{2} Q X^2)\}$, from (7), (8) and lemma (11),

$\geqslant QX^2/10 > 0$, from C (13).

Lemma 18. Every N satisfying all the conditions given, is the sum of at most $s + 2l$, kth powers.

This immediately follows from lemma (17).

Some More Lemmas

Lemma 19. $|A(p)| \leqslant (d-1)^s/p^{(s-1)/2}$ or $\leqslant (1-1/p)(d-1)^{s-1}/p^{(s-2)/2}$, according as $p \nmid n$ or $p \mid n$.

When $p \nmid n$, this follows from the proof of Satz 317 in Landau's *Zahlentheorie*.

When $p \mid n$, from the above,

$$A(p) = p^{-s} \sum_{r=1}^{p-1} \left(\sum_{\psi \neq \psi_0} \bar{\psi}(r) \tau_\psi \right)^s$$

$$= p^{-s} \sum_{\psi_1, \cdots, \psi_s,} \tau_{\psi_1} \cdot \cdots \cdot \tau_{\psi_s} \sum_{r=1}^{p-1} \bar{\psi}_1(r) \cdot \cdots \cdot \bar{\psi}_s(r).$$

Now $\psi_s(r) = e^{2\pi i m/d}$, $m = 1, 2, \cdots, (d-1)$.

So $\bar{\psi}_1(r) \cdot \cdots \cdot \bar{\psi}_s(r) = E\{2\pi i (m_1 + \cdots + m_s)/d\} = 1$,

when $m_1 + \cdots + m_s \equiv 0 \pmod{d}$, $1 \leqslant m \leqslant d-1$.

The number of solutions of the above congruence is $(d-1)^{s-1}$.

If $m_1 + \cdots + m_s \equiv h \pmod{d}$, where $h \neq 0$,

$$\sum \bar{\psi}_1(r) \cdots \bar{\psi}_s(r) = \sum_{h=1}^{p-1} E\{2\pi i h/d\} = 0.$$

Hence, $|A(p)| \leqslant p^{-s}(p-1) p^{s/2} (d-1)^{s-1} = \left(1 - \frac{1}{p}\right)(d-1)^{s-1}/p^{(s-2)/2}$

Lemma 20. $|S_{a,q}/q^{1-\nu}| \leqslant \Pi_1 \times \Pi_2 \times \Pi_3$,

where $\Pi_1 = \Pi p$, where $p \mid k$,

$\Pi_2 = \Pi p^\nu$, where $p \nmid k$, but $p \leqslant (d-1)^2$,

and $\Pi_3 = \Pi (d-1)/p^{\frac{1}{2}-\nu}$, where $p \nmid k$, $(d-1)^2 < p \leqslant (d-1)^{\frac{2k}{k-2}}$.

We know that, if $l = mk + n$, $1 \leqslant n \leqslant k$,

then $|S_{a,} p^l| \leqslant p^{mk(1-\nu)} |S_{a,} p^n|$

and if $p \nmid k$ and $2 \leqslant n \leqslant k$,

$$|S_{a,} p^n| = p^{n-1}.$$

From these, the lemma follows.

Lemma 21. $|b_l(x)| < 1$ when $1 \leqslant l \leqslant 10$

This can be verified by direct calculation following Satz 329 in Landau's *Zahlentheorie*.

Put $k = 6$, $s = 19$, $r = 10$, $\rho = 1 - \frac{g(6)}{20}$; $\log P \geqslant 400$. $l = 27$.

Lemma 22.

$$\mathfrak{S} \geqslant e^{-11}$$

To avoid lengthening the paper, I do not give the calculation here. Lemma (19) is used.

Lemma 23. $\quad A \geqslant e^{-2\cdot 4}$

Lemma 24. $\quad S_{a,q} = \theta\,(e^{5\cdot 3}\, q^{1-1/6})$

That is, $\quad M = e^{5\cdot 3}$

From lemma (20),

$$M \leqslant 6\,(7\cdot 13\cdot 19)^{1/6}\,(5)^{10}\,(31\cdot 37\cdot 43\cdot 61\cdot 67\cdot 73\cdot 79\cdot 97\cdot 103\cdot 109)^{-1/3} < e^{5\cdot 3}$$

C (5) $\quad 1-(r+k)(1-\rho) = 1-\frac{16}{200} = \frac{1}{5}$. So $P^{\frac{1}{5}} \geqslant e^{80} > 9\cdot M^6$.

C (6) $\quad 1-\rho-\dfrac{\rho}{rk} > \frac{1}{200} - \frac{1}{600} = \frac{1}{300}$

$$P^{1/30} > e^{10} > 2\pi k. \quad \text{Hence } P^{f-\rho\nu} > A_1$$

C (7) $\quad P^{1-\rho} > e^{20}$

and $\quad \{40\, s\, A_1\, 2^{s\nu}\,(k+1)\,(jM)^{s-1}/(A\,\mathfrak{S})\}^{1/\nu} < e^{18}$.

So C (7) is satisfied.

C (8) is obviously satisfied.

C (9) $\quad \rho\,(s-k+s\nu-1)-(s-k) > \rho\,(s-k+2)-(s-k)$

$$= 2 - \tfrac{1}{200}\,(s-k+2) = 2 - \tfrac{15}{200} > 1.$$

C (10) $\quad$ Put $i = 2$. Then $t = 12$.

$$H = \tfrac{1}{2}\,\{(P^{\rho}/_{6})^{\frac{1}{2}}\,(\log P+1)^{-12}\}^{1/32}$$

$$\geqslant \tfrac{1}{2} \times 6^{-1/64}\cdot P^{\frac{\rho}{64}-\frac{3}{8}}\,\log(\log P+1)/\log P.$$

$$\geqslant \tfrac{1}{2} \times 6^{-1/64}\, P^{\frac{1}{64}-\frac{1}{1280}-\frac{3}{8}\cdot\frac{6}{400}}$$

$$\tfrac{6\phi}{19} \leqslant \tfrac{1}{400}$$

Hence, $\quad H\,P^{-k\phi/s}$

$$\geqslant 2^{-1} \times 6^{-1/64}\, P^{43/6400} > 2^{-1}\; 6^{-1/64}\cdot e^{\cdot 43/16}$$

$$> e^{1\cdot 9661}$$

But $\quad 2^{\nu+2/s}\;[k^k/(A\,\mathfrak{S})]^{1/s} < e^{1\cdot 4626}$

So C (10) is also satisfied.

C (11) $\quad 1-\rho-k\,\phi/s \geqslant \frac{1}{200} - \frac{1}{400} = \frac{10}{400}$

So $\quad P^{1-\rho-k\phi/s} > e^{19}$.

But $7.2^{\nu}\{20.6^6/(A\ \mathfrak{S})\}^{1/19} < e^{19}$.

Hence C (11) is satisfied.

So all the conditions are satisfied. Therefore, we get from lemma (18),

Lemma 25. When $\log N > 2400$, every N is the sum of at most 73, 6th powers.

Lemma 26. Every one of the 537 numbers between 2,120,044 and 2,120,581, is the sum of at most 23, 6th powers.

This follows from Shook's table. R (4).

Lemma 27. Every number between 2,120,044 and 3,589,516 is the sum of 37, 6th powers.

This follows by applying Dickson's result [Lemma 6. R (3)] repeatedly to lemma (26).

Lemma 28. Every number between 2,120,044 and e^{2400} is the sum of 73, 6th powers.

This follows by applying Dickson's result (Lemma 7. R (3)) to lemma (27).

Lemma 29. Every number between 704 and 2,120,044 is the sum of 61, 6th powers.

Since $704 = 11 \times 2^6$, $728 = 704 + 24$ and $729 = 3^6$.

Every number between 704 and 763 is the sum of 35, 6th powers.

Applying to this interval Dickson's lemma mentioned in lemma (27) 26 times, we get the present lemma.

Lemma 30. Every number < 704 is the sum of 73, 7th powers.

This can be easily verified.

Lemma 31. 703 requires 73, 6th powers.

$$703 = 10 \times 2^6 + 63.$$

THEOREM I. $g(6) = 73$.

This follows from lemmas (25), (28), (29), (30) and (31).

REFERENCES

R (1) Van Der Corput .. "Un inegalite relative aux sommes de Weyl," *Proceedings of the Amsterdam Royal Society*, **42**, No. 6.

R (2) Eastermann .. "Proof that every positive integer is the sum of seventeen biquadrats," *Proceedings of the London Math. Society*, **41**, Part, 2.

R (3) S. S. Pillai "On Waring's Problem," *The Journal of the Indian Math. Society*, **2**, No. 1.

R (4) L. E. Dickson .. *The Bulletin of the American Mathematical Society*, 1933, pp. 701–27.

WARING'S PROBLEM WITH INDICES $\geqslant n$

By S. S. Pillai

Received April 25, 1940
(Communicated by Prof. B. S. Madhava Rao)

Introduction

Let $u = u_i$ be a number of the form x^m where $m \geqslant n$. $g_2(n)$ is the least value of s, such that the equation $N = u_1 + u_2 + \ldots + u_s$ is solvable for every N.

$$l = [(3/2)^n]\ ;\ 3^n = l \cdot 2^n + r = l \cdot 2^n + 2^n - t;\ k = [\log l/\log 2] \quad (1)$$

Then Mary Haberzetle* has proved that, if $r \leqslant 2^n - k - 3$, then $g_2(n) = 2^n + k - 1$ when $n \geqslant 9$; and verified that the above hypothesis holds good as far as 400.

The object of this note is to prove

Theorem: $g_2(n) = 2^n + k - 1$ for all $n \geqslant 32$.

In other words, Mary Haberzetle's result is proved without any hypothesis.

Further Notations

$$K = K(n) = 2^n + k - 1$$

U(M) is the least value of s, such that the equation $M = u_1 + u_2 + \ldots + u_s$ is solvable.

$\log \beta = 12 \cdot 5 \cdot n^{5\frac{1}{2}}$.

$$s = [\log \beta/\log 2] + 2 \quad (2)$$

$a = (2^n - s - 2n)/r$ and $F = al\,2^n$ when $r \leqslant 2^n - 2s - 4n$,

$a = [(2^n - s - 2n)/t]$ and $F = (al + a - 1)\,2^n$ otherwise. (3)

$h_j(n)$ is the sum of the digits when n is expressed in the scale of j.

From (1),

$$2^n - 1 \geqslant r \geqslant 1;\ 2^n - 1 \geqslant t \geqslant 1;\ 2^k \leqslant l \leqslant 2^{k+1} - 1 \quad (4)$$

We assume that

$$n \geqslant 6, \text{ and } 2^n \geqslant 4s + 8n \quad (5)$$

---

* *Duke Mathematical Journal*, 5, No. 1.

Lemmas

Lemma 1. $U(x \cdot j^n) \leqslant h_j(x)$

If $x = c_0 + c_1 \cdot j + \ldots + c_i \cdot j^{n+i}$, (6)

then $x \cdot j^n = c_0 \cdot j^n + c_1 \cdot j^{n+1} + \ldots + c_i \cdot j^{n+i}$.

Lemma 2. $h_j(x) \leqslant (j-1) \log x / \log j + j - 1$.

Lemma 3. $h_2(x) \leqslant [\log (x+1)/\log 2)]$.

Lemma 4. $h_3(a) \leqslant 2n$ and $h_2(F/2^n) \leqslant 2n$.

This follows from (3), (5) and lemma 2.

Lemma 5. (Mary Haberzetle). $U(2^{n+k} - 1) = K$.

Since $2^{n+k} - 1 \leqslant 2^n \cdot l - 1 < 3^n$,

$$2^{n+k} - 1 = 2^n + 2^{n+1} + \ldots + 2^{n+k-1} + (2^n - 1) \cdot 1^n$$

is the best representation.

In the above, there are K terms.

Lemma 6. If $M \leqslant 3^n$, $U(M) \leqslant K$.

$M = d \cdot 2^n + 2^n - i$, where $d \leqslant l$.

When $i = 0$, the result is obvious.

So we assume that $i \geqslant 1$.

(*i*) Let $d \leqslant l - 1$.

Then $U(M) \leqslant h_2(d) + 2^n - i \leqslant [\log (d+1)/\log 2] + 2^n - 1 \leqslant K$.

(*ii*) Let $d = l$.

$M = l \cdot 2^n + 2^n - i = 3^n + t - i$.

If $t \geqslant i$, $U(M) \leqslant 1 + t - i < 2^n$.

If $t < i$, $U(M) \leqslant h_2(l) + 2^n - i \leqslant k + 1 + 2^n - (t+1) \leqslant K$.

From (*i*) and (*ii*), the lemma follows.

Lemma 7. When $r \leqslant 2^n - 2s - 4n$ and $M \leqslant F - 1$, $U(M) \leqslant K$.

$M = (bl + d) 2^n + 2^n - i$, where $b \leqslant a - 1$ and $d \leqslant l - 1$ (7)

$= b \cdot 3^n + d \cdot 2^n + 2^n - i - br$.

Since the result is obvious when $i = 0$, we assume that $i \geqslant 1$.

(*i*) Let $i \geqslant 2n$.

Then $U(M) \leqslant h_2(bl + d) + 2^n - i$

$\leqslant [\log (bl + d + 1)/\log 2] + 2^n - i$, from lemma 3,

$\leqslant \log (al)/\log 2 + 2^n - i$, from (7),

$\leqslant \log (3^n)/\log 2 + 2^n - i \leqslant 2^n$.

(*ii*) Let $i < 2n$.

Then $i + br < i + ar < 2^n$.

So, from the second form for M,

$$\begin{aligned} U(M) &\leqslant b + h_2(d) + 2^n - i - br \leqslant [\log(d+1)/\log 2] + 2^n - i \\ &\qquad - b(r-1) \\ &\leqslant k + 2^n - i < K; \text{ for } d + 1 \leqslant l \leqslant 2^{k+1} - 1. \end{aligned}$$

From (*i*) and (*ii*), the lemma follows:

Lemma 8. When $n \geqslant 3$, $t \geqslant 2$.

If $3^n = (l+1)2^n - 1$, then $(l+1)2^n = 3^n + 1$.

But $3^n + 1$ is not a multiple of 8. So the lemma follows.

Lemma 9. When $r > 2^n - 2s - 4n$ and $3^n \leqslant M \leqslant F - 1$,

$U(M) \leqslant K$.

In this case, $M = b \cdot 3^n + d \cdot 2^n + 2^n - i$, where $1 \leqslant b \leqslant a - 1$; $d \leqslant l$. (8)

$$= (bl + b + d)2^n + 2^n - i - bt.$$

As before, we can assume that $i \geqslant 1$.

(*i*) Let $i \geqslant 2n + 2$.

Then, $U(M) < h_3(b) + h_2(d) + 2^n - i$

$\leqslant 2n + \log(d+1)/\log 2 + 2^n - i$, from lemmas 4, 3.

$\leqslant 2n + k + 1 + 2^n - i$, from (8), (4).

$\leqslant K$.

(*ii*) Let $i \leqslant 2n + 1$.

Then $i + bt < 2^n$.

So, from the second form for M,

$$\begin{aligned} U(M) &\leqslant h_2(bl + b + d) + 2^n - i - bt \\ &\leqslant [\log\{(b+1)(l+1)\}/\log 2] + 2^n - 1 - 2b, \\ &\qquad \text{from (8) and lemmas (3), (8).} \\ &\leqslant k + 1 + [\log(b+1)/\log 2] + 2^n - 1 - 2b \\ &= K - \{2b - [\log(b+1)/\log 2] - 1\} \\ &\leqslant K; \text{ for } b \geqslant 1. \end{aligned}$$

From (*i*) and (*ii*), the lemma follows :

Lemma 10. If $F \leqslant M \leqslant F + 2^n - 1$, then $U(M) \leqslant 2^n - s$

(*a*) Let $r \leqslant 2^n - 2s - 4n$. (9)

(*i*) $al \cdot 2^n \leqslant M \leqslant a \cdot 3^n - 1$.

Then $M = al \cdot 2^n + (M - al \cdot 2^n)$.

So, $U(M) \leqslant h_2(al) + M - al \cdot 2^n$

$\leqslant \log(al+1)/\log 2 + a \cdot 3^n - 1 - al \cdot 2^n$, from lemma 3,

$\leqslant \log(3^n)/\log 2 + ar - 1$, from (3), (1).

$\leqslant 2n + ar - 1$

$\leqslant 2^n - s$; from (3).

(*ii*) $a \cdot 3^n \leqslant M \leqslant (al+1) \cdot 2^n - 1$.

$M = a \cdot 3^n + (M - a \cdot 3^n)$.

So $U(M) \leqslant h_3(a) + M - a \cdot 3^n \leqslant h_3(a) + (al+1) \cdot 2^n - 1 - a \cdot 3^n$

$\leqslant 2n + 2^n - 1 - ar$, from lemma 4,

$\leqslant 2n + 2^n - r\{(2^n - s - 2n)/r - 1\}$, from (3),

$= s + 4n + r \leqslant 2^n - s$; from (9).

(*b*) Let $r > 2^n - 2s - 4n$, so that $t < 2s + 4n$ (10)

(*i*) $(al + a - 1) \cdot 2^n \leqslant M \leqslant a \cdot 3^n - 1$.

Then $U(M) \leqslant h_2(al + a - 1) + \{M - (al + a - 1) \cdot 2^n\}$

$\leqslant h_2(3^n) + a \cdot 3^n - (al + a - 1) \cdot 2^n - 1$

$\leqslant 2n + 2^n - at$, from (1)

$\leqslant 2n + 2^n - \left(\frac{2^n - s - 2n}{t} - 1\right) t$, from (3),

$= t + s + 4n \leqslant 3s + 8n$, from (10),

$\leqslant 2^n - s$; from (5).

(*ii*) $a.3^n \leqslant M \leqslant (al + a) \cdot 2^n$.

Then $U(M) \leqslant h_3(a) + M - a \cdot 3^n \leqslant h_3(a) + (al + a) \cdot 2^n - a \cdot 3^n$

$\leqslant 2n + at$ from lemma 4 and (1)

$\leqslant 2^n - s$; from (3).

From all these and the definition of F, the lemma follows.

Lemma 11. Every integer greater than β is the sum of at most $n^2 + 2 + [12n \log n]$, nth powers.

This follows from § 3·7 of my paper 'On Waring's Problem' in Vol. II, No. 1, of the *Journal of the Indian Mathematical Society*.

Lemma 12. When $n \geqslant 9$ and $M \geqslant \beta$, $U(M) \leqslant K$.

When $n \geqslant 9$, $n^2 + 2 + 12\,n \log n < 2^n$.

So the lemma follows from the previous one.

Proof of the Theorem

If $F \leqslant M \leqslant \beta$,

$M = x \cdot 2^n + y$, where $F \leqslant y \leqslant F + 2^n - 1$ and $x \leqslant \beta/2^n$. (11)

So $U(M) \leqslant U(x \cdot 2^n) + U(y)$

$\leqslant h_2(x) + 2^n - s$, from lemmas 1, 10.

$\leqslant \log x/\log 2 + 2^n - s + 1$

$\leqslant \log(\beta/2^n)/\log 2 + 2^n - s + 1$, from (11)

$\leqslant 2^n$; from (2). (12)

Further, when $n \geqslant 32$,

$$\log 2^n - \log(4s + 8n) \geqslant \log 2^n - \log(4 \log \beta/\log 2 + 4 + 8n)$$

$$\geqslant n \log 2 - \log(50 \cdot n^{5\frac{1}{8}} + 8 + 8n)$$

$$\geqslant 32 \log 2 - \log(50 \times 32^{5\frac{1}{8}} + 264) > 0.$$

So (5) is satisfied.

Hence from (12) and lemmas 6, 7, 9, 10, we get that, when $n \geqslant 32$, for every M, $U(M) \leqslant K$. (13)

From (13) and lemma 5, we get,

THEOREM. When $n \geqslant 32$, $g_2(n) = 2^n + k - 1$.

It may be noted that Dickson's lemma on ascent is not required to prove the above result.

STUDIES IN THE FRIEDEL-CRAFTS REACTION

Part V. The Action of Acetic Anhydride and Benzoyl Chloride on β-Methyl Resorcylate

By R. D. Desai and (Miss) K. S. Radha

(From the Department of Chemistry, St. Xavier's College, Bombay)

Received March 20, 1940

In Part IV of this series, it was shown by Desai and Ekhlas[1] that whereas orcinol and resacetophenone underwent simultaneous β- and γ-substitutions, β-methyl resorcylate gave the exclusive β-substitution. As these results were at variance with those of Shah and co-workers[2] who obtained exclusive γ-substitution during the Gattermann and Pechmann Reactions (using $AlCl_3$) with this substance, it was deemed highly necessary to study the action of acetic anhydride and benzoyl chloride on this ester in order to decide once for all whether γ-substitution was at all possible during the course of these reactions.

The action of one mol. of acetic anhydride gave exclusively methyl 2:4-dihydroxy-5-acetyl benzoate as reported before, unaccompanied by the detectable trace of the isomeric methyl 2:4-dihydroxy-3-acetyl benzoate. Excess of acetic anhydride gave methyl 2:4-dihydroxy-3:5-diacetyl benzoate (I) as the corresponding free acid gave, on decarboxylation, 2:4-diacetyl resorcinol (II). Incidentally this reaction provides a better method of preparing 2:4-diacetyl resorcinol in a state of purity, as compared with Baker's method.[3] Similarly one molecule of benzoyl chloride or benzoic anhydride gave methyl 2:4-dihydroxy-5-benzoyl benzoate (III) in an unsatisfactory yield, as it was impossible to avoid the formation of methyl 2:4-dihydroxy-3:5-dibenzoyl benzoate (IV) which was exclusively formed if two mols. of benzoyl chloride were taken. The constitution of (III) was proved by the fact that its acid gave 4-benzoyl-resorcinol, on decarboxylation. The ester (III) reacted readily with acetic anhydride giving methyl 2:4-dihydroxy-3-acetyl-5-benzoyl-benzoate (V). The free acid corresponding to (IV) gave on decarboxylation, 2:4-dibenzoyl resorcinol, prepared by Japp and Meldrum[4] by oxidising the condensation product of benzoin and resorcinol.

Thus we conclude from our results that γ-substitution is not possible in the case of the Friedel-Crafts Reaction between acid chlorides or anhydrides and methyl β-resorcylate. The possible explanation is that the

chelation between the hydroxyl and the carbomethoxy groups with the consequent fixation of the double bond between the carbon atoms to which these groups are attached, as assumed by Shah and Laiwalla (*loc. cit.*) is destroyed under the conditions employed. The absence of such a fixed double bond will not favour the γ-substitution of the acyl groups in the resorcinol nucleus. Moreover, as γ-substitution is partly possible in the case of resacetophenone during the course of this reaction according to Desai and Ekhlas (*loc. cit.*), it follows that the chelation between hydroxyl and acetyl groups is far more stable than between hydroxyl and carbomethoxy groups.

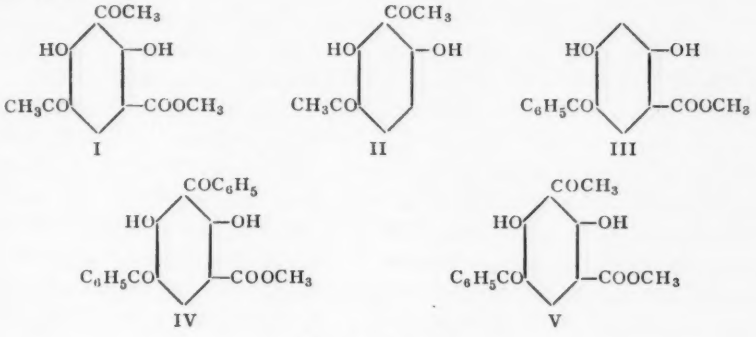

Experimental

Methyl 2 : 4-*dihydroxy*-5-*acetylbenzoate* was prepared in a better yield by a slight modification of Desai and Ekhlas' method. Anhydrous β-methylresorcylate (6·75 g.) was gradually added with cooling to the solution of anhydrous aluminium chloride (11 g.) in dry nitrobenzene (100 c.c.). Acetic anhydride (4·5 c.c.) was cautiously added to the cooled mixture, which was kept overnight and heated at 110° in an oil-bath for 6 hours. After decomposing the aluminium chloride with ice and hydrochloric acid, the nitrobenzene was removed in steam. The solid that separated out on cooling the mixture was filtered off, and the residue treated with a dilute sodium bicarbonate solution. On purification through alkali treatment, the crude solid melting at 106–110° was crystallised from hexane, when colourless needles, m.p. 124°, were obtained. The sodium bicarbonate soluble portion gave on acidification with hydrochloric acid an acid m.p. 256°. When esterified with methyl alcohol and concentrated sulphuric acid, it gave a *methyl ester* whose m.p. and mixed m.p. with the above ester was 124°. The alcoholic solution of the methyl ester as well as of the free acid gave a wine-red colouration with aqueous ferric chloride.

Methyl 2:4-*dihydroxy*-3:5-*diacetylbenzoate* (I).—This was obtained by the usual method either from β-methyl resorcylate and two mols. of acetic anhydride or from methyl 2:4-dihydroxy-5-acetyl-resorcylate and one mol. of acetic anhydride. After the usual pruification, it crystallised from dilute alcohol in colourless, lustrous needles, m.p. 113°. Its alcoholic solution gave intense red colouration with ferric chloride solution. (Found: C, 56·8; H, 4·7; $C_{12}H_{12}O_6$ requires C, 57·1; H, 4·8 per cent.)

2:4-*dihydroxy*-3:5-*diacetyl-benzoic acid* obtained by hydrolysing the above ester with 10 per cent. caustic soda solution crystallised from hot water in flat needles, m.p. 175°. (Found: C, 55·6; H, 4·2; $C_{11}H_{10}O_6$ requires C, 55·5; H, 4·2 per cent.) Its aqueous solution gave an intense red colouration with ferric chloride. It was easily soluble in alcohol, acetone, and acetic acid, but sparingly in benzene and almost insoluble in petrol. On heating its glacial acetic acid solution containing a few drops of hydrochloric acid in a sealed tube at 160-70° for 7–8 hours, it was converted into a product cystallising from alcohol in long needles, m.p. 95–96°, and identified as 2:4-diacetyl resorcinol (Baker, *loc. cit.*, gives m.p. 85–87°). The 4-*nitrophenylhydrazone of the acid* was prepared by heating the solution of 4-nitrophenylhydrazine (0·5 g.), and the acid (0·5 g.) in glacial acetic acid (15 c.c.) for 3 hours on a water-bath and crystallised from the same solvent in orange needles, m.p. above 280°. (Found: N, 10·8; $C_{17}H_{15}O_7N_3$ requires N, 11·3 per cent.)

The semicarbazone prepared in the usual manner was a microcrystalline solid sparingly soluble in alcohol; and did not melt upto 280°. (Found: N, 13·9; $C_{12}H_{13}O_6N_2$ requires N, 14·2 per cent.)

Methyl 2:4-*dihydroxy*-5-*benzoyl-benzoate* was obtained in the usual manner by using anhydrous β-methyl resorcylate (7·7 g.), benzoyl chloride (5·4 c.c.), anhydrous aluminium chloride (11 g.). The ester crystallised from methyl alcohol in fine, lustrous needles, m.p. 129–30°.

The 2:4-*dinitrophenyl hydrazone* of the ester crystallised in tiny orange-red needles which did not melt upto 270°. (Found: N, 12·1; $C_{12}H_{16}O_8N_4$ requires N, 12·4 per cent.)

The semicarbazone was a microcrystalline powder unmelted below 270°.

2:4-*dihydroxy*-5-*benzoyl-benzoic acid* obtained by hydrolysing the ester with caustic soda crystallised from benzene in needles, m.p. 232–33°. Its alcoholic solution gave an intense red colour with alcoholic ferric chloride. (Found: C, 65·4; H, 3·9; $C_{14}H_{10}O_5$ requires C, 65·1; H, 3·9 per cent.) When the acid was decarboxylated by heating in a sealed tube, 4-benzoyl resorcinol was obtained, and this was confirmed by comparison with an

authentic specimen. Methyl-2: 4-dihydroxy-5-benzoyl-benzoate, when condensed with acetic anhydride in the usual way gave *Methyl*-2: 4-*dihydroxy*-3-*acetyl*-5-*benzoyl-benzoate* which crystallised from dilute alcohol in needles, m.p. 126–27°.

The 2: 4-*dinitrophenylhydrazone of the ester* was an orange-red crystalline powder which did not melt upto 280–90°. (Found: N, 11·1; $C_{23}H_{18}O_9N_4$ requires N, 11·3 per cent.)

Methyl 2: 4-*dihydroxy*-3: 5-*dibenzoyl benzoate* was readily obtained from methyl β-resorcylate and two mols. of benzoyl chloride or benzoic anhydirde in the usual manner, and crystallised from alcohol in white needles, m.p. 119–20°.

2: 4-*dihydroxy*-3: 5-*dibenzoyl benzoic acid* obtained in the usual manner crystallised from dilute alcohol in fine needles, m.p. 235–36°. (Found: C, 66·4; H, 4·2; $C_{21}H_{14}O_6 + H_2O$ requires C, 66·3; H, 4·2 per cent.) Its alcoholic solution gave deep red colour with alcoholic ferric chloride solution. On decarboxylation, it gave 2: 4-dibenzoyl-resorcinol, m.p. 102°, identified by comparison with an authentic specimen.

The 2: 4-*dinitrophenylhydrazone of the acid* was a microcrystalline, orange-red powder which did not melt upto 280°. (Found: N, 10·1; $C_{27}H_{18}O_9N_4$ requires N, 10·3 per cent.)

The semicarbazone was a greyish powder unmelted below 290°.

In conclusion, we thank Prof. R. N. Bhagwat, M.A., B.Sc., the Director of the Laboratories, and Rev. G. Palacios, S.J., Ph.D., D.D., the Principal, for their kind interest and provision of the facilities.

Summary

The action of acetic anhydride as well as benzoyl chloride on methyl β-resorcylate gives only the β-substitution products. The probable cause of the absence of γ-substitution has been discussed.

REFERENCES

1. Desai and Ekhlas .. *Proc. Ind. Acad. Sci.*, (A), 1938, **8**, 194.
2. Shah and co-workers .. *J.*, 1938, **228**, 1828.
3. Baker .. *Ibid.*, 1934, 1684.
4. Japp and Meldrum .. *Ibid.*, 1899, **75**, 1035.

MEASUREMENT OF POINT DISCHARGE CURRENT DURING DISTURBED WEATHER AT COLABA

By M. W. Chiplonkar, M.Sc.

Received June 26, 1940
(Communicated by Dr. K. R. Ramanathan)

Introductory

In a former communication, some preliminary measurements of discharge currents from an elevated metal point made at Colaba during the post-monsoon months of 1936 were reported and discussed.[1] The discharging point used for the purpose did not have a sufficiently open exposure so that its effective height was much smaller than its actual height above ground. Moreover the currents passing through the galvanometer were only observed visually and noted down in quick succession with the corresponding times. The method is therefore not suitable for measurements extending over a long period and was therefore later modified.

In the present communication a recording arrangement is described and the results obtained with it during the period May to October 1938 are discussed.

Experimental Arrangement

Exposure of Discharging Point—

The mast carrying the discharging system was erected on open ground near the sea-shore in the observatory compound. It will be seen from the photograph that the exposure of the point discharger was satisfactory. There were no tall objects nearby, except an old Kelvin water dropper (out of use) and the low electrograph room (seen to the right in the photograph), which are 15 m. and 20 m. away respectively from the mast.

Discharging Systems—

(*a*) *Single Point.*—The discharging system used before was slightly modified in the new experiments. Instead of a fine wire at the end of a stout copper wire, used as a discharging point in the former experiments, the stout copper wire itself was now made pointed and nickel-plated over a length of $1\frac{1}{2}$ inches of this wire.

(*b*) *Multiple Point.*—In order to investigate the effect of increasing the number of points at the top of the discharging system, a multiple point,

shown in Fig. 2, was prepared. It consisted of four copper wires about 8" long, tapered and electroplated in the same manner as the single point discharger and mounted on a thick copper base as shown in the figure. Either the single or the multiple point discharger could at any time be easily screwed on the top of the discharging system.

Recording System—

The lead-covered insulated wire connecting the point discharger to the galvanometer was brought down along the mast and then taken over short wooden pegs to the electrograph room, in which the recording system was housed. The current passed through a Moll Galvanometer to the earth and the deflections were recorded photographically. This galvanometer was chosen particularly for its stability of zero. Even in those few cases when the zero had shifted no difficulty was encountered in making accurate measurements of the current.

A clockwork was used to move the photographic paper on which a single trace of the point discharge current was obtained. The run of the paper was 14 cms. per hour which was very accurately maintained throughout the period of observation. The width of the photographic paper was 8 cms. and sometimes the spot of light would go out of the paper. In order therefore to secure observations of the discharge current when it was high, the galvanometer was shunted with known resistances. The corresponding reductions in sensitivity of the galvanometer were once for all known. The range of sensitiveness so adjusted during these experiments was from $2 \cdot 88 \times 10^{-9}$ to $1 \cdot 6 \times 10^{-7}$ amp. per mm. deflection at a distance of one metre.

Electric Field Measurements—

The corresponding values of electric field were obtained from the records of the electrograph which is housed in the same room. The instrument has been in continuous run since 1930. The radio-active spiral of the collector projects out of the wall on the same side as the point discharge mast. During times of high potential gradient it is generally drawn in and the sensitiveness is reduced in definite known ratios, so that even high values are not lost. The usual run of the paper is only 1·5 cms. per hour, but occasionally during thunderstorms it was made to run more rapidly so that corresponding values of field and current could be obtained with greater accuracy.

Experimental Results—

The above arrangement was in use from May to October 1938 the period in which practically the whole rainfall of the year took place. Generally the

recording of the discharge current was started only when a thunderstorm, or a shower or dark clouds were seen coming towards the observatory. This naturally caused a great deal of saving in the photographic paper but it also entailed a loss of record on some occasions of high field. It was possible, however, with this plan to secure about 20 good records of point discharge current. Many of them were accompanied by rain. A few typical records are shown in Fig. 3. The corresponding traces of the field,

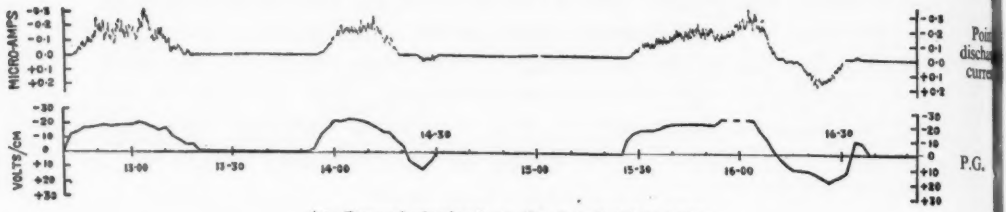

(*a*) Record obtained on the 1st October 1938

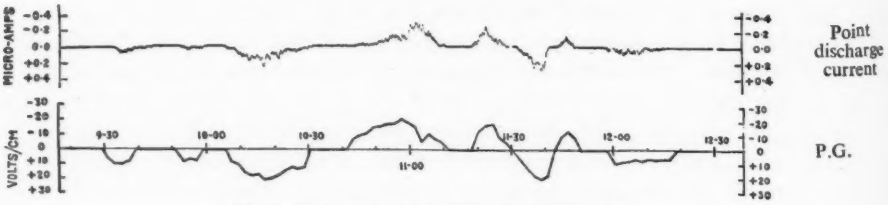

(*b*) Record obtained on the 7th August 1938

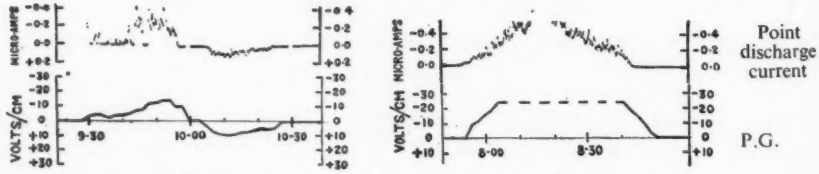

(*c*) Record obtained on the 24th June 1938

(*d*) Record obtained on the 7th August 1938

FIG. 3

obtained from the electrograph records, are also snown below each. Time (Bombay Mean Time) is marked along the abscissæ and current in micro-amperes and field in volts/cm. are marked along the ordinates. Most of the records show a great similarity in the behaviour of the two elements. Records (*a*) and (*c*) were obtained on 1st October 1938 and 24th June 1938 respectively, when the single point discharger was used; records (*b*) and (*d*) were obtained on 7th August 1938, with the multiple point discharger.

During the period of observation, apart from occasional large kicks due to neighbouring lightning flashes, the steady point discharge current averaged over an interval of two minutes, attained a maximum value of 1·75 micro amp. while the average steady field reached a value of 47·3 volts/cm.

Relation between the Current and Field—

In order to make a statistical comparison of the field and the corresponding current, values of both taken during periods when there were no rapid fluctuations of field and averaged over an interval of two minutes (and in the case of qucik run records, one minute) were plotted in Fig. 4. The points

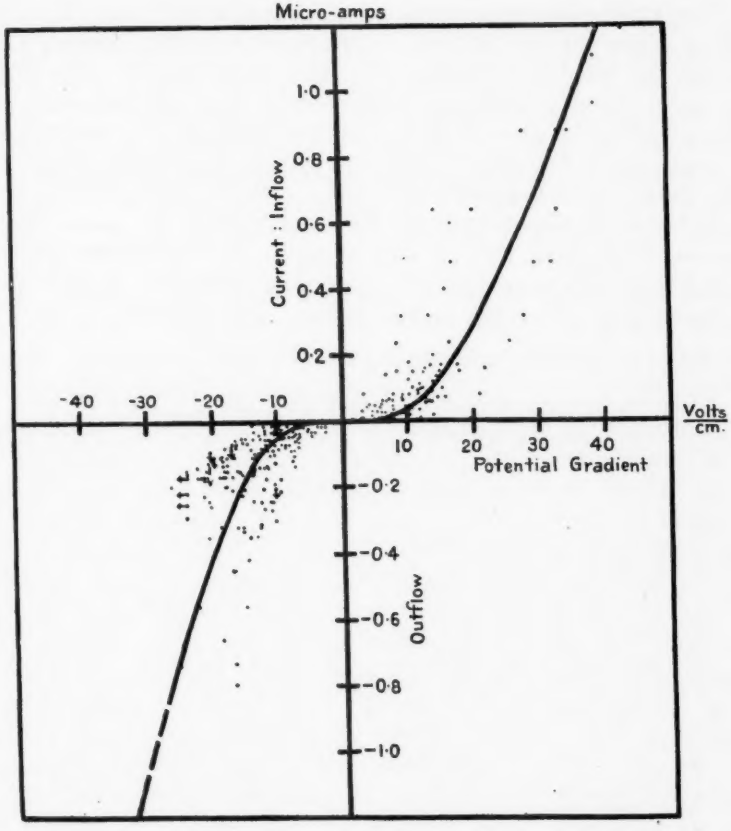

FIG. 4

marked by arrow-heads show that the point ought to be shifted in the direction of the arrow in order to get the exact position. Because the deflection in such cases was too large to be accommodated on the recording paper and so the value marked by the point represents only a lower limit to the actual one. There is a general scatter of points, but the mean curve drawn shows fairly well the relation between the field and the current. It will be noticed that there is a much larger number of points showing a negative field and a negative current than those showing + ve field and + ve current. This means that the discharge of positive electricity from the point into the air occurred more often than in the opposite direction. As a matter of fact, the two periods of discharge are in the ratio of 5 : 2.

The Colaba discharger consisted of a single point raised to a height of 8·3 m. above the ground level. The curve is nearly identical with that obtained by Whipple and Scrase[2] at Kew with a point at a height of 8·4 metres. Larger fields and currents were more often observed at Kew than at Colaba in spite of the equally good efficiency of the discharger at the latter place. The reason for this is perhaps to be found in the relatively lower cloud base in England than in India. This may also be expected from the fact that lightning flashes from the cloud base to the ground are more frequent in England than in this country. In Schonland's[3] experiments much higher fields were present but because of the less effective height of his discharging system only feeble currents were observed.

The Effect of Multiple Point discharger—

In order to investigate, as was mentioned earlier, the effect of a bunch of sharp points on the discharge current from a lightning rod, records were taken on some days with a multiple point discharger containing four points instead of one. From these records a similar diagram was prepared showing the mean current against the mean field over an interval of two minutes. This is shown as curve B in Fig. 5. A comparison of this curve with curve A in the same figure shows that for the same potential gradient at the ground, the total current passing through the multiple point discharger is markedly less than that passing through a single point. If the different points of a bunch effectively reduce the field at each point, the total effect may be to reduce the total number of ions brought to the bunch. A similar effect would occur to an even more pronounced degree in the case of Schonland's tree. The question therefore arises whether the actual discharge currents from trees under natural conditions can be calculated by taking them to be the same as those from metal points at the same height and requires further experiments for its answer.

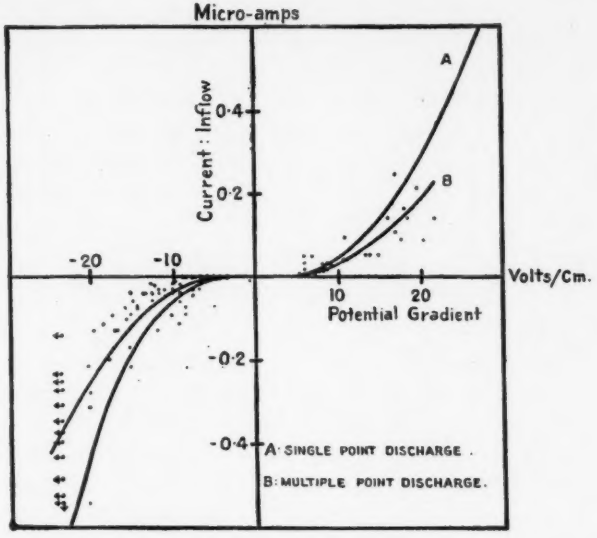

FIG. 5

Total Point Discharge—

The records of the point discharge current were next utilised to find the total amount of electric charge that passed through the point. During the 18 days on which there was direct observation, only on 5 days there was a nett transfer of positive charge into the earth, while on 13 days, positive charge was discharged to the air. The nett transfer of positive charge from the earth to the air as measured from these point discharge current records, all obtained during the period May to October 1938 was 10·4 millicoulombs (Table I). It was mentioned before that some occasions of high potential gradient were lost. In order to make an estimate of the total point discharge during those periods the curve of Fig. 4 was used and from the known potential gradients recorded by the electrograph, corresponding current values were read. These estimates are given separately in Table II. The sum of these two quantities represents the total point discharge for the whole year since there were no occasions of high field during the rest of the period (Table III). It is also interesting to notice that the months in which the largest point discharges took place were June and October—the months of setting in and withdrawal of the monsoon respectively.

TABLE I

Total point-discharge directly recorded at Colaba, Bombay, in 1938

Date	Duration hr.	Duration m.	Charge in millicoulombs		
			− Inflow	+ Outflow	+ Nett Outflow
June 6	1	38	0·355	0·238	− 0·117
13	0	37	0·002	0·098	+ 0·096
14	1	3	0·265	0·084	− 0·181
23	1	28	0·066	0·394	+ 0·328
24	0	41	0·060	0·185	+ 0·125
July 6	0	17	0·000	0·009	+ 0·009
9	0	23	0·000	0·017	+ 0·017
11	1	9	0·285	0·000	− 0·285
17	0	24	0·017	0·042	+ 0·025
23	0	18	0·042	0·078	+ 0·036
24	0	7	0·032	0·000	− 0·032
Aug. 7 .. .	3	36	0·271	1·494	+ 1·223
Sep. 14	3	31	1·024	1·544	+ ·0520
30	0	33	0·081	0·057	− 0·024
Oct. 1	3	5	0·107	1·149	+ 1·042
3	2	55	0·342	2·166	+ 1·824
5	4	16	0·000	2·563	+ 2·563
6	8	0	2·908	6·467	+ 3·559

TABLE II

Total point-discharge estimated from potential gradient records and current-potential gradient curve at Colaba (1938)

Month	Charge in millicoulombs		
	Inflow	Outflow	Nett Outflow
May	1·443	3·470	+ 2·027
June	1·789	7·646	+ 5·859
July	0·107	0·135	+ 0·028
August	0·088	1·041	+ 0·953
September	0·861	0·832	− 0·029
October	0·217	0·885	+ 0·668

TABLE III

Total Discharge of Electricity in each Month
Sum of Discharges tabulated in Tables I and II

Month	Charge in millicoulombs		
	Inflow	Outflow	Nett Outflow
May	1·443	3·470	+ 2·027
June	2·537	8·645	+ 6·126
July	0·483	0·251	− 0·232
August	0·359	2·535	+ 2·176
September ..	1·976	2·433	+ 0·457
October	3·573	13·230	+ 9·656
May–Oct.: Total ..	10·37	30·56	+ 20·19

Discussion

In fine weather, a positive potential gradient exists near the surface of the earth, which means that the surface of the earth is normally negatively charged. This causes a positive current to flow from the air to earth. The

mean magnitude of this current obtained by multiplying the potential gradient by the positive conductivity is about $1 \cdot 0 \times 10^{-16}$ amp./cm.^{2} C. T. R. Wilson suggested[4] that during disturbed weather and especially during thunderstorms owing to the existence of strong negative fields, the earth must be losing a large amount of positive charge through the sharp points on its surface such as tops of buildings, trees, mountain peaks, etc., and that this loss of positive electricity in disturbed weather is made up by the gain in normal weather and that is how the normal fine weather positive gradient at the earth's surface is maintained. Wormell[5] estimates that the point discharge current from an area of one square mile of ground near Cambridge is about 100 coulombs per year. Wormell's point discharge measurements showed a net outflow of 130 millicoulombs of positive electricity per year from a single point at a height of 4·8 metres, while the measurements of Whipple and Scrase at Kew gave the amounts as 60 millicoulombs. The point discharge estimated at Bombay is even smaller, being only 20 millicoulombs per year. The result is surprising, especially if Bombay results are taken as representing average conditions in the tropics, Bombay having neither an exceptionally large nor exceptionally small number of thunderstorms in a year. It may be pointed out that the average value of the potential gradient at Bombay during disturbed weather was smaller than those in higher latitudes and it is also possible that the greater density of discharge points in low latitudes may reduce the amount of discharge from each point.

The ratio of the total amount of positive charge flowing out of the point to that flowing into it under the influence of the high fields of thunder clouds gives statistically an idea of the electric fields of the overhead clouds. The values of this ratio as found at the three places: Cambridge, Kew and Colaba are 2·0, 1·7 and 2·9, respectively. The total quantity of electricity discharged by the point at Cambridge was about six times, and at Kew about three times that handled by the point at Colaba. But the ratios of the two quantitites outflow/inflow at the three places are very much less different. It shows that on the whole the field of the overhead clouds causing the point discharge at the earth's surface is two to three times as often $-$ve as $+$ve. The results are in agreement with those of Simpson and Scrase,[6] who found from their measurements of the signs of the electric fields inside clouds that the upper part of a thunderstorm was always positively charged and the main part of the base negatively charged.

The measurements described in this paper were carried out at the Colaba Observatory, Bombay, in 1938 and I am thankful to Dr. K. R. Ramanathan who was then in charge of the Observatory for giving me all facilities for the work.

FIG. 1

Point Discharger and its Surroundings

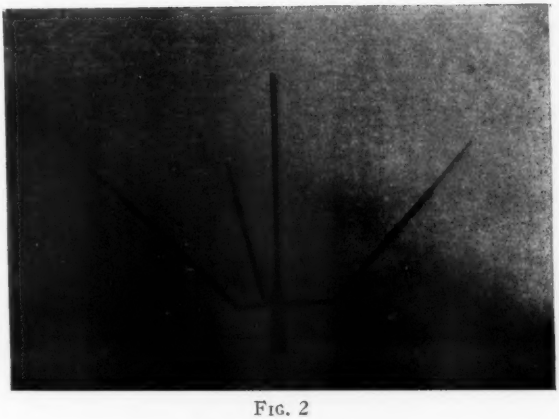

FIG. 2

Multiple Point Discharger

Summary

The paper describes the results of measurements of point discharge currents made at the Colaba Observatory, Bombay, in 1938. A discharging point was erected on a pole at a height of 8·3 metres above ground and connected to earth through a Moll galvanometer; the deflections of the galvanometer were recorded photographically on as many occasions of disturbed weather as possible. A current-potential gradient curve was prepared and on occasions when the current records were missed, the electric discharges through the point were estimated from this curve. The results show that during the year, there was an outflow of 30·6 millicoulombs of positive electricity from earth to air and an inflow of 10·4 millicoulombs from air to earth, giving a nett outflow of 20·2 millicoulombs and a ratio of outflow to inflow equal to 2·9.

Experiments made with a bunch of four points at the same height showed that the discharge through the bunch of points was markedly smaller than that through a single point at the same height.

REFERENCES

1. M. W. Chiplonkar .. *Jour. University of Bombay*, 1937, **6**, Pt. II, pp. 9–17.
2. F. J. W. Whipple and F. J. Scrase — *Met. Office, Geophys. Memoir*, 1936, No. 68.
3. B. F. J. Schonland .. *Proc. Roy. Soc.*, A, 1928, **118**, p. 252.
4. C. T. R. Wilson .. *Proc. Roy. Soc.*, A, 1916, **92**, p. 555; *Phil. Trans.*, A, 1921, **221**, p. 73.
5. T. W. Wormell .. *Phil. Trans.*, 1939, A, **238**, No. 791, p. 267; *Proc. Roy. Soc.*, 1930, **127**, 567.
6. G. C. Simpson and F. J. Scrase — *Ibid.*, A, 1937, **171**, 309.

ON THE ABSOLUTE WEIGHT OF AN INTEGER

By Hansraj Gupta

(From the Department of Mathematics, Government College, Hoshiarpur)

Received April 23, 1940

(Communicated by Dr. B. L. Bhatia)

1. The problem discussed in this paper, has already been considered by Rao[1] and Pillai[2]. I believe that my method of attack is more direct.

Let n be an integer such that

$$(a+1)^k > n \geqslant a^k ;$$

then $$n = a^k + n_1, \text{ where } n_1 \geqslant 0.$$

If $$(b+1)^k > n_1 \geqslant b^k ;$$

then $$n_1 = b^k + n_2, \text{ where } n_2 \geqslant 0 ;$$

so that $$n = a^k + b^k + n_2.$$

Proceeding in this manner, we obtain a unique expression for n as the sum of k-th powers of non-zero positive integers. If the number of k-th powers required to express n in this way be s, then we say that the absolute weight of n in terms of k-th powers is s. We express this relation by writing

$$\mathrm{A}b\,(n, k) = s, \text{ or simply } \mathrm{A}b\,(n) = s.$$

2. We proceed to obtain the form of n for which the absolute weight of n is greater than that of any and every integer less than n.

If N_j be any such integer, then the integer N_{j+1} next greater than N_j and such that

$$\mathrm{A}b\,(\mathrm{N}_{j+1}) = \mathrm{A}b\,(\mathrm{N}_j) + 1,$$

is given by the relation:

$$\mathrm{N}_{j+1} = \mathrm{N}_j + a_j^k, \tag{1}$$

where a_j is the least solution in integers of the inequality:

$$(x+1)^k - x^k > \mathrm{N}_j \tag{2}$$

Since $$k\,(x+1)^{k-1} > (x+1)^k - x^k \geqslant k\,(x+\tfrac{1}{2})^{k-1},$$

for all positive integral values of $k \geqslant 2$, the above inequality evidently holds if

$$x \geqslant (\mathrm{N}_j/k)^{\frac{1}{k-1}} - \tfrac{1}{2}; \tag{3}$$

the sign of equality being read only if $k \geqslant 3$.

Moreover the inequality (2) cannot hold if

$$x \leqslant (N_j/k)^{\frac{1}{k-1}} - 1. \tag{4}$$

Hence $a_j = [(N_j/k)^{\frac{1}{k-1}}]$ or $[(N_j/k)^{\frac{1}{k-1}} + \frac{1}{2}]$.

3. In what follows, we write h for $1/k$, g for $1/(k-1)$, u for $k/(k-1)$, and t_j for $(h\,N_j)^g$. We thus have

$$\begin{aligned} N_{j+1} &\geqslant N_j + (t_j - \tfrac{1}{2})^k \\ &\geqslant N_j + t_j^k - \tfrac{1}{2} N_j + \tfrac{1}{48} k(k-1)\, t_j^{k-3} (6\, t_j - k + 2) + \cdots \end{aligned}$$

If $t_j \geqslant (k-2)/6$, we get

$$N_{j+1} > t_j^k = (h\,N_j)^u. \tag{5}$$

Let N_0 be the least integer $< (2k)^k$ of which the absolute weight is not less than that of any other integer $< (2k)^k$.

Then $N_1 > (2k)^k$, and $t_j > t_1 > k$, $j \geqslant 1$.

Hence $$\begin{aligned} N_{j+1} &> h^u N_j^u > h^{u+u^2} N_{j-1}^{u^2} > \cdots \\ &> h^v N_1^{u^j}; \end{aligned}$$

where $v = u + u^2 + u^3 + \cdots + u^j = k(u^j - 1)$.

Therefore $$\begin{aligned} \log N_{j+1} &> u^j \log N_1 - v \log k, \\ &> u^j \log (2k)^k - v \log k; \end{aligned}$$

i.e., $$\begin{aligned} \log N_{j+1} &> u^j \log 2^k + k \log k, \\ &> u^j \log 2^k. \end{aligned}$$

Hence $\log \log N_{j+1} > j \log u + \log \log 2^k$,

so that $j \leqslant [(\log \log N_{j+1} - \log \log 2^k)/\log u]$. (6)

Again $N_{j+1} < (a_j + 1)^k < (t_j + 1\frac{1}{2})^k$

Now $(t_j + 1\frac{1}{2}) < N_j^g$, $k \geqslant 2$. (7)

Proof of (7).

(7) is true if $(h\,N_j)^g + \frac{3}{2} < N_j^g$,

i.e., if $N_j^g > \dfrac{3m}{2(m-1)}$, $m = k^g$.

Since $N_j > (2k)^k$, $j \geqslant 1$; (7) holds if

$$2k > \frac{3m}{2(m-1)} \quad \text{or} \quad m > \frac{4k}{4k-3}, \text{ i.e., } k > \left(\frac{4k}{4k-3}\right)^{k-1} \tag{8}$$

(8) is readily seen to hold when $k = 2$ or 3.

when $k > 3$, we have

$$\left(\frac{4k}{4k-3}\right)^{k-1} = \left(1-\frac{3}{4k}\right)^{-(k-1)} = 1+\frac{3(k-1)}{4k}+\frac{(k-1)k}{2}\left(\frac{3}{4k}\right)^2+\cdots$$

$$< 1+\tfrac{3}{4}+(\tfrac{3}{4})^2+\cdots < 4.$$

Hence (8) holds for all values of $k \geqslant 2$.

From (7) it now follows that

$$N_{j+1} < (N_j)^u < N_{j-1}^{u^2} < \cdots < N_0^{u^{j+1}} < (2k)^{ku^{j+1}}.$$

Hence $$\log N_{j+1} < u^{j+1} \log (2k)^k,$$

i.e., $$\log \log N_{j+1} < (j+1)\log u + \log \log (2k)^k;$$

whence $$j \geqslant [(\log \log N_{j+1} - \log \log (2k)^k)/\log u]. \tag{9}$$

From (6) and (9) we get

$$j = [(\log \log N_{j+1} - \log \log r^k)/\log u],\ 2 \leqslant r \leqslant 2k.$$

In my choice of N_0, I am mainly led by Pillai.

REFERENCES

1. *Jour. Indian Math. Soc.*, 1939, **3**, 262–65.
Rao's proof of his Theorem 1 is incorrect.
2. *Ibid.*, 1939, **3**, 266–67.

A NOTE ON GUPTA'S PREVIOUS PAPER

By S. S. Pillai

(From the Department of Mathematics, Annamalai University, Annamalainagar)

Received May 18, 1940

Let $S_k(x) = Ab(x, k)$*; $M(n) = \text{Max. } S_k(x)$ when $1 \leqslant x \leqslant n$; $\nu = 1/(k-1)$;

$$t = k\nu;\ K = 1/\log t;\ l_2 x = \log\log x.$$

Then Gupta's result implies that

$$\text{Max. } S_k(x) = K\{l_2 x - \log k\} + M(2^k k^k) + O(k l_2 k).$$

In this note, I refine Gupta's method to prove

Theorem I. $\text{Max. } S_k(x) = K\{l_2 x - l_2(2^{k-1} k^{k-1})\} + M(2^{k-1} \cdot k^{2k-1}) + O(1)$, where the constant in O is independent of k.

The same method can be applied to prove

Theorem II. $\text{Max. } S_k(x) = K\{l_2 x - \log k\} + M(2^k k^k) + O(k)$.

N_1 is the least integer $> 2^{k-1} k^{2k-1}$ such that $S_k(N_1) > S_k(N')$ for all $N' < N_1$; and N_{j+1} is the least integer for which $S_k(N_{j+1}) = S_k(N_j) + 1$, $j = 1, 2, 3, \cdots$.

$$h = 1/k;\ N_0 = N_1 h^k;\ f = 1/(h N_1)^\nu;$$

$$M_j = K\{l_2 N_{j+1} - l_2 N_0\};\ Y_j = M_j - K \cdot k \log k/(t^j \log N_0).$$

a_j is the least integral solution of the inequality $(x+1)^k - x^k > N_j$. (1)

$$b = b_j = (h N_j)^\nu;\quad P = N_j$$

$$d = d_j = t^j.$$

It may be convenient to remember that

$$N_j > N_{j-1} > \cdots > N_1 \geqslant 2^{k-1} k^{2k-1}.$$

Since $(b+\frac{1}{2})^k - (b-\frac{1}{2})^k = P + \cdots > P$,

and $b^k - (b-1)^k = P - + \cdots \leqslant P$,

$$b - 1 < a_j \leqslant b + \tfrac{1}{2} \tag{2}$$

From definitions, we get that

$$N_{j+1} = N_j + a_j^k \tag{3}$$

* Refer to Gupta's paper.

From (2) and (3),

$$N_{j+1} \geqslant (b-1)^k + N_j > b^k = h^t N_j^t > h^{t+t^2} N_{j-1}^{t^2} > \cdots > h^v \cdot N_1^d,$$

where $$v = t + t^2 + \cdots + t^j = k(d-1) \tag{4}$$

Hence $$N_{j+1} \geqslant N_0^d \cdot k^k$$

Again from (2), (3),

$$N_{j+1} \leqslant N_j + (b+\tfrac{1}{2})^k \leqslant (b+\tfrac{3}{2})^k = h^t N_j^t \{1 + \tfrac{3}{2}/(h N_j)^v\}^k$$
$$\leqslant h^t N_j^t (1 + \tfrac{3}{2} f)^k.$$

By applying the above repeatedly for $j = 1, 2, \ldots$, we get that

$$N_{j+1} \leqslant N_0^d k^k (1 + \tfrac{3}{2} f)^{k^{(k-1)(d-1)}}$$

So $$\log N_{j+1} \leqslant d \log N_0 + k \log k + k(k-1) d \times \tfrac{3}{2} f.$$

Hence $$j \geqslant Y_j - \tfrac{3}{2} k(k-1) f/(\log N_0 \log t). \tag{5}$$

Similarly from (4), $$j \leqslant Y_j. \tag{6}$$

Since $k(k-1) f/(\log N_0 \log t) < 1$, from (5), (6), we get

Lemma 1: $$j = [Y_j].$$

When $j \geqslant k \nu \log N_1$, $K\{k(k-1) \times \tfrac{3}{2} f + k \log k/t^j\}/\log N_0 < 1$;

and so $$M_j > j > M_j - 1.$$

Now j is an integer. Therefore, we get

Lemma 2: When $j \geqslant k \nu \log N_1$,

$$j = [M_j].$$

It is easy to veirfy that

$$K l_2 N_0 = K l_2 (2^{k-1} k^{k-1}) + O(1). \tag{7}$$

From (7) and lemma 2, theorem I follows.

ALTERATION OF TREMOLITE TO TALC IN THE DOLOMITE MARBLES OF YELLANDU WARANGAL DISTRICT (HYDERABAD, DN.)

By N. Jayaraman

(From the Department of Pure and Applied Chemistry, Indian Institute of Science, Bangalore)

Received March 12, 1940

(Communicated by Dr. K. R. Krishnaswami)

It was noticed while working on the tremolite specimens gathered from the Munditok (Yellandu) marble quarries that some of them had a higher silica and magnesia content and an unusually low calcium content. This led the author to suspect the presence of talc in the mineral most probably as an alteration product and it was indeed found to be so. The alteration of tremolite to talc seemed to be due to meteoric solutions, and to the atmosphere, because the alteration was found to be always a surface phenomenon. Generally speaking the alteration was noticeable only till a depth of about six feet. Instances of alteration at lower depths could be ascribed to the vicinity of yawning cracks in the marble. The gradual conversion of ferrous iron to the ferric state observed in the samples of the mineral in progressive stages of alteration also lends support to this view. Further, it was found that some of the larger altered samples had unaltered cores although their shells showed complete alteration.

Though the alteration of tremolite to talc was observed previously, the exact mechanism of alteration is still a matter of doubt. To get a clear picture of the process of alteration it is necessary to collect numerous data obtained from a systematic work on specimens of secondary talc derived from tremolite and also on the various intermediate products of alteration. With this idea in view the present work was undertaken and it is hoped that the results of this investigation would throw some light on this matter.

A microscopic examination of such samples of tremolite revealed the presence of large patches of talc which bore a pseudomorphic replacement relation to its tremolite host. A careful examination of the locality showed that there were numerous samples of almost pure talc derived from the alteration of tremolite. Specimens of tremolite which had been acted upon by meteoric solutions and by long exposure to atmosphere were found to be

completely altered to the fibrous variety of talc. Unexposed portions of tremolite were found to show no alteration. One large crystal which was completely altered to talc had a thickness of about nine inches and a length of about eighteen inches. Though the talc derived from the alteration of tremolite generally retained the original shape and size and was also rather rigid, this particularly large specimen showed signs of crushing and corrosion and was found to be very soft and somewhat pliable.

The material derived from the alteration of tremolite, *viz.*, the secondary talc, has the following properties : It has a pale-white to pale-green colour, a fibrous appearance and pearly lustre. The white variety seems to be more abundant than the greenish type. In this work only the white variety was studied in detail as the green coloured one was found to be admixed with serpentine and chlorite and so had a large alumina and iron content. Perhaps, the green variety of talc is derived mostly from the actinolite bands in the marble which provide iron, the alumina being taken up at the same time from the circulating underground meteoric solutions. The white variety has the characteristic soapy feel of talc and a hardness of about 1·5. The pure altered substance (talc) has a specific gravity of 2·7165 while the unaltered tremolite has a specific gravity of 2·9962. The mean index of refraction of the secondary talc is found to be 1·5743 while that of the unaltered tremolite from which it is derived is 1·6241. This altered end-product shows a stronger birefringence than the unaltered tremolite. This secondary talc was found to be insoluble in acids.

The intermediate products of alteration (Table I) excepting specimen No. 4, were found to be heterogeneous mixtures of the two end-members in varying proportions and their indices of refraction were found to be very variable. But they showed a gradual decrease in the value of their specific gravities from the tremolite end to the talc end. Specimen No. 4, though it showed the presence of a very few minute unaltered tremolite needles, is rather homogeneous and seems to denote a definite intermediate stage in the alteration of tremolite to talc. It has a specific gravity of 2·8261 and a mean refractive index of 1·6023. A similar intermediate product was noticed by Pelisek[1] while working on the alteration of tremolite to talc in a crystalline limestone at Petrov. Various other specimens collected from different quarries and having the same characteristics as specimen No. 4 showed approximately the same density and refractive index. Of all the intermediate products specimen No. 4 was the most definite and widespread. It is found to be more abundant than the final product of alteration and is always found wherever alteration has proceeded. As for the general physical

properties, its resemblance to the end-product of alteration is very striking. However, it differs from talc in still retaining to some extent the platy habit of tremolite. It shows incipient development of the fibrous texture of the secondary talc and the soapy feel also is well pronounced. Specimen No. 5 was found to be a mixture of specimens Nos. 4 and 6 the final product of alteration. This was deduced by a heavy-liquid separation of this specimen, *viz.*, No. 5, when two fractions were obtained one of which resembled specimen No. 4, in specific gravity and chemical composition, and the other which was the lighter fraction, resembled specimen No. 6.

Preparation of the Samples for Examination.—The specimens were initially obtained by picking from the crushed marble. They were then roughly powdered and carefully examined under a low-power microscope, and marble pieces, if present, were removed by picking. Part of this material was utilised for the specific gravity determination and the other part for the complete chemical analysis. Ferrous iron determination was made with a portion of the sample and the rest of the material was then treated with very dilute hot hydrochloric acid to remove traces of calcium carbonate derived from the marble. It was then washed well with distilled water and dried at 105° and then taken for analysis.

Method of Analysis.—As usual with other silicates, fusion with sodium carbonate was resorted to and silica, alumina, iron, magnesium and calcium were determined as usual. As fluorine was found to be present only in traces in specimen No. 1 no special precautions were taken for the estimation of silica. Ferrous iron was determined by heating the substance with a mixture of hydrofluoric and sulphuric acids in a platinum crucible in an atmosphere of carbon dioxide and steam and then taking the solution in a saturated solution of boric acid and titrating it against standard potassium permanganate. Water was determined by strong ignition of separate portions of the substance. Prolonged heating at about 900° was found to be necessary to drive off the water completely. The loss on ignition thus obtained gave the total water present in the tremolite. This water in the tremolite was found to be liberated in stages at three different temperatures, *viz.*, 300°, 650° and 900°.

Six specimens showing a gradual transition from almost pure tremolite (Specimen No. 1) to a definite end-product, *viz.*, the secondary talc (Specimen No. 6), were taken for chemical analysis, and the results obtained are given below in Table I.

TABLE I

Percentage Compositions of Various Specimens

Oxides	SPECIMENS*					
	1	2	3	4	5	6
SiO_2 ..	% 57·98	% 58·56	% 58·92	% 59·61	% 60·59	% 61·07
Al_2O_3 ..	0·16	0·38	0·55	1·85	2·23	2·42
Fe_2O_3 ..	0·11	0·52	0·63	1·07	1·32	1·49
FeO ..	1·12	0·98	0·78	0·36	nil	nil
MgO ..	24·39	25·53	26·97	27·82	28·69	29·13
CaO ..	13·92	10·71	9·26	5·63	2·48	0·75
F ..	Trace	..	..	..	..	..
H_2O ..	1·85	2·14	2·59	3·99	4·56	4·82
TOTAL ..	99·53	98·82	99·70	100·33	99·87	99·68
Sp. Gr. ..	2·9962	2·9407	2·9114	2·8261	2·7495	2·7165

* Specimens 1, 2, 4 and 6 were taken from pit No. 1 and specimens Nos. 3 and 5 were taken from pit No. 3 of the Munditok (Yellandu) marble quarry.

Table I shows that all the constituents of the original mineral (Specimen No. 1) undergo changes during the alteration process. All the other constituents excepting calcium and ferrous iron show a definite increase during alteration. The increase shown by silica is only apparent and not real, as can be gathered later (Table II). Calcium and ferrous iron decrease in quantity and while the latter is completely absent in the altered mineral calcium is present only in traces. The changes of the major constituents during the alteration of 100 grams of original substance, involved a loss of 13 grams, (out of about 14 grams originally present) of CaO while 3 grams of SiO_2, 5 grams of MgO and 3 grams of combined water were gained.

It is clear that there is no volume change in the alteration of tremolite to talc in these marbles. Because, the dolomite crystals surrounding the inclusions of tremolite both in specimens wherein the tremolite is fresh and in specimens wherein it is completely altered to talc, have similar optical properties. They show no strain effect and therefore indicate that the volume of the mineral did not increase or decrease during its alteration.

Further, it is found that the process of alteration effected the porosity of the mineral only very slightly.

So now it would be instructive to calculate the weights of the constituents involved in the alteration. By comparing the amounts of the various constituents in 100 c.c. of the fresh mineral with those in an equal volume of the completely altered mineral, the gains and losses involved during the alteration can be obtained. The results of such comparison are given in Table II.

TABLE II

Gains and losses in grams due to the alteration of 100 *c.c. of Tremolite to an equal volume of Talc*

Oxides	Tremolite g.	Secondary talc g.	Change in weight g.
SiO_2	173·8	165·9	− 7·9
Al_2O_3	0·5	6·6	+ 6·1
Fe_2O_3	0·3	4·0	+ 3·7
FeO	3·4	nil	− 3·4
MgO	73·1	79·1	+ 6·0
CaO	41·8	2·0	−39·8
H_2O	5·5	13·1	+ 7·6
TOTAL ..	298·4	270·7	−27·7

Table II shows that 39·8 grams of CaO, 3·4 grams of FeO and 7·9 grams of SiO_2 were lost, and 6·0 grams of MgO, 7·6 grams of combined water, 6·1 grams of Al_2O_3 and 3·7 grams of Fe_2O_3 were gained during the alteration of 100 c.c. of the mineral. Therefore, a total loss of 27·7 grams of matter results and the specific gravity falls from 2·9962 to 2·7165. This loss of 27·7 grams of matter, however, has not increased very much the porosity of the mineral.

The gradual change in chemical composition taking place during the alteration of fresh tremolite to secondary talc is shown graphically in Fig. 1 (relating to the percentage composition) and also in Fig. 2 (relating to the weights of the various constituents in 100 c.c. of the mineral during alteration).

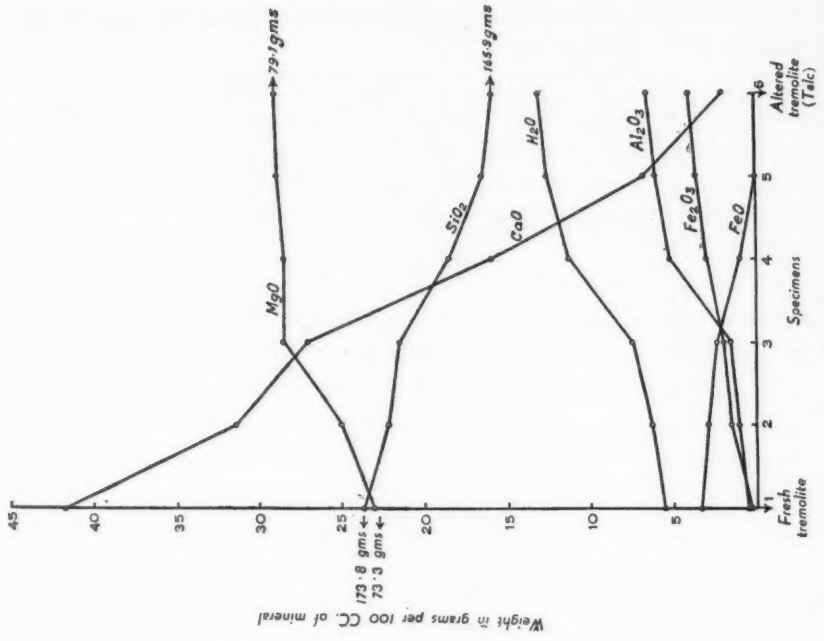
MgO
SiO2
CaO
H2O
Al2O3
Fe2O3
FeO
73·1gms
145·9gms
173·8 gms
73·3 gms
Weight in grams per 100 CC. of mineral
Fresh tremolite
Specimens
Altered tremolite (Talc)

FIG. 2

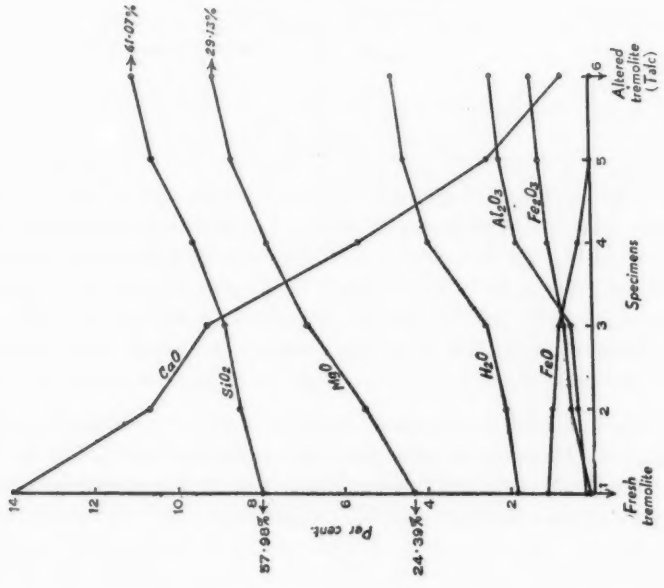
61·07%
29·13%
CaO
SiO2
MgO
H2O
Al2O3
Fe2O3
FeO
57·98%
24·39%
Per cent.
Fresh tremolite
Specimens
Altered tremolite (Talc)

FIG. 1

Fig. 1 indicates a definite increase in weight of silica while Fig. 2 shows a definite decrease. This anomaly is brought about by the lowered density of the altered mineral. As the volume of the mineral remains constant during its alteration, Fig. 2 represents more correctly the various stages of alteration.

Summary

1. Specimens of tremolite from the dolomite marbles of Yellandu showed variations in composition indicating that they have undergone alteration.

2. The end-product of alteration was identified to be talc.

3. Six different specimens in varying stages of alteration were examined and they revealed a gradual change in specific gravity and chemical composition.

4. A definite intermediate stage of alteration was confirmed by examination of some specimens.

5. It was established by chemical analysis that during the progress of alteration the following changes take place: (*a*) almost all the calcium is lost, (*b*) water of constitution and alumina accumulate and (*c*) ferrous iron gets fully oxidised.

6. It is suggested that meteoric solutions and atmospheric action were mainly responsible for the alteration of tremolite to talc.

7. The gains and losses of the various constituents when 100 c.c. of tremolite undergo alteration to an equal volume of talc can be calculated because no change in volume occurs during the alteration of the mineral. The results of such are tabulated in this paper.

In conclusion, the author wishes to express his indebtedness to Dr. K. R. Krishnaswami, D.Sc. (Lond.), F.I.C., for his keen interest and advice and also for much helpful criticism.

REFERENCE

1. Pelisek .. "Priroda", Brno, 1935, **28**, pp. 115.; *Mineralog. Abts.*, **6**, p. 510.

EXPLANATION OF FIGURES

FIG. 1.—Dolomite marble from Yellandu with the characteristic inclusions of tremolite blades—actual size.

FIG. 2.—Four specimens of tremolite in various stages of alteration—actual size.

(*a*) Original unaltered tremolite

(*b*) and (*c*) Intermediate products of alteration

(*d*) Final product of alteration—talc.

FIG. 3.—The dolomite marble with the definite intermediate product of alteration present as white streaks—$\frac{1}{2}$ natural size.

FIG. 4. The marble with the final product of alteration—the fibrous talc.—Actual size.

M–Marble, *Tc*–Talc.

MICROPHOTOGRAPHS

FIG. 5.—Unaltered tremolite in the dolomite marble.

M–Marble, *Tr*–Tremolite. × 30. Between + nicols.

FIG. 6.—The definite intermediate product of alteration.

I–Intermediate product, *Tr*–Tremolite. × 30. Between + nicols.

FIG. 7.—Shows the intermediate product of alteration and the secondary talc in addition to the original tremolite.

Tr–Tremolite, *I*–Intermediate product and *Tc*–Talc. × 30. Between + nicols.

FIG. 8.—Shows the final stage of alteration.

I–Intermediate product, *Tc*–Talc. × 30. Between + nicols.

Fig.1

Fig.2

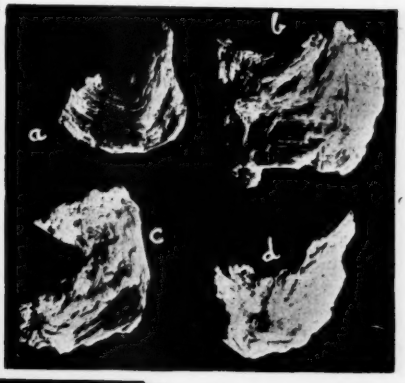

Fig.3

Fig.4

Fig.5

Fig.8

Fig.6

Fig.7

SOME RESULTS INVOLVING ANGELESCU'S POLYNOMIAL $\pi_n(x)$

By N. A. Shastri

(From the College of Science, Nagpur)

Received April 30, 1940

(Communicated by Prof. B. S. Madhava Rao)

In a recent paper[1] I have obtained some properties of the Angelescu's polynomial $\pi_n(x)$. This polynomial being of the type of Generalized Laguerre polynomial belongs to the family of confluent hypergeometric functions. It is to be anticipated, therefore, that some relations should exist between it and functions like Whittaker's function, Laguerre polynomial, Parabolic cylinder function, Bateman's k-function, Sonine's polynomial, etc. These relations have been established in this paper. Also some integrals involving Bessel functions and $\pi_n(x)$ are obtained. Finally a recurrence formula for $\pi_n(x)$ is given.

I. The operational representation of the polynomial $\pi_n(x)$ is given[1] by

$$\pi_n(0) - \pi_n(x) \doteqdot \sum_{r=0}^{n-1} \frac{n!}{r!}\, \pi_r(0)\, \frac{(p-1)^{n-r-1}}{p^{n-r}} \qquad (1\cdot1)$$

Therefore from theorems of operational calculus we get

$$e^{-x}[\pi_n(0) - \pi_n(x)] \doteqdot \sum_{r=0}^{n-1} \frac{n!}{r!}\, \pi_r(0)\, \frac{p^{n-r}}{(p+1)^{n-r+1}} \qquad (1\cdot2)$$

and

$$e^{-ax}[\pi_n(0) - \pi_n(ax)] \doteqdot \sum_{r=0}^{n-1} \frac{n!}{r!}\, \pi_r(0) \cdot \frac{p^{n-r}}{a^{n-r}\left(1+\frac{p}{a}\right)^{n-r+1}} \qquad (1\cdot3)$$

But

$$e^{-x} \doteqdot \frac{p}{p+1}. \qquad (1\cdot4)$$

Hence applying Parseval's theorem

$$\int_0^\infty \frac{h_1(x)\, f_2(x)}{x}\, dx = \int_0^\infty \frac{h_2(x)\, f_1(x)}{x}\, dx,$$

if $f_1(p) \doteqdot h_1(x)$ and $f_2(p) \doteqdot h_2(x)$,

to (1·3) and (1·4), we get

$$\int_0^\infty \frac{e^{-ax}}{1+x}\,[\pi_n(0)-\pi_n(ax)]\,dx = \sum_{r=0}^{n-1}\frac{n!}{r!}\pi_r(0)$$

$$\times \frac{1}{a^{n-r}}\int_0^\infty e^{-x}\,x^{n-r-1}\left(1+\frac{x}{a}\right)^{-n+r-1}dx.$$

$$= \sum_{r=0}^{n-1}\frac{n!}{r!}\,\Gamma(n-r)\,\pi_r(0)\,e^{\frac{1}{2}a}\,W_{-(n-r),-\frac{1}{2}}(a) \quad (1\cdot5)$$

using the integral[2]

$$W_{k,m}(z) = \frac{e^{-\frac{1}{2}z}\,z^k}{\Gamma(\frac{1}{2}-k+m)}\int_0^\infty e^{-t}\,t^{-k-\frac{1}{2}+m}\left(1+\frac{t}{z}\right)^{k-\frac{1}{2}+m}dt\,;\,R(k-\tfrac{1}{2}-m)\leqslant 0. \quad (1\cdot6)$$

If we take the result[3]

$$2^{s/2}\,\Gamma\left(\frac{s+1}{2}\right)\sqrt{p}\,e^{\frac{1}{2}p}\,D_{-s}(\sqrt{2p}) \doteqdot \frac{x^{\frac{1}{2}(s-1)}}{(1+x)^{s/2}}\quad R(s) > -1 \quad (1\cdot7)$$

with (1·2) and apply Parseval's theorem we obtain

$$\int_0^\infty \frac{e^{-\frac{x}{2}}}{\sqrt{x}}\,[\pi_n(0)-\pi_n(x)]\,D_{-s}(\sqrt{2x})\,dx.$$

$$= \sum_{r=0}^{n-1}\frac{n!}{r!}\,\frac{\pi_r(0)}{2^{s/2}\,\Gamma\left(\frac{s+1}{2}\right)}\cdot\int_0^\infty \frac{x^{n-r+\frac{1}{2}s-\frac{3}{2}}}{(1+x)^{n-r+\frac{s}{2}+1}}\,dx$$

$$= \sum_{r=0}^{n-1}\frac{n!\,\sqrt{\pi}\,\pi_r(0)\,\Gamma\left(n-r+\frac{s-1}{2}\right)}{r!\,2^{\frac{s+2}{2}}\,\Gamma\left(\frac{s+1}{2}\right)\Gamma\left(n-r+\frac{s}{2}+1\right)} \quad (1\cdot8)$$

II. We now apply the theorem:

$$p\,f(p) \doteqdot h'(x) \qquad \text{if } f(p) \doteqdot h(x) \text{ and } h(0)=0,$$

to (1·1) and we get

$$\pi_n'(x) \doteqdot -\sum_{r=0}^{n-1}\frac{n!}{r!}\,\pi_r(0)\left(\frac{p-1}{p}\right)^{n-r-1} \quad (2\cdot1)$$

$$= -\sum_{r=0}^{n-1}\frac{n!\,\pi_r(0)}{r!\,(n-r-1)!}\,L_{n-r-1}(x) \quad (2\cdot2)$$

after interpreting with the help of the result $L_n(x) \doteqdot n!\left(1-\frac{1}{p}\right)^n$. The equation (2·1) can be transformed into

$$e^{-x}\,\pi_n'(x) \doteqdot -\sum_{r=0}^{n-1}\frac{n!}{r!}\,\pi_r(0)\left(\frac{p}{p+1}\right)^{n-r} \quad (2\cdot3)$$

But $$e^{-ax} \doteqdot \frac{p}{p+a}.$$

Applying Parseval's theorem to these results we get

$$\int_0^\infty \frac{e^{-x}\,\pi_n'(x)}{x+a}\,dx = -\sum_{r=0}^{n-1} \frac{n!}{r!}\,\pi_r(0) \int_0^\infty e^{-ax}\,\frac{x^{n-r-1}}{(1+x)^{n-r}}\,dx.$$

$$= -\sum_{r=0}^{n-1} \frac{n!\,\pi_r(0)\,2^{n-r}\,\Gamma(n-r+\tfrac{1}{2})}{r!} \cdot \frac{e^{\frac{1}{2}a}}{\sqrt{a}} \cdot \mathrm{D}_{-2n+2r}(\sqrt{2a}) \tag{2·4}$$

using the integral

$$\int_0^\infty \frac{e^{-ax}\,x^{\frac{1}{2}(n-1)}}{(1+x)^{\frac{1}{2}n}}\,dx = 2^{\frac{n}{2}}\,\Gamma\left(\frac{n+1}{2}\right)\frac{e^{\frac{1}{2}a}}{\sqrt{a}}\,\mathrm{D}_{-n}(\sqrt{2a}).$$

III. We have[4]

$$e^{\frac{1}{2}x}\,\mathrm{D}_{2n+1}(\sqrt{2x}) \doteqdot \sqrt{\frac{\pi}{2}} \cdot \frac{(2n+1)!}{2^n\,n!} \cdot \frac{1}{\sqrt{p}}\left(\frac{1-p}{p}\right)^n \tag{3·1}$$

Therefore

$$\sum_{r=0}^{n-1} \frac{n!}{r!}\,\pi_r(0)\,\frac{2^{n-r-\frac{1}{2}}\,(n-r-1)!\,(-)^{n-r}}{\sqrt{\pi}\,(2n-2r-1)!}\,e^{\frac{1}{2}x}\,\mathrm{D}_{2n-2r-1}(\sqrt{2x})$$

$$\doteqdot \frac{1}{p}\sqrt{p}\sum_{r=0}^{n-1}(-)^{n-r}\frac{n!}{r!}\,\pi_r(0)\left(\frac{1-p}{p}\right)^{n-r-1}$$

We now apply the product theorem of the operational calculus remembering that

$$\sum_{r=0}^{n-1}(-)^{n-r}\frac{n!}{r!}\,\pi_r(0)\left(\frac{1-p}{p}\right)^{n-r-1} \doteqdot \pi_n'(x)$$

and

$$\sqrt{p} \doteqdot \frac{1}{\sqrt{\pi x}}.$$

and interpret the right-hand side as $\displaystyle\int_0^x \frac{\pi_n'(\xi)}{\sqrt{(x-\xi)\,\pi}}\,d\xi.$

Therefore

$$\int_0^x \frac{\pi_n'(\xi)}{\sqrt{x-\xi}}\,d\xi = \sum_{r=0}^{n-1}(-)^{n-r}\frac{n!}{r!}\,\pi_r(0)\left\{\frac{2^{n-r-\frac{1}{2}}(n-r-1)!}{(2n-2r-1)!}\right\}e^{\frac{1}{2}x}\,\mathrm{D}_{2n-2r-1}(\sqrt{2x})$$

$$\text{or} \quad = \sum_{r=0}^{n-1}(-)^{n-r}\frac{n!\,\sqrt{\pi}\,\pi_r(0)}{r!\,2^{n-r-\frac{1}{2}}\,\Gamma(n-r+\frac{1}{2})}\,e^{\frac{1}{2}x}\,\mathrm{D}_{2n-2r-1}(\sqrt{2x}) \tag{3·2}$$

using the duplication formula of the gamma functions. This gives a relation between the parabolic cylinder functions and the polynomial $\pi_n(x)$. In the previous paper another relation was obtained between these functions but it involved a double series. To get a result involving a generalized Laguerre polynomial we proceed as follows: we have

$$e^{-x}\, x^{\alpha}\, \mathrm{L}_{n-r-1}^{(\alpha)}(x) \doteqdot \frac{\Gamma(\alpha+n-r)}{\Gamma(n-r)}\, \frac{p^{n-r}}{(p+1)^{\alpha+n-r}} \quad \alpha > 1. \tag{3·3}$$

Hence

$$\sum_{r=0}^{n-1} \frac{n!}{r!}\, \pi_r(0)\, \frac{\Gamma(n-r)}{\Gamma(\alpha+n-r)}\, e^{-x}\, x^{\alpha}\, \mathrm{L}_{n-r-1}^{(\alpha)}(x)$$

$$\doteqdot \frac{1}{p} \cdot \frac{p}{(1+p)^{\alpha-1}} \sum_{r=0}^{n-1} \frac{n!}{r!}\, \pi_r(0)\, \frac{p^{n-r}}{(p+1)^{n-r+1}}$$

$$= \int_0^x \frac{e^{-(x-\xi)}\,(x-\xi)^{\alpha-2}\, e^{-\xi}\,[\pi_n(0)-\pi_n(\xi)]}{\Gamma(\alpha-1)}\, d\xi \quad \alpha > 1.$$

after interpreting the right-hand side by applying the product theorem to (1·2) and

$$e^{-x}\, x^{\alpha-2} \doteqdot \frac{p\,\Gamma(\alpha-1)}{(p+1)^{\alpha-1}} \quad \alpha > 1. \tag{3·4}$$

Hence

$$\int_0^x (x-\xi)^{\alpha-2}\,[\pi_n(0)-\pi_n(\xi)]\, d\xi = \sum_{r=0}^{n-1} \frac{n!}{r!}\, \frac{\Gamma(\alpha-1)\,\Gamma(n-r)}{\Gamma(\alpha+n-r)} \cdot \pi_r(0)\, x^{\alpha}\, \mathrm{L}_{n-r-1}^{(\alpha)}(x)$$

$$\alpha > 1. \tag{3·5}$$

We will now obtain the relation with the confluent hypergeometric functions of the type $\mathrm{N}_{k,m}(x)$ and $\mathrm{M}_{k,m}(x)$.

For this we have[5]

$$\mathrm{N}_{k,m}(x) \doteqdot \frac{p\,(p-\tfrac{1}{2})^{k-m-\frac{1}{2}}}{(p+\tfrac{1}{2})^{k+m+\frac{1}{2}}} \qquad m > -\tfrac{1}{2}.$$

Therefore

$$e^{\frac{1}{2}x}\, \mathrm{N}_{n-r-\frac{1}{2},m}(x) \doteqdot \frac{p\,(p-1)^{n-r-m-1}}{p^{n-r+m}} \tag{3·6}$$

Hence

$$-\sum_{r=0}^{n-1} \frac{n!}{r!}\, \pi_r(0)\, e^{\frac{1}{2}x}\, \mathrm{N}_{n-r-\frac{1}{2},m}(x) \doteqdot -\sum_{r=0}^{n-1} \frac{n!}{r!}\, \pi_r(0)\, \frac{p\,(p-1)^{n-r-m-1}}{p^{n-r+m}}$$

$$\doteqdot -\frac{1}{p} \cdot \frac{p\,(p-1)^{-m}}{p^{m}} \sum_{r=0}^{n-1} \frac{n!}{r!}\, \pi_r(0) \left(\frac{p-1}{p}\right)^{n-r-1}$$

$$= \int_0^x \pi_n'(\xi)\, e^{\frac{1}{2}(x-\xi)}\, \mathrm{N}_{0,m-\frac{1}{2}}(x-\xi)\, d\xi$$

after interpreting the right-hand side with the help of the product theorem as applied to (3·6) and (2·1). Hence

$$-\sum_{r=0}^{n-1}\frac{n!}{r!}\pi_r(0)\,\mathrm{N}_{n-r-\frac{1}{2},m}(x)=\int_0^x e^{-\frac{1}{2}\xi}\pi_n'(\xi)\,\mathrm{N}_{0,m-\frac{1}{2}}(x-\xi)\,d\xi \qquad (3\cdot7)$$

From this we get the corresponding result involving $\mathrm{M}_{k,m}$ functions if we use the relation $\dfrac{x^{m-\frac{1}{2}}\mathrm{M}_{k,m}(x)}{\Gamma(2m+1)}=\mathrm{N}_{k,m}(x)$

$$-\frac{1}{2m}\sum_{r=0}^{n-1}\frac{n!}{r!}\pi_r(0)\,x^{m-\frac{1}{2}}\mathrm{M}_{n-r-\frac{1}{2},m}(x)=\int_0^x e^{-\frac{1}{2}\xi}\pi_n'(\xi)\times$$

$$\times(x-\xi)^{m-1}\mathrm{M}_{0,m-\frac{1}{2}}(x-\xi)\,d\xi \qquad (3\cdot8)$$

But[5]

$$\mathrm{M}_{0,m}(x)=2^{2m}e^{-\frac{m\pi i}{2}}\Gamma(m+1)\sqrt{x}\,\mathrm{J}_m\left(\frac{x}{2}e^{\frac{\pi}{2}i}\right)=2^{2m}\Gamma(m+1)\sqrt{x}\,\mathrm{I}_m\left(\frac{x}{2}\right)$$

if m is a + ve integer.

Hence

$$\int_0^x e^{-\frac{1}{2}\xi}\pi_n'(\xi)(x-\xi)^{m-\frac{1}{2}}\mathrm{I}_{m-\frac{1}{2}}\left(\frac{x-\xi}{2}\right)d\xi.$$

$$=-\frac{1}{m\,2^{2m}\,\Gamma(m+\frac{1}{2})}\sum_{r=0}^{n-1}\frac{n!}{r!}\pi_r(0)\,x^{m-\frac{1}{2}}\mathrm{M}_{n-r-\frac{1}{2},m}(x) \qquad (3\cdot9)$$

if $m-\frac{1}{2}$ is a positive integer.

The relation involving Bateman's k-function has already been obtained in the previous paper while that involving Sonine's polynomial can be derived from (3·5) by the help of

$$\mathrm{L}^{(n)}{}_s(x)=(-)^s(s+n)!\,\mathrm{T}_n{}^s(x).$$

IV. We now proceed to evaluate the integrals involving $\pi_n(x)$ and Bessel functions. From the definition of the operational representation

$$\pi_n(0)-\pi_n(x)\doteqdot\sum_{r=0}^{n-1}\frac{n!}{r!}\pi_r(0)\frac{(p-1)^{n-r-1}}{p^{n-r}}$$

it follows that

$$\int_0^\infty e^{-ps}[\pi_n(0)-\pi_n(s)]\,ds=\sum_{r=0}^{n-1}\frac{n!}{r!}\pi_r(0)\frac{(p-1)^{n-r-1}}{p^{n-r+1}}.$$

In this write $\beta+\dfrac{1}{p}$ for p throughout and multiply by $p^{-\nu}$, $\mathrm{R}(\nu)>-1$ and interpret the expression $e^{-\frac{s}{p}}p^{-\nu}$ occurring under the integral sign on

the left-hand side by

$$e^{-\frac{s}{p}} p^{-\nu} \doteqdot \left(\frac{x}{s}\right)^{\frac{\nu}{2}} J_\nu (2\sqrt{sx}). \qquad R(\nu) > -1$$

we get after a little simplification on the right-hand side

$$\int_0^\infty e^{-\beta s} \left(\frac{x}{s}\right)^{\frac{\nu}{2}} J_\nu (2\sqrt{sx}) [\pi_n(0) - \pi_n(s)]\, ds$$

$$\doteqdot \sum_{r=0}^{n-1} \frac{n!}{r!} \frac{\pi_r(0)\,[(\beta-1)p+1]^{n-r-1}}{(\beta p+1)^{n-r+1}\, p^{\nu-2}} \qquad R(\nu) > -1. \tag{4·1}$$

Four cases can be considered (*a*) β and ν can take general values; (*b*) β can take general value while ν is constant say unity; (*c*) β is constant while ν has a general value; (*d*) both β and ν have particular values. We will take the first case and suppose that $f(x)$ is the function of which the expression under the summation sign on the right-hand side is the operational representation. Therefore

$$e^{-\frac{x}{1-\beta}} f(x) \doteqdot \frac{n!}{r!} \pi_r(0) \frac{p\left[(\beta-1)\left(p+\frac{1}{1-\beta}\right)+1\right]^{n-r-1}}{\left(p+\frac{1}{1-\beta}\right)^{\nu-1}\left[\beta\left(p+\frac{1}{1-\beta}\right)+1\right]^{n-r+1}}$$

$$\doteqdot \frac{n!}{r!} \frac{\pi_r(0)\,(-)^{n-r-1}}{[\beta(1-\beta)]^{1-\nu}} \cdot \left(\frac{1-\beta}{\beta}\right)^{n-r} \frac{[p\beta(1-\beta)]^{n-r}}{[p\beta(1-\beta)+1]^{n+\nu-r}} \times$$

$$\times \left[1 - \frac{1-\beta}{p\beta(1-\beta)+1}\right]^{1-\nu}. \tag{4·2}$$

The right-hand side can be expanded and interpreted with the help of the relation

$$e^{-\frac{x}{\beta(1-\beta)}} \left(\frac{x}{\beta(1-\beta)}\right)^{\nu} L_n^{(\nu)}\left(\frac{x}{\beta(1-\beta)}\right) \doteqdot \frac{\Gamma(n+\nu+1)}{n!} \times$$

$$\times \frac{[p\beta(1-\beta)]^{n+1}}{[p\beta(1-\beta)+1]^{n+\nu+1}} \tag{4·3}$$

Therefore the value of the integral can be expressed as a double series containing in its general term an expression of the form

$$e^{-\frac{x}{\beta}} \left(\frac{x}{\beta(1-\beta)}\right)^{\nu} L_n^{(\nu)}\left(\frac{x}{\beta(1-\beta)}\right).$$

This will be the case when β and ν are taken in the most general form subject to the condition that the operational representations have meaning and the integral remains convergent. This case being of a complicated nature is

excluded from consideration. We will next take the case when β is positive and general while ν is equal to one. Then (4·1) changes into

$$\int_0^\infty e^{-\beta s}\left(\frac{x}{s}\right)^{\frac{1}{2}} J_1(2\sqrt{sx})\,[\pi_n(0)-\pi_n(s)]\,ds \doteqdot \sum_{r=0}^{n-1}\frac{n!}{r!}\frac{\pi_r(0)\,[(\beta-1)p+1]^{n-r-1}}{(\beta p+1)^{n-r+1}}p$$

In this case, for the interpretation of the right-hand side with the same assumption as before we have

$$e^{-\frac{x}{1-\beta}} f(x) \doteqdot \frac{n!}{r!}\pi_r(0)(-)^{n-r-1}\left(\frac{1-\beta}{\beta}\right)^{n-r}\frac{[p\,\beta(1-\beta)]^{n-r}}{[p\,\beta(1-\beta)+1]^{n+1-r}}$$

$$=\frac{n!\,\pi_r(0)}{r!\,n-r}(-)^{n-r-1}\left(\frac{1-\beta}{\beta}\right)^{n-r}e^{-\frac{x}{\beta(1-\beta)}}\left(\frac{x}{\beta(1-\beta)}\right)L_{n-r-1}^{(1)}\left(\frac{x}{\beta(1-\beta)}\right)$$

Therefore

$$f(x)=\frac{n!\,\pi_r(0)}{r!\,(n-r)}\,\frac{(\beta-1)^{n-r-1}}{\beta^{n-r+1}}\,e^{-\frac{x}{\beta}}\,x\,L_{n-r-1}^{(1)}\left(\frac{x}{\beta(1-\beta)}\right).$$

Hence we get

$$\int_0^\infty e^{-\beta s}\left(\frac{x}{s}\right)^{\frac{1}{2}} J_1(2\sqrt{sx})\,[\pi_n(0)-\pi_n(s)]\,ds.$$

$$=\sum_{r=0}^{n-1}\frac{n!}{r!}\,\frac{\pi_r(0)}{(n-r)}\cdot\frac{(\beta-1)^{n-r-1}}{\beta^{n-r+1}}\cdot e^{-\frac{x}{\beta}}\,x\,L_{n-r-1}^{(1)}\left(\frac{x}{\beta(1-\beta)}\right) \tag{4·4}$$

$$=\sum_{r=0}^{n-1}\frac{n!}{r!}\left(\frac{1-\beta}{\beta}\right)^{n-r}\pi_r(o)\exp\left[\tfrac{1}{2}x\left(\frac{1}{1-\beta}-\frac{1}{\beta}\right)\right]k_{2n-2r}\left(\frac{x}{2\beta(1-\beta)}\right) \tag{4·5}$$

using the result

$$x\,L_n^{(1)}(x)=(-)^n(n+1)\,e^{\frac{x}{2}}\,k_{2n+2}\left(\frac{x}{2}\right)$$

where k_n is a Bateman function. This gives us the operational representation:

$$\sqrt{\frac{s}{x}}\cdot J_1(2\sqrt{sx})\cdot[\pi_n(0)-\pi_n(x)] \doteqdot \sum_{r=0}^{n-1}\frac{n!\,\pi_r(0)}{r!\,(n-r)}\,\frac{(p-1)^{n-r-1}}{p^{n-r}}\times$$

$$\times\, e^{-\frac{s}{p}}\,s\,L_{n-r-1}^{(1)}\left(\frac{s}{p(1-p)}\right).$$

$$\doteqdot \sum_{r=0}^{n-1}\frac{n!}{r!}\pi_r(0)\,\frac{(1-p)^{n-r}}{p^{n-r-1}}\,e^{\frac{1}{2}s\left[\frac{1}{1-p}-\frac{1}{p}\right]}\,k_{2n-2r}\left(\frac{s}{2p(1-p)}\right) \tag{4·6}$$

The next case is one in which β is taken as one and ν an integer greater than one. (4·1) gives us

$$\int_0^\infty e^{-s}\left(\frac{x}{s}\right)^{\frac{\nu}{2}} J_\nu(2\sqrt{sx})\,[\pi_n(0)-\pi_n(s)]\,ds \doteqdot \sum_{r=0}^{n-1}\frac{n!}{r!}\,\frac{\pi_r(0)}{(p+1)^{n-r+1}\,p^{\nu-2}} \tag{4·7}$$

This result could also have been obtained if we had used Tricomi's theorem[6]

$$\frac{1}{p^{\nu-1}} f\left(\frac{1}{p}\right) \doteqdot \int_0^\infty \left(\frac{x}{S}\right)^{\frac{\nu}{2}} J_\nu\,[2\sqrt{xs}]\; h\,(S)\; dS, \text{ if } h\,(x) \doteqdot f(p)$$

where for $h\,(x)$ we take $e^{-x}\,[\pi_n\,(0) - \pi_n\,(x)]$ so that $f(p)$ becomes

$$\sum_{r=0}^{n-1} \frac{n\,!}{r\,!}\,\pi_r\,(0)\,\frac{p^{n-r}}{(p+1)^{n-r+1}}.$$

To interpret the right-hand side of (4·7) we write the expression in its general term as

$$\frac{1}{p}\cdot\frac{1}{p^{\nu-2}}\cdot\frac{p}{(p+1)^{n-r+1}}$$

and apply the product theorem to the results

$$\frac{1}{p^{\nu-2}} \doteqdot \frac{x^{\nu-2}}{\Gamma(\nu-1)}\;\nu>1\;;\quad \frac{p}{(p+1)^{n-r+1}} \doteqdot \frac{e^{-x}\,x^{n-r}}{\Gamma(n-r+1)}$$

we get

$$\frac{1}{\Gamma(\nu-1)\,\Gamma(n-r+1)} \int_0^x e^{-\xi}\,(x-\xi)^{n-r}\,\xi^{\nu-2}\,d\xi$$

$$= \frac{(-)^{-\frac{1}{2}(n-r+\nu)}}{\Gamma(n-r+\nu)}\,e^{-\frac{1}{2}x}\,x^{\frac{1}{2}(n-r+\nu-2)}\,M_{\frac{1}{2}(n-r-\nu+2),\,\frac{1}{2}(n-r+\nu-1)}\,(-x)$$

using a slight modification of the integral*

$$M_{k,m}\,(z) = \frac{\Gamma\,(2m+1)\,z^{m+\frac{1}{2}}\,2^{-2m}}{\Gamma\,(\tfrac{1}{2}+m+k)\,\Gamma\,(\tfrac{1}{2}+m-k)}\cdot\int_{-1}^{+1} e^{\frac{1}{2}zu}\,(1+u)^{-\frac{1}{2}+m-k}\,(1-u)^{-\frac{1}{2}+m+k}\,du.$$

Hence

$$\int_0^\infty e^{-s}\left(\frac{x}{s}\right)^{\frac{\nu}{2}} J_\nu\,(2\sqrt{sx})\;[\pi_n(0) - \pi_n\,(s)]\;ds$$

$$= \sum_{r=0}^{n-1} \frac{n\,!\;\pi_r\,(0)\,(-)^{-\frac{1}{2}(n-r+\nu)}}{r\,!\;\Gamma\,(n-r+\nu)}\,e^{-\frac{1}{2}x}\,x^{\frac{1}{2}(n-r+\nu-2)}\,M_{\frac{1}{2}(n-r-\nu+2),\,\frac{1}{2}(n-r+\nu-1)}\,(-x) \tag{4·8}$$

Change x into $-x$ and use $J_\nu\,(2\,i\,\sqrt{xs}) = i^\nu\,I_\nu\,(2\sqrt{xS})$ we get

$$(-)^{\nu+1} \int_0^\infty e^{-s}\left(\frac{x}{s}\right)^{\frac{\nu}{2}} I_\nu\,(2\sqrt{sx})\;[\pi_n\,(0) - \pi_n\,(s)]\;ds$$

$$= \sum_{r=0}^{n-1} \frac{n\,!}{r\,!}\,\frac{\pi_r\,(0)\,e^{\frac{1}{2}x}\,x^{\frac{1}{2}(n-r+\nu-2)}}{\Gamma\,(n-r+\nu)}\,M_{\frac{1}{2}(n-r-\nu+2),\,\frac{1}{2}(n-r+\nu-1)}\,(x) \tag{4·9}$$

[* Whittaker and Watson, *Modern Analysis*, p. 352.]

We now take the case when both β and ν are each equal to one, we get from (4·1)

$$\int_0^\infty e^{-S}\sqrt{\frac{x}{S}}\,J_1(2\sqrt{xS})\,[\pi_n(0)-\pi_n(S)]\,dS$$

$$\doteqdot \sum_{r=0}^{n-1}\frac{n!}{r!}\pi_r(0)\frac{p}{(p+1)^{n-r+1}}$$

$$=\sum_{r=0}^{n-1}\frac{n!}{r!}\frac{\pi_r(0)}{(n-r)!}e^{-x}\,x^{n-r} \qquad (4\cdot10)$$

after interpretation. This result could have been obtained by the direct application of the theorem: $f\left(\frac{1}{p}\right)\doteqdot\int_0^\infty\sqrt{\frac{x}{S}}\,J_1(2\sqrt{xS})\,h(S)\,dS$ to

$$e^{-x}\,[\pi_n(0)-\pi_n(x)]\doteqdot\sum_{r=0}^{n-1}\frac{n!}{r!}\pi_r(0)\frac{p^{n-r}}{(1+p)^{n-r+1}}.$$

If we put in (4·4) $\beta=\frac{1}{2}$ we get after a small transformation

$$\int_0^\infty e^{-\frac{s}{2}}\sqrt{\frac{x}{4s}}\;J_1(\sqrt{sx})\,[\pi_n(0)-\pi_n(s)]\,ds$$

$$=\sum_{r=0}^{n-1}\frac{n!\,\pi_r(0)}{r!\,(n-r)}(-)^{n-r-1}\,x\,L_{n-r-1}^{(1)}(x)\,e^{-\frac{x}{2}} \qquad (4\cdot11)$$

$$=\sum_{r=0}^{n-1}\frac{n!}{r!}\pi_r(0).\;k_{2n-2r}\left(\frac{x}{2}\right). \qquad (4\cdot12)$$

V. To get the recurrence formula for $\pi_n(x)$ differentiate with respect to t the generating function of $\pi_n(x)$:

$$\frac{1}{(1-t)}\exp\left[-\frac{xt}{1-t}\right]\phi\left(-\frac{t}{1-t}\right)=\sum_{s=0}^{\infty}\frac{t^s}{s!}\;\pi_S(x)$$

we get

$$-x(1-t)^{-2}\left\{\frac{1}{1-t}\exp\left[-\frac{xt}{1-t}\right]\phi\left(-\frac{t}{1-t}\right)\right\}$$

$$+(1-t)\left[\frac{1}{1-t}\exp\left(-\frac{xt}{1-t}\right)\right]\left[\frac{d}{dt}\left\{\frac{1}{1-t}\phi\left(-\frac{t}{1-t}\right)\right\}\right]$$

$$=\sum_{s=0}^{\infty}\frac{t^S}{S!}\pi_{S+1}(x).$$

Now use the following results

$$\frac{1}{(1-t)}\exp\left(-\frac{xt}{1-t}\right)=\sum_{s=0}^{\infty}\frac{t^s}{S!}L_s(x);\text{ and }\frac{1}{1-t}\phi\left(-\frac{t}{1-t}\right)=\sum_{s=0}^{\infty}\frac{t^s}{S!}\pi_s(0)$$

and obtain

$$-x\left\{\sum_{n=0}^{\infty}(n+1)\,t^n\right\}\left\{\sum_{s=0}^{\infty}\frac{t^s}{S!}\,\pi_s(x)\right\}+(1-t)\left\{\sum_{s=0}^{\infty}\frac{t^s}{S!}\,L_s(x)\right\}\times$$

$$\times\left\{\sum_{m=0}^{\infty}\frac{\pi_{m+1}(0)\,t^m}{m!}\right\}=\sum_{s=0}^{\infty}\frac{t^s}{S!}\,\pi_{S+1}(x)$$

or

$$-x\sum_{s=0}^{\infty}\left[\sum_{r=0}^{s}\frac{s-r+1}{r!}\,\pi_r(x)\right]t^s+(1-t)\sum_{s=0}^{\infty}\left[\sum_{r=0}^{s}\frac{\pi_{S-r+1}(0)\,L_r(x)}{(S-r)!\,r!}\right]t^s$$

$$=\sum_{s=0}^{\infty}\frac{t^s}{S!}\,\pi_{S+1}(x).$$

Equate the coefficients of t^S on both sides and get

$$-x\sum_{r=0}^{s}\frac{S-r+1}{r!}\,\pi_r(x)+\sum_{r=0}^{s}\frac{\pi_{S-r+1}(0)\,L_r(x)}{r!\,(s-r)!}-\sum_{r=0}^{s-1}\frac{\pi_{S-r}(0)\,L_r(x)}{r!\,(s-r-1)!}$$

$$=\frac{\pi_{S+1}(x)}{S!}$$

or

$$\pi_1(0)\,L_S(x)-x\,\pi_S(x)-\pi_{S+1}(x)=\sum_{r=0}^{s-1}\frac{S!}{r!}\left[(S-r+1)\,x\,\pi_r(x)\right.$$

$$\left.-\frac{\pi_{S-r+1}(0)\,L_r(x)}{(S-r)!}+\frac{\pi_{S-r}(0)\,L_r(x)}{(S-r-1)!}\right] \qquad (5\cdot1)$$

The particular case $s=1$, $r=o$ gives

$$\pi_2(x)+x\,\pi_1(x)+2\,x\,\pi_0(x)=\pi_1(0)\,L_1(x)+[\pi_2(0)-\pi_1(0)]\,L_0(x). \qquad (5\cdot2)$$

REFERENCES

1. Shastri .. *Proc. Ind. Acad. Sci.*, 1940, **11**, 314.
2. Whittaker and Watson .. *Modern Analysis*, 1927, 340.
3. Varma .. *Phil. Mag.*, (7), 1936, **22**, 32.
4. Goldstein .. *Proc. Lond. Math. Soc.*, 1932, **34**, 124.
5. Erdelyi .. *Math. Zeit.*, 1936, **42**, 132.
6. Tricomi .. *Rend. dei Lincei.*, 1935, **22**, 564.

QUANTUM THEORY OF X-RAY REFLECTION AND SCATTERING

Part I. Geometric Relations

By Sir C. V. Raman and Dr. N. S. Nagendra Nath
(*From the Department of Physics, Indian Institute of Science, Bangalore*)

Received July 16, 1940

1. Introduction

The simplest example of the optical excitation of the vibrations of a crystal lattice is that afforded by the absorption of infra-red radiations by the crystal. In this case, the material vibrations of the lattice and the electromagnetic waves by which they are excited have the same frequency. When the incident radiations lie in the visible or ultra-violet region of the spectrum, they have a much higher frequency than the possible lattice vibrations, but may nevertheless excite the latter, as is shown by the fact that the light scattered by the crystal includes radiations of diminished frequency. The possibility of excitation in this case is due to the lattice vibrations altering the optical polarisability of the material of the crystal. In both cases, the excitation is essentially an optical process, as is clear from the fact that it occurs irrespective of the temperature of the crystal. That it is also a quantum-mechanical effect is particularly evident in the case of light scattering; the intensity of the lines appearing with diminished frequency in the spectrum of the scattered light is proportional to the Planck constant of action and varies but little with temperature, so long as this is moderate and the lattice vibrations are of sufficiently high frequency.

That the lattice vibrations of a crystal may be excited by X-rays in much the same way as in the case of ordinary light has been suggested and supported by experimental evidence in a recent series of papers in these *Proceedings*.* It was there shown that the character of the resulting phenomena is different in the cases where the lattice vibrations lie respectively in the acoustic and the optical range of frequencies. This is to be expected, because in the vibrations of the acoustic class, the average electron density

* Raman and Nilakantan, 1940, **11**, 379–408.

in the unit cell of the lattice varies periodically while its distribution within the cell remains nearly constant, while on the other hand, in the vibrations of the optical class, the mean electron density in the unit cell remains approximately constant while its distribution within the cell varies periodically with time. The possibility of the vibrations of these two classes being induced by the incidence of X-rays therefore arises in different ways. In one case, it is the time-variation of the mean polarisability of the crystal and in the other case the time-variation of the structure amplitudes (Fourier components) of the electron density that is responsible for the excitation of the vibrations. It is not surprising therefore that the effects produced on the incident radiation differ even in respect of their geometric characters in the two cases.

It is proposed in these papers to develop in mathematical form the ideas outlined in the papers quoted above. In this first instalment, the purely geometric aspects of the phenomena will be discussed, the important question of intensities being only touched upon incidentally. The fuller treatment of the latter will be given in Part II.

2. *The Acoustic Case*

From the remarks made above, it is evident that the cases in which the frequency of the lattice vibrations lie respectively in the acoustic and optical ranges must be considered separately. We shall proceed on the assumption that exchanges of energy and momenta take place between the incident X-radiation and the waves excited by it in the crystal, the substance of the latter otherwise taking no part in the phenomena. The conservation of energy and momentum requires

$$h\nu = h\nu' + h\nu^* \tag{1}$$

$$\frac{\vec{h}}{\lambda} = \frac{\vec{h}}{\lambda'} + \frac{\vec{h}}{\lambda^*} \tag{2}$$

ν, ν' and ν^* being respectively the frequency of the incident and scattered X-rays and of the excited acoustic waves; λ, λ' and λ^* are the corresponding wave-lengths. Equation (1) shows that the frequency of the scattered X-rays is diminished relatively to the incident X-rays by the frequency of the sound-waves excited in the process. As, however, ν is far larger than ν^* we may in equation (2) take $\lambda = \lambda'$ without sensible error and proceed to solve it geometrically as shown in Fig. 1.

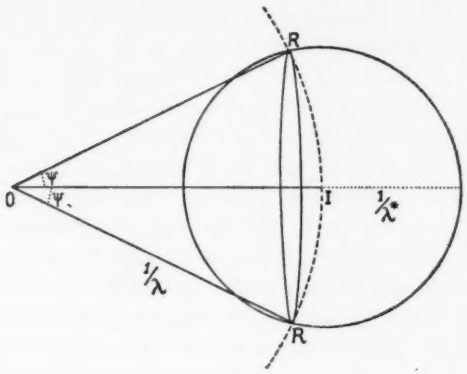

FIG. 1

With O as centre, we draw a sphere having a radius equal to $1/\lambda$. The particular radius OI of the sphere which is parallel to the incident X-rays being marked out, we draw a second sphere with I as centre and $1/\lambda^*$ as radius which intersects the first sphere along the circle R R. It is evident that the generating lines of the cone ORR represent the possible directions of the scattered X-rays corresponding to the acoustic wave-length λ^*. The semivertical angle of this cone ψ is given by the relation

$$2\lambda^* \sin \psi/2 = \lambda \qquad (3)$$

When λ^* is infinite, ψ vanishes and the cone of scattered X-rays collapses to a line along the incident ray. As λ^* diminishes however, the cone opens out, reaching its maximum semi-vertical angle when the wave-length of the acoustic waves is the minimum physically possible in the crystal. In the case of a cubic crystal, this minimum wave-length would certainly be greater than the grating constant of the crystal, and it is clear from (3) that in any setting of the crystal, the directions in which the Bragg reflections by the crystal could be observed would lie outside the cone of monochromatic radiations scattered by it. The distribution of energy in the cone of scattered X-rays is a special problem into which we shall not here enter. It is obvious, however, that if the acoustic spectrum of the crystal has a concentration of energy at or near a particular wave-length which may be greater than the minimum possible, the scattered X-rays may be expected to show a concentration of intensity in the vicinity of a corresponding cone of rays.

3. The Optical Case

Equations (1) and (2) are equally applicable in the optical case, ν^* being now one of the characteristic optical frequencies of the crystal lattice and

λ^* is the wave-length of the periodic stratifications of electron density resulting from the lattice vibrations of that frequency excited in the crystal by the incident X-rays. ν^* is, of course, much larger than in the acoustic case, but even so, it is small compared with the X-ray frequency. Hence, though the change of frequency in the act of reflection indicated by equation (1) is an essential part of the phenomenon, we may without sensible error take $\lambda = \lambda'$ in equation (2). We shall, however, retain the ascent in λ' to indicate that the vector $1/\lambda'$ refers to the direction of the reflected X-ray. In the acoustic case, the vector $1/\lambda^*$ has an arbitrary direction and an arbitrary magnitude subject to only a maximum limit, with the result that the vector $1/\lambda'$ representing the direction of the scattered X-rays has an arbitrary direction lying within a certain cone. In the optical case, however, the conditions are different, as we shall presently see, with the result that the vector $1/\lambda'$ is restricted to specifiable directions and the observed effect is in the nature of a well-defined reflection and not an irregular scattering.

We shall first consider the particular case in which the optical vibrations excited in the cells of the crystal lattice are everywhere of identical phase; in other words, the phase-waves of the lattice vibrations have an infinite wave-length ($\Delta = \infty$). As already remarked, the possibility of optical excitation of the lattice vibrations depends on the fact that these vibrations produce time-periodic variations in the Fourier components of the space distribution of electron density, in other words, produce periodic pulsations of the structure amplitudes of the crystal. When $\Delta = \infty$ the wave-length of these pulsations is the same as that of the crystal spacings, or a harmonic thereof, and the wave-fronts also run parallel to the crystal spacings. Accordingly, we may write

$$\frac{\vec{1}}{\lambda^*} = \frac{\vec{n}}{d} \tag{4}$$

where n is an integer (1, 2, 3, $\cdot\ \cdot\ \cdot$) and $1/d$ is a vector normal to any chosen set of crystal spacings, its magnitude being the reciprocal of that spacing. Combining (2) and (4), we have

$$\frac{\vec{1}}{\lambda} - \frac{\vec{1}}{\lambda'} = \frac{\vec{n}}{d} \tag{5}$$

Representing this graphically, (Fig. 2), we derive the formula $2d \sin\theta = n\lambda$, θ being the glancing angle of incidence and of reflection. Equation (5) thus shows that *when the phase-wave length Δ of the lattice vibrations is assumed to be infinite, the quantum reflection of X-rays with diminished frequency occurs under the same geometric conditions as the classical X-ray reflections.*

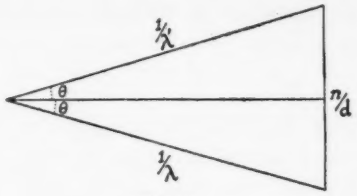

FIG. 2

The case when Δ is finite corresponds to a lattice vibration in which the phase of the atomic vibrations alters progressively from cell to cell. The phase of the pulsation of structure-amplitude will therefore also alter from cell to cell, and *in general*, both the direction of the wave-fronts along which this phase is constant, and the spacing between successive such wave-fronts will differ from the crystal spacings. These quantities are indicated by the vector $1/\lambda^*$ and the reciprocal of its magnitude. We may readily find the relation between λ^*, the lattice wave-length Δ and the crystal spacing d/n (see Fig. 3).

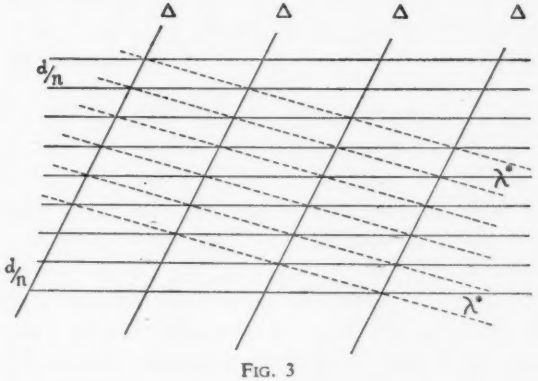

FIG. 3

The crystal spacings are a set of equidistant planes marked d/n in the figure and the phase waves of the lattice vibrations are another set of planes marked Δ crossing them at an angle as in Fig. 3. It is evident that the planes along which the phase of the pulsations of electron density would be constant would be the set of planes crossing both diagonally and marked λ^* in the figure. The spacings of the three sets of planes are evidently connected by the vector relationship between their reciprocals (see note at the end of the paper).

$$\frac{\vec{1}}{\lambda^*} = \frac{\vec{n}}{d} + \frac{\vec{1}}{\Delta} \tag{6}$$

Combining (6) with (2), we have, in the most general case

$$\frac{\vec{1}}{\lambda} - \frac{\vec{1}}{\lambda'} = \frac{\vec{n}}{d} + \frac{\vec{1}}{\Delta} \tag{7}$$

Equation (7) reduces, as it should, to equation (5) when Δ is infinite. It states the most general law of the quantum reflection of X-rays which may be put into words thus: *We combine vectorially the reciprocals of the crystal spacing and of the wave-length of the optical vibrations of the crystal lattice. The reciprocal of the resultant gives the spacing of the dynamic stratifications of electron density and its direction that of their normal: these dynamic stratifications give a geometric reflection of the X-rays with diminished frequency.*

The optical vibrations of a crystal lattice have well-defined frequencies, as is shown by the sharpness of the lines observed in the spectrum of the light scattered by the crystal. The fact that the frequency shifts observed in light scattering have not so far been found to depend appreciably on the angle of scattering is also significant and shows that the lattice frequencies are approximately independent of the lattice wave-lengths. Regarding the observed frequencies as due to the characteristic vibrations of the unit cells in the lattice, it is evident that the frequency as observed with an actual crystal would be N-fold degenerate, N being the number of lattice cells in the fragment of crystal used. Actually, the N frequencies should be regarded as forming an aggregate which is densest at the frequency corresponding to an infinite lattice wave-length ($\Delta = \infty$) and rapidly thins out as Δ diminishes. These considerations enable us to understand the effects to be expected on the basis of equation (7). Δ can always be considered as large compared with d/n. Hence, the effect of its appearance in the right-hand side of equation (7) on its scalar magnitude is a small quantity of the first order. It serves, however, to alter the orientation of the wave-fronts of the dynamic stratifications with respect to the crystal spacings. Indeed this would be its only effect if the vectors $1/\Delta$ and n/d are mutually perpendicular, as the resultant of their addition would then be practically n/d. In the limiting case when Δ is infinite, equation (7) shows that the quantum reflection appears under the same conditions as the classical reflection and coincides with it in position. It is also then of maximum intensity, as the N-fold aggregate of optical frequencies of the lattice is densest for infinite values of Δ. As the crystal is tilted away from the setting for the ordinary Bragg reflection, equation (7) shows that Δ must diminish in magnitude, and the intensity of the quantum reflection must therefore fall off in proportion to the diminished density of the aggregate

of frequencies for smaller values of Δ. As we shall see presently, the quantum reflection also then separates out from the Bragg reflection and can be observed by itself.

4. *Geometric Law of Quantum Reflection*

The geometric interpretation of equation (7) is facilitated by first considering a case in which the vector $1/\Delta$ besides being small compared with n/d is perpendicular to it and lies in the same plane with it as the incident X-rays. In this case, it is evident that the result of combining $1/\Delta$ and n/d vectorially is to tilt the reflecting planes in the plane of incidence with respect to the crystal spacings but without any alteration of these spacings. If therefore we consider a case in which the crystal-spacings are so inclined to the incident monochromatic X-rays that they *cannot* give a Bragg reflection, in other words, when

$$\frac{\vec{1}}{\lambda} - \frac{\vec{1}}{\lambda'} \neq \frac{\vec{n}}{d} \tag{8}$$

they would nevertheless give a quatum reflection according to the formula

$$\frac{\vec{1}}{\lambda} - \frac{\vec{1}}{\lambda'} = \frac{\vec{n}}{d'} \tag{9}$$

where d' has the same magnitude as the crystal spacing d, but its direction has been altered so as to satisfy the vectorial relation (9). This relation indicates that *the incident X-rays give a reflection with diminished frequency in the plane of incidence even when the Bragg reflection is not possible*, and *that the direction in which it appears with reference to the incident X-rays is unaffected by the setting of the crystal*, though as remarked above, *its intensity would fall off rapidly as the crystal is turned away from the Bragg setting*.

Equation (9) is represented graphically in Fig. 4 for two cases in which the crystal has been turned away from the Bragg setting in one direction or

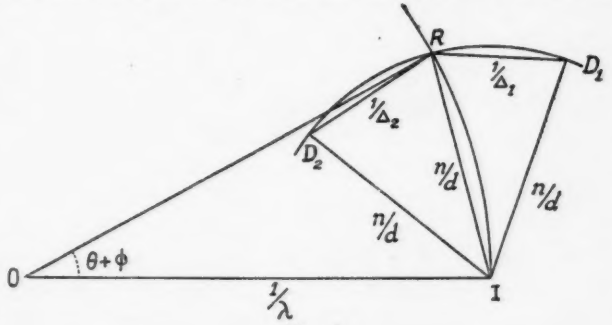

FIG. 4

the other. In both cases, the direction of the reflected ray OR is the same and is given by the trigonometric formula

$$2\,d \sin \tfrac{1}{2}(\theta + \phi) = n\,\lambda \qquad (10)$$

where θ and ϕ are the glancing angles of incidence and reflection with respect to the crystal spacings.

The postulate made above which results in the formulæ (9) and (10), namely, that the vectors $1/\Delta$ and $1/d$ are perpendicular to each other, physically interpreted, means that the lattice-waves excited by the X-rays have wave-fronts perpendicular to the crystal spacings giving the quantum reflection. There is good reason to believe that this must be actually the case with most crystals. For, the atomic vibrations which are effective in altering the structure-amplitude of any particular spacing are those in which the displacements are normal to the crystal spacing. If the lattice wave-fronts are parallel to the crystal spacings, the phase of the atomic vibrations would alter as we pass from one spacing to the next, whereas if they are perpendicular to the crystal spacings, the phase of the vibration would change along the crystal spacings but not perpendicular to them. The forces brought into play between the neighbouring cells of the lattice by such phase-changes would obviously be much greater in the former case than in the latter. Accordingly, the N-fold aggregate of frequencies would be spread out over a much wider range of frequencies when Δ and d are parallel than when they are perpendicular. So far as the reflection of X-rays is concerned, therefore, we would be justified in considering only the case where Δ and d are perpendicular and ignoring the case where they are parallel. Equation (10) could then be regarded as the generally valid geometric law for the quantum reflection of X-rays with diminished frequency.

It must be recognised, however, that there may be cases where the considerations set forth above cannot reasonably be expected to be valid. It may, for instance, be possible that the binding forces which hold the crystal lattice together are of such a nature that though the atomic vibrations are normal to the crystal planes under consideration, a change in the phase of such vibrations along the crystal planes may evoke forces and disturb their frequencies quite as much as a change of phase normal to them. In such a case, the postulate that the vectors $1/\Delta$ and $1/d$ are perpendicular may cease even to be approximately true. In such cases, that is, when the effective lattice-waves have an arbitrary inclination to the crystal spacings, an alternative principle suggests itself giving the selection rule for the vector $1/\Delta$, namely, that the direction of the vector is such that its scalar magnitude necessary to satisfy equation (9) is a minimum. Such a principle would not

be unreasonable in view of the remark already made that the frequency-aggregate of the optical vibrations becomes rapidly less dense for increasing values of Δ. It can readily be shown that this principle gives the same result as equation (10) when θ and ϕ are nearly equal to each other, that is to say when the setting of the crystal is not far from the Bragg position. More generally, however, it deviates from that result.

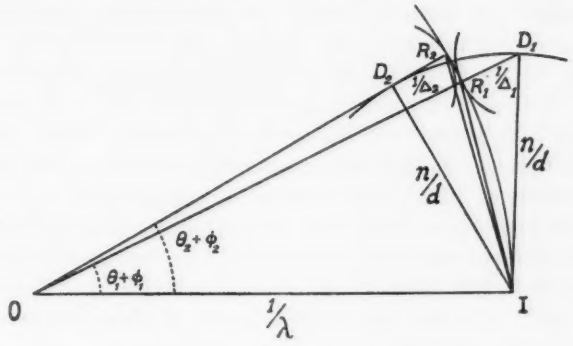

FIG. 5

Fig. 5 represents equation (7) graphically for two cases in which the crystal has been turned away from the Bragg setting in one direction or the other, and Δ is chosen to have the minimum necessary length required to satisfy the equation. The direction of the reflected ray is OR_1 in one case and OR_2 in the other. It will be noticed that the effective resulting spacing is in one case greater than d/n, and in the other case less than d/n. At the correct Bragg setting, therefore, OR_1 and OR_2 become coincident. The geometric law of the quantum reflection is seen from Fig. 5 to be

$$d \sin (\theta + \phi) = n \lambda \cos \phi. \qquad (11)$$

Equations (10) and (11) give results which differ the more widely, the greater the difference between θ and ϕ, but become identical when $\theta = \phi$. It will be noticed that they correspond respectively to the results which have been found experimentally valid for the cases of sodium nitrate and diamond. The divergence between the results given by the two formulæ when $\theta \neq \phi$, and the fact that they have been derived on quite different considerations suggests that when the crystal is tilted away from the correct Bragg setting, the definition of the quantum reflection should progressively deteriorate. Such an effect is actually observed, but whether it is due solely to the cause stated or is due partly also to other disturbing effects, *e.g.*, thermal agitation or the mosaic structure of the crystal, is a matter for further investigation.

Summary

When X-rays fall upon a crystal, the characteristic vibrations of the crystal lattice may be excited thereby, in much the same way as in the phenomenon of the scattering of light in crystals with diminished frequency, the excitation being a quantum mechanical effect. From the equations for the conservation of energy and momentum, the geometrical relations entering in this effect are deduced theoretically for the two cases in which the lattice vibrations fall within (1) the acoustic range of frequency and (2) the optical range. In the first case, the incident X-rays are scattered in directions falling within a cone having the incident ray as axis and with a semi-vertical angle $2 \sin^{-1} \lambda/2 \lambda^*$ where λ^* is the minimum acoustical wave-length. In the second case, we have a quantum-mechanical reflection of the X-rays with diminished frequency in a direction which generally follows the geometric formula $2 d \sin \frac{1}{2} (\theta + \phi) = n \lambda$ where θ and ϕ are the glancing angles of incidence and reflection on the crystal spacings. For crystals with specially rigid bindings, the alternative fomula $d \sin (\theta + \phi) = n \lambda \cos \phi$ is indicated as being more appropriate. In either case, the intensity of the reflection should fall off rapidly as θ and ϕ diverge.

Note :—Equation (6) may be very simply derived from the construction shown in Fig. 3. The vector sum of the two sides of a triangle is equal to the third side. Dividing this equation by the area of the triangle, we get a vector relation between the reciprocals of the three perpendiculars from the vertices on the sides.

ANALYSIS OF THE RAMAN AND INFRA-RED SPECTRA OF α-QUARTZ

By Bishambar Dayal Saksena

(From the Department of Physics, Indian Institute of Science, Bangalore)

Received July 5, 1940

(Communicated by Sir C. V. Raman, F.R.S., N.L.)

1. Introduction

It was remarked by the late Lord Rutherford (1930) that the Raman effect has proved and will prove an instrument of great power in the theory of solids. But although the number of investigations on the Raman spectra of crystals has been quite large, in relatively few cases has any attempt been made to consider the significance of the observed results in relation to the structure of the crystal as revealed by X-ray studies. That an intimate relationship exists between the Raman spectrum and the crystal structure has however been evident from the first. As in the parallel case of the infra-red spectrum, this relationship is determined in the main by the symmetry properties of the crystal and the geometrical character of the vibrations involved. Brester (1924) considered this problem for the infra-red spectrum and worked it out in detail for the case of calcite, while Placzek (1930) developed the corresponding theory for the Raman effect. It is therefore a little surprising that during the past ten years, more extensive use has not been made of the theoretical ideas in analysing and interpreting the Raman data for crystals. It must however be remarked that to take full advantage of the theory, we require more information than a mere catalogue of the observed frequencies. The selection rules for the crystal take the form of a statement regarding the components of the polarisability tensor for each particular class of vibration, and to utilize these rules, it is necessary to have data with single crystals in specific orientations obtained with polarised exciting light. Work of this kind has been attempted by comparatively few investigators. It is, in general, necessary also to have the corresponding data for the infra-red spectrum as these are complementary to those obtained from the Raman effect. When such data are available, the next step is to correlate them with the possible modes of vibration of the known crystal structure, and to determine the binding forces and the normal modes and frequencies. In making the necessary calculations, the

methods of the group theory developed by Wigner (1930) are of great assistance.

A detailed investigation of the kind referred to above for the case of quartz would evidently be laborious, but would be well justified. In the first place, quartz is a substance of basic importance and plays the same part in mineral chemistry and glass technology as benzene does in organic chemistry. Then again, the numerous technical and scientific applications of this crystal invest its physical properties with very great interest, and it is evident that an investigation of the kind indicated above would open the way to a fuller understanding of these properties. Such a detailed investigation has been undertaken by the author and the present paper reports the results so far obtained.

2. *Review of Existing Data*

The infra-red spectrum of α-quartz has been investigated by numerous workers, namely, Rubens (1892), Merritt (1895), Nichols (1897), Rosenthal (1899), Coblentz (1906), Reinkober (1911), Liebisch and Rubens (1919), Dreisch (1927), Plyler (1929), Parlin (1929), and Czerny (1929). The region extending from $8\,\mu$ to about $30\,\mu$ has been investigated by the earlier workers using the reflection method, *i.e.*, measuring the wave-lengths at which the reflecting power is a maximum. The frequency deduced in this way is usually lower than the frequency of maximum absorption. The difference may be evaluated by using the Havelock (1912) formula; it is of the order of ten to twenty wave-numbers for the lowest frequencies and less for the higher ones. As the positions of the reflection maxima for the ordinary and extra-ordinary rays are not the same, it is necessary to use quartz plates cut parallel and perpendicular to the optic axis respectively. Liebisch and Rubens worked with the polarised radiation reflected by a plane selenium mirror, whereas Reinkober used unpolarised radiation and evaluated his results with the aid of the formula $R_0 = R_\perp$ and $R_e = 2R_\parallel - R_\perp$, where R_0 and R_e are the reflecting powers for the ordinary and the extraordinary rays and $R_\perp$ and $R_\parallel$ are the reflecting powers for unpolarised radiation of a quartz plate cut respectively perpendicular and parallel to the optic axis. According to Reinkober the crystal shows normal reflection in the region 1 to $7{\cdot}5\,\mu$. A high peak in the curve representing the reflecting power as a function of wave-length occurs at $8{\cdot}5\,\mu$ both for the ordinary and the extra-ordinary rays, with a subsidiary maximum at $8{\cdot}35\,\mu$. This is followed by strong maxima at 8·9 and $9{\cdot}05\,\mu$ which are sharply separated both in the ordinary and the extraordinary rays. Between 12 and $13\,\mu$ there occurs a maximum which was first noticed by Coblentz with unpolarised radiation. Actually, however, in this region the crystal shows dichroism, the maximum

for the extraordinary ray lying at 12·87 μ and for the ordinary ray at 12·52 μ, these being quite distinctly separated. Another weak maximum is observed at 14·55 μ for the ordinary ray only. The dichroism extends throughout the whole long wave-length region. Liebisch and Rubens observed maxima for the ordinary ray at 21·0 μ and 26·0 μ, and at 19·7 μ and 27·5 μ for the extraordinary ray. The maxima are broad, the one at 26·0 μ being weak, but they are well separated. Czerny has investigated the infra-red spectrum in the long wave-length region from 38 to 80 μ by the absorption method using quartz plates cut parallel and perpendicular to the axis. An absorption at 38 μ was found with a quartz plate 1 mm. thick cut perpendicular to the optic axis and at 78 μ with a plate 3·5 mm. thick cut similarly. Both the absorption maxima are weak, the one at 78 μ being weaker. The region near 48 μ was investigated with quartz plates 1 mm. thick cut parallel and perpendicular to the optic axis but no absorption could be found, the transmission curve showing no dip in this region. Several weak absorption bands have been observed in the region between 2·9 μ and 8 μ by various investigators, but we need not consider them in detail, as they are undoubtedly due to combination frequencies. Omitting these, we may summarise the existing data regarding the wave-lengths of maximum absorption and reflection in the infra-red in the following table.

TABLE I

Infra-red Wave-lengths in μ

Ordinary Ray	Extraordinary Ray
78 (weak)	..
38 (weak)	..
26·0 (medium weak)	27·5 (medium strong)
21·0 (very strong)	19·7 (very strong)
14·55 (weak)	..
12·52 (medium weak)	12·87 (medium weak)
9·05 (strong)	9·05 (strong)
8·9 (strong)	8·9 (strong)
..	8·7 (strong)
8·5 (strong)	8·5 (strong)

The Raman spectrum of α-quartz has been investigated by Landsberg and Mandelstam (1928), Rao (1928), Krishnan (1928, 1929), Pringsheim and

Rosen (1928), Daure (1929), Gross and Romanova (1929), Nisi (1929, 1932), Hollaender and Williams (1931), Rasetti (1932), Weiler (1932), Kujumzelis (1936), Nedungadi (1940). The frequency shifts observed in light scattering at room temperature are listed in Table II. The first column shows the results of the present author deduced from numerous spectrograms, the relative intensities being those determined from microphotometric curves for the case in which the optic axis of the crystal is perpendicular to the incident and scattered rays, the illuminating beam being unpolarised; without such specification, the intensity data for crystals are of doubtful value. The second and third columns show the results of Rasetti and of Nedungadi for comparison.

TABLE II

Comparison of Raman and Infra-red Frequencies

Raman Frequencies				Raman Wave-length in μ	Infra-red Wave-length in μ	Ordinary (O) or Extra-ordinary (E)	
Author	Rasetti	Nedungadi	Mean				
128 (13)	128 (5)	127 (20)	128	78·13	78	O	Abs.
207 (10 br)	207·3 (10)	207 (15 br)	207	48·31	Absent		
267 (5)	265·9 (2)	263 (4)	265	37·74	38	O	Abs.
358 (4)	356·5 (3)	354 (6)	356	28·09			
391 (3)	394·4 (1)	397 (4)	392	25·51	27·5	E	Ref.
					26·0	O	Ref.
403 (3)	403·9 (1)		403	24·81			
452 (3)	..	453 (3)	452	22·12			
466 (30)	466·4 (20)	465 (30)	466	21·46			
479 (0)	..	..	479	20·90	21·0	O	Ref.
505 (1)	..	501 (1)	503	19·88			
695 (2)	696·8	694 (3)	695	14·39	19·7	E	Ref.
					14·55	O	Ref.
795 (2)	796·9 (1)	794 (3)	795	12·58	12·87	E	Ref.
					12·52	O	Ref.
806 (3)	809·3 (2)	805 (3)	807	12·39			
1063 (1)	1063·1 (1)	1064 (2)	1063	9·43			
1082 (2)	1082·5 (2)	1082 (2)	1082	9·28			
					9·05	E & O	Ref.
					8·9	E & O	Ref.
1160 (4)	1160·2 (2)	1158 (5)	1159	8·63	8·7	E	Ref.
					8·5	E & O	Ref.
1228 (1)	1227 (1)	1228 (2)	1228	8·15	8·35	O	Ref.

A few remarks are desirable in respect of the entries appearing in Table II. It will be noticed that the author's results agree closely with those of Rasetti and Nedungadi. The former's result that there are two distinct frequencies at 394 and 404 is confirmed. They are seen clearly resolved in Plate III, Fig. 6 (*f*) and Plate IV, Fig. 8 (*o*), in which the 466 line excited by the 4339 A. U. radiation is of negligible intensity and cannot therefore be confused with the 404 line excited by the 4358 A. U. radiation. The two lines at 452 and 479 recorded in the table are of special interest. Usually, they are masked by the very intense and rather broad line midway between them at 466. But by suitably polarising the incident light, the 466 line may be greatly weakened, and its two companions can then be observed. The 452 line was first noticed by Cabannes and Bouhet (1937), while the 479 line was first noticed by the present author. Its observation is of importance as it evidently coincides with the very intense infra-red reflection at $21 \cdot 0 \mu$.

Lines of zero intensity at 320, 526, 585, 632, 746, 943 and 1020 cm.$^{-1}$ have been reported by Gross and Romanova (1929). No trace of these lines is to be observed even in the clearest and most heavily exposed spectrograms obtained by Nedungadi nor in any of the author's plates, though a special search was made for them. These lines have not also been reported by any except the Russian workers. In the circumstances, they have been omitted from Table II. Even if they existed, it appears extremely unlikely that any of them could represent fundamental frequencies of the quartz lattice.

A comparative study of the Raman and the infra-red data listed in Table II reveals the following important features: (1) In the region extending from 80μ down to 10μ the crystal exhibits dichroism. The infra-red absorption and reflection maxima observed with the ordinary ray do not appear in the extraordinary ray, and *vice versa*. The strongest reflection maxima for the ordinary ray in this region have however corresponding maxima for the extraordinary ray not greatly different from them either in wave-length or in intensity. (2) There is no infra-red absorption corresponding to the intense Raman lines at 207 and 466 cm.$^{-1}$ though a special search for the former was made by Czerny. These two frequencies are therefore clearly inactive in the infra-red. (3) Every one of the six infra-red absorption or reflexion maxima appearing in the region 80μ to 10μ in the ordinary ray has a corresponding Raman frequency which may reasonably be identified with it, provided account is taken of the frequency difference between the absorption and reflection maxima in the infra-red. (4) There is no Raman frequency agreeing sufficiently closely with the strong and well-defined infra-red reflexion maxima appearing in the extraordinary rays at $27 \cdot 5 \mu$, $19 \cdot 7 \mu$

and 12·87 μ to justify its being identified with any of them after the correction just mentioned has been made.

Any theoretical interpretation of the Raman and infra-red spectra of quartz should be capable of explaining the facts mentioned above.

3. *Thermal Behaviour of Quartz*

No account of the Raman and infra-red spectra of quartz would be complete without a mention of the manner in which they are influenced by change of temperature. The data available in this respect with regard to the infra-red spectrum are however not complete. Rubens and Hertz (1912) investigated the reflecting power in the region 8 μ to 10 μ at 20° C. and at − 186° C. and found only minor changes. On the other hand, it was noticed that in the long wave-length region temperature has a notable influence. The absorption coefficient was determined at a series of temperatures down to that of liquid air for selected wave-lengths namely, 7 μ, 11 μ, 16·5 μ, 52 μ and 110 μ. In all cases, the absorption diminishes steadily with falling temperature, and for the longer wave-lengths tends almost to zero. The work of Rubens and Hertz was extended by Reinkober and Kipcke (1928) over the region 1 μ to 7 μ.

The effect of temperature on the Raman spectrum of quartz has been studied by several workers, namely, Landsberg and Leontowitch (1929), Brickwedde and Peters (1929), Landsberg and Mandelstam (1929), Ney (1931) and Ornstein and Went (1935). More recently, a very thorough investigation has been made by Nedungadi (1940), whose main results are stated below:

1. The most remarkable feature is the behaviour of the symmetric oscillation of lowest frequency which gives an intense Raman scattering. This appears in the spectrum at liquid air temperature as a sharp line of frequency shift 220 cm.$^{-1}$ At room temperature, it becomes more diffuse and has a breadth of about 20 wave-numbers, the mean frequency shift being 207. As the temperature is raised above 200° C., it broadens very rapidly and in an unsymmetrical manner with reference to its original position, finally becoming a very diffuse continuous band, covering the region of frequency shift from 130 to 212 cm.$^{-1}$

2. The two other intense lines with frequency shifts of 127 and 465 at room temperature are both sharp at liquid air temperature. They broaden and shift towards the exciting line as the temperature is raised; these effects are, however, much less marked than for the 207 line. The 127 line shifts at an accelerated rate at temperatures above 200° C., the frequency reaching the value of 98 cm.$^{-1}$ at 530° C.

3. The fainter lines at 265, 354 and 397 are fairly sharp even at the high temperatures, the 265 line however, shifting noticeably to lower frequency. Changes are also noticed with the other lines which will be mentioned later.

According to Raman and Nedungadi (1940), the remarkable behaviour of the line 207 with the rise of temperature has a special significance in relation to the transformation of quartz from the α form to the β form which takes place at 575° C., and in relation to the notable changes in the physical properties of quartz (such as elasticity, thermal expansion and piezo-electricity) which occur in the temperature range above 200° C. and precede the α-β transformation. They have indeed suggested that the increasing excitation of the particular mode of vibration of the crystal lattice represented by the 207 band is responsible for these changes in physical properties and ultimately also for the α-β transformation itself. One of the principal aims with which the present investigation was undertaken was to ascertain the nature of the 207 oscillation and to find whether, as suggested by Raman and Nedungadi, its excitation would favour an alteration of the structure of quartz from trigonal to hexagonal symmetry.

The specific heat of quartz, except at the very lowest temperatures, would obviously be determined by the excitation of the fundamental modes of vibration of the crystal lattice. The analysis of the Raman and infra-red spectra, by enabling us to determine the fundamental frequencies, would allow us to evaluate the specific heat of quartz over a wide range of temperature. This will be done later in the course of this paper. The heat capacity of quartz has been experimentally investigated by Nernst (1911) from 26° to 93° K. and by Koref (1911) from 80° K. to 223° K. The latest determinations at higher temperatures are due to Moser (1936) and cover the range from 50° to 700° C. The earlier work in this region is due to Regnault (1841), Weber (1895), White (1919), Weitzel (1921), Cohn (1924), also Perrier and Roux (1923).

4. *Structure of α-Quartz*

According to the theories of Brester, Placzek and Wigner—references to which have already been made in the Introduction—the interpretation of the Raman and the infra-red spectra of α-quartz has to be based upon the geometric picture of its crystalline structure. This has been investigated by numerous workers, but the one generally accepted is that which was put forward by R. E. Gibbs (1926). The latter based his determination on the structure of β-quartz which was established by Wyckoff (1926) and by himself and W. H. Bragg (1925). Low quartz belongs to the trigonal

subdivision of the hexagonal system, the symmetry class being trigonal enantiomorphous hemihedral or trigonal trapezohedral, the Schonflies notation being D_3. The lattice in low quartz is hexagonal Γ_h which is made by the intersection of two vertical sets of planes inclined at 60° with each other and one horizontal set perpendicular to both. The space group of α-quartz is represented by D_3^4 (or the enantiomorphous D_3^6) in the Schonflies notation. The structure, accordingly, has in addition to the threefold screw axis, three twofold axes perpendicular to the same which carry the three SiO_2 triplets spaced at equal intervals along the vertical axis, each turned through 120° in respect of its predecessor. The repeating unit in low quartz thus contains 3 silicons and 6 oxygen atoms. In crystallographic notation, using the trigonal axes (a, a, c)—the two equal 'a' axes inclined at 120° in the plane, and the c-axis perpendicular to this plane—the positions of the nine atoms in α-quartz are given as (see also Wyckoff's *Structure of Crystals*, Part I)

Silicons → (1, 2, 3) in order (u, o, o), $(o, u, -\frac{1}{3})$, $(\bar{u}, \bar{u}, \frac{1}{3})$,

Oxygens → (4, 5, 6, 7, 8, 9)—in order (x, y, z), $(y, x, \bar{z}+\frac{2}{3})$,

$(\bar{y}, x-y, z-\frac{1}{3})$, $(\bar{x}, y-x, \bar{z}+\frac{1}{3})$, $(y-x, \bar{x}, z+\frac{1}{3})$, $(x-y, \bar{y}, \bar{z})$.

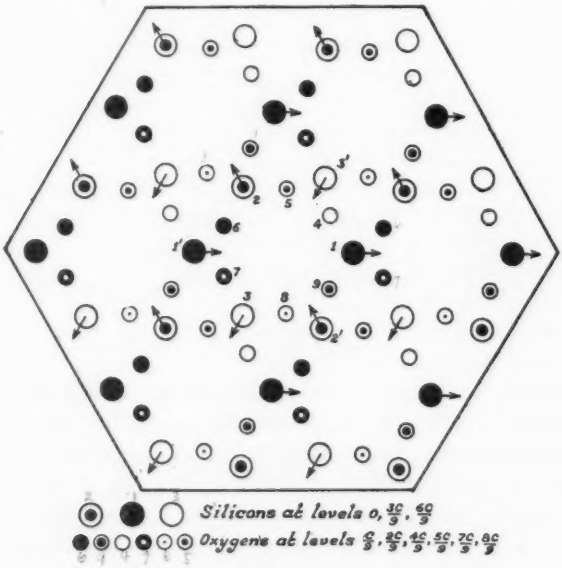

FIG. 1

Projection of the Structure on the Basal Plane

The silicons and oxygens are arranged in parallel planes, the distance between two silicon planes being 1·8 A. U. The oxygens are assumed to lie in planes spaced c/9 above and below the horizontal silicon planes, and the linear distance of the oxygen centre from the line joining the silicon centres is 0·44 A. U. Each silicon atom thus appears surrounded by four oxygen atoms, and each oxygen atom has two silicon atoms as near neighbours. The four oxygen atoms round a silicon atom do not form a regular tetrahedron, *i.e.*, the $O\overset{Si}{\diagup\diagdown}O$ angle departs from the usual tetrahedral value (109°–28′). The positions of the silicon atoms (1, 2, 3, 1′, 2′, 3′) and oxygen atoms (4, 5, 6, 7, 8, 9) in the plane perpendicular to the *c*-axis are shown in Fig. 1, and the descriptions are given thereunder.

5. *Optical Excitation of Lattice Vibrations*

It is evidently necessary for us to consider the various possible modes of vibration of the crystal lattice in quartz and their respective frequencies and to discuss the conditions necessary for these vibrations to be excited, either as the result of absorption of incident infra-red radiation or as the result of the scattering of light with diminished frequency.

The normal modes of vibration of an extended crystal lattice cover a wide range of frequencies which may be divided into two parts, one of lower frequency which is designated as the acoustic spectrum, and the other including the higher frequencies which is the optical spectrum of the crystal. There are important differences in the character of the vibrations falling into these two groups. In the acoustic spectrum, we are concerned with vibrations in which the deformations of the crystal lattice are similar to those of an elastic solid considered as a continuum, and when regarded as progressive waves, travel with the usual acoustic velocities. The positions of the atoms within the cells of the crystal lattice undergo displacements, but these are small in comparison with the translatory movements of the individual cells. In the optical spectrum of vibrations, on the other hand, the relative displacements of the atoms within the cell assume greater importance than the translatory movements of the cell, the latter vanishing in the limiting case of a vibration of identical phase in all the cells of the crystal lattice. In spectroscopic language, the acoustic vibrations form what is essentially a continuous spectrum in which the frequency increases as the wave-length diminishes, while in the optical spectrum we have a concentration of the energy at or near discrete frequencies, large changes in the length of the lattice waves involving changes of frequency which are proportionately quite small. This

analysis of the possible deformations of the crystal lattice into normal vibrations which are independent of each other is, of course, only an approximation, and its consequences would cease to be strictly valid when the amplitude of the disturbances is not infinitesimal. One result of the non-independence of the normal vibrations then resulting is the appearance of vibrations with frequencies which are overtones and combinations of the normal frequencies. There are various other consequences into which we need not here enter.

It is evident that for one of the normal modes of vibration of the the crystal lattice to be excited by the incident radiations, there should be a suitable relationship in phase at every point of the crystal between the radiations and the material vibrations. In the case of the infra-red radiation this would only be possible if there is a complete identity of the wave-lengths of the electric and material vibrations within the crystal. In other words, only that vibration of the crystal lattice would be excited which has wave-fronts parallel to and coincident with those of the radiation within the crystal. Since the wave-lengths are large in comparison with the crystal spacings, we may consider them without appreciable error as infinitely large. The characteristic vibrations appearing in infra-red absorption may accordingly be identified with those in which the internal vibrations in the cells of the crystal lattice are everywhere of identical phase.

In the case of the scattering of light, the frequency of the incident radiation is much higher than that of the lattice vibrations. To enable the latter to be excited, the necessary uniformity of phase-relationship may be secured by considering the incident radiation and the radiation scattered in any particular direction as forming a stationary wave-pattern, the wave-fronts in this pattern being parallel to and coincident with the lattice wave-fronts in the crystal. The scattering of the incident radiation by the lattice-waves in the crystal could then be regarded as equivalent to a reflection by them of the incident light-waves. A change of frequency occurs in this process which is equal to the frequency of the lattice vibration (Tamm, 1930; Raman, 1940). The wave-length of the lattice-waves necessary for such coherent reflection to be possible would be infinite for scattering in the forward direction and half the wave-length of the incident light-waves for backward scattering. In any case, this is large compared with the crystal spacings.

It is thus evident that in analysing the Raman and infra-red spectra of a crystal, we are justified in proceeding on the assumption that the vibrations of the atoms within a cell of the crystal lattice have exactly the same frequency and phase as the vibrations in the neighbouring cells.

6. *The Character Table*

The vibrating unit in α-quartz is obviously not the simple SiO_4 group suggested by Weiler (1933), as the actual number of distinct lines observed in the Raman spectra is far larger than can be accounted for in that way. We need not, therefore, stop to discuss Weiler's suggestion in further detail, but will proceed to consider the possible modes of vibration of the group of three silicon and six oxygen atoms, present in the unit cell of the crystal lattice. The elements of symmetry of this group are:

(1) Identity;

(2) a double threefold screw axis, $2C_3$;

(3) three twofold axes each passing through one silicon atom, $3\,C_2$.

These may be written as:

$2\,C_3$ (screw)—	(1, 2, 3);	(4, 6, 8);	(5, 7, 9)		
	(1, 3, 2);	(4, 8, 6);	(5, 9, 7)		
$3\,C_2$ —(1);	(2, 3);	(4, 9);	(5, 8);	(6, 7)	—(C_2^1)
(2);	(1, 3);	(4, 7);	(5, 6);	(8, 9)	—(C_2^2)
(3);	(1, 2);	(4, 5);	(6, 9);	(7, 8)	—(C_2^3)

In explanation of the symbols, we may indicate that (4, 6, 8) means an operation by which 4 changes to the place occupied by 6, and 6 changes to the place occupied by 8, and 8 changes to the place occupied by 4. (1) means that 1 is an invariant point in the operation. The character table for the point group D_3 has been given by Tisza (1933). The selection rules in the infra-red and the Raman effect as well as the number of vibrations belonging to each class of the group can be calculated according to the rules given by Wigner. The number of oscillations a_p of the type of vibration p is given by

$$a_p = 1/h \, \Sigma \, \chi^{(p)} \, \epsilon \, (\mathrm{R})$$

where

$$\epsilon \, (\mathrm{R}) = \underset{\text{rotation pure}}{\Sigma \, u_r \, (1 + 2 \cos \phi)} + \underset{\text{rotation and reflection}}{\Sigma'' u_r \, (2 \cos \phi - 1)}$$

for all vibrations including translations and reflection rotations, and h is the number of elements of symmetry for a particular group, ϕ is the angle of rotation for any particular element of symmetry (axis) which does not alter the character of the group after the operation, u_r is the number of invariant points in any element of symmetry, and $\chi^{(p)}$ is the character of the irreducible representation of various types of elements of the group. If a vibration is forbidden in the infra-red, we have

$$\Sigma \, \chi^{(p)} \, \epsilon' \, (\mathrm{R}) = 0$$

where $$\epsilon'(R) = \underset{\text{rotation}}{\Sigma(1 + 2\cos\phi)} + \underset{\text{rotation and reflection}}{\Sigma'(2\cos\phi - 1)}$$

and if a vibration is forbidden in the Raman effect, we have

$$\Sigma \chi^{(p)} \epsilon''(R) = 0$$

where $$\epsilon''(R) = \underset{\text{rotation}}{\Sigma(2 + 2\cos\phi + 2\cos 2\phi)} + \underset{\text{rotation and reflection}}{\Sigma'(2 - 2\cos\phi + 2\cos 2\phi)}$$

The selection rules have also been derived by Placzek (1930) in a different way. In Placzek's theory, the activity in the Raman effect is indicated by the six components (ϵ_{ii} and ϵ_{ik}) of the change of polarisability tensor—namely, three longitudinal, $\epsilon_{\alpha\alpha}$, $\epsilon_{\beta\beta}$, $\epsilon_{\gamma\gamma}$ and three transverse $\epsilon_{\alpha\beta}$, $\epsilon_{\beta\gamma}$, $\epsilon_{\gamma\alpha}$; and the activity in the infra-red is given by the change in the electric moment along the three principal directions, namely, M_α, M_β and M_γ. Table III gives the number of vibrations and the selection rules for each class of the point group D_3.

7. *The Selection Rules*

It will be seen from the character table that the 27 degrees of freedom resolve themselves into four vibrations in class A, four in class B and eight (doubly degenerate) in class E, besides three translations. The vibrations in class A are allowed in the Raman effect but forbidden in the infra-red. The vibrations in class B are forbidden in the Raman effect and allowed in the infra-red, but only in respect of electrical vibrations parallel to the optic axis. The vibrations in class E are allowed both in the Raman effect and in the infra-red, but in the latter case, only in respect of the electrical vibrations perpendicular to the optic axis.

The selection rules for the Raman effect appearing in the character table may be readily interpreted. In respect of the vibrations belonging to class A, the transverse components of the polarisability tensor vanish. In consequence, the lines of this class would be completely polarised. Geometrically interpreted, the tensor indicates that the ellipsoid of polarisability remains a spheroid while expanding and contracting along its axes, the directions of the latter also remaining fixed. The selection rules for class E result in a subdivision of the vibrations in this class into three sub-groups in all of which, however, the polarisability along the optic axis remains invariant. If therefore, the crystal is illuminated by a beam with its electric vector along the optic axis, the component of the vibration in the scattered light parallel to the optic axis would in every case vanish. Further, in all the sub-groups, as the result of the degeneracy, the two directions

TABLE III

TABLE III

Character Table

D_3	E	$2C_3^{\gamma}$	$3C_2$ $(C_\alpha, 2C_2)$	Total Number of vibrations	Translations	Number of vibrations	Selection rules in Raman Effect	Selection rules in Infra-red
A	1	1	1	4	0	4	$\epsilon_{\alpha\alpha} = \epsilon_{\beta\beta} = \epsilon_{\gamma\gamma}$; $\epsilon_{ik} = 0$	Forbidden
B	1	1	−1	5	1 (Q_γ)	4	Forbidden	$\begin{cases} M_\alpha = 0 \\ M_\beta = 0 \end{cases}$
E	2	−1	0	9	1 (Q_α, Q_β)	8	1. $\epsilon_{\alpha\alpha} = -\epsilon_{\beta\beta} = \epsilon_{\alpha\beta}$; $\epsilon_{\alpha\gamma} = \epsilon_{\beta\gamma}$; $\epsilon_{\gamma\gamma} = 0$ 2. $\epsilon_{\alpha\alpha} = -\epsilon_{\beta\beta} = \epsilon_{\alpha\beta} = 0$; $\epsilon_{\alpha\gamma}$; $\epsilon_{\beta\gamma}$; $\epsilon_{\gamma\gamma} = 0$ 3. $\epsilon_{\alpha\alpha} = -\epsilon_{\beta\beta} = \epsilon_{\alpha\beta}$; $\epsilon_{\alpha\gamma} = \epsilon_{\beta\gamma} = \epsilon_{\gamma\gamma} = 0$	$M_\gamma = 0$
U_R	9	0	1	EXPLANATION : α, β, γ are three perpendicular directions fixed relatively to the crystal, γ being the direction of the optic axis.				
t_R	27	0	−3					

TABLE IV

Tensor Components in Different Orientations

Direction of optic axis	Values of x, y, and z	Depolarisation			Total intensities		
		Electric vector along OY	Electric vector along OZ	Electric vector along OY and OZ	Electric vector along OY	Electric vector along OZ	Electric vector along OY and OZ
OZ	$z = \gamma$ $y = \beta$ $x = \alpha$	$\frac{\epsilon_{\beta\alpha}^2}{\epsilon_{\beta\gamma}^2}$	$\frac{\epsilon_{\gamma\alpha}^2}{\epsilon_{\gamma\gamma}^2}$	$\frac{\epsilon_{\alpha\beta}^2 + \epsilon_{\gamma\alpha}^2}{\epsilon_{\beta\gamma}^2 + \epsilon_{\gamma\gamma}^2}$	$\epsilon_{\alpha\beta}^2 + \epsilon_{\beta\gamma}^2$	$\epsilon_{\gamma\alpha}^2 + \epsilon_{\gamma\gamma}^2$	$\epsilon_{\alpha\beta}^2 + \epsilon_{\beta\gamma}^2 + \epsilon_{\gamma\alpha}^2 + \epsilon_{\gamma\gamma}^2$
OY	$y = \gamma$ $x = \beta$ $z = \alpha$	$\frac{\epsilon_{\beta\gamma}^2}{\epsilon_{\alpha\gamma}^2}$	$\frac{\epsilon_{\alpha\beta}^2}{\epsilon_{\alpha\alpha}^2}$	$\frac{\epsilon_{\beta\gamma}^2 + \epsilon_{\alpha\beta}^2}{\epsilon_{\alpha\gamma}^2 + \epsilon_{\alpha\alpha}^2}$	$\epsilon_{\beta\gamma}^2 + \epsilon_{\alpha\gamma}^2$	$\epsilon_{\alpha\beta}^2 + \epsilon_{\alpha\alpha}^2$	$\epsilon_{\alpha\beta}^2 + \epsilon_{\beta\gamma}^2 + \epsilon_{\alpha\gamma}^2 + \epsilon_{\alpha\alpha}^2$
OX	$x = \gamma$ $z = \beta$ $y = \alpha$	$\frac{\epsilon_{\gamma\alpha}^2}{\epsilon_{\alpha\beta}^2}$	$\frac{\epsilon_{\gamma\beta}^2}{\epsilon_{\beta\beta}^2}$	$\frac{\epsilon_{\gamma\alpha}^2 + \epsilon_{\gamma\beta}^2}{\epsilon_{\alpha\beta}^2 + \epsilon_{\beta\beta}^2}$	$\epsilon_{\gamma\alpha}^2 + \epsilon_{\alpha\beta}^2$	$\epsilon_{\gamma\beta}^2 + \epsilon_{\beta\beta}^2$	$\epsilon_{\gamma\alpha}^2 + \epsilon_{\gamma\beta}^2 + \epsilon_{\alpha\beta}^2 + \epsilon_{\beta\beta}^2$

perpendicular to the optic axis are equivalent. This has an important consequence, namely, that the scattered light observed along the optic axis would be always fully depolarised ($\rho = 1$). The second sub-class is distinguished by the fact that when the incident beam has its electric vibrations perpendicular to the optic axis, the light vector in the scattered radiation would have no components transverse to the optic axis. In the third sub-class, on the other hand, when the incident beam has its electric vibrations parallel to the optic axis the scattered radiations would vanish completely. The behaviour described above is readily understood in terms of the geometric behaviour of the ellipsoid of polarisability in the respective cases. The tensor relations indicate that in the second sub-class of vibrations, the ellipsoid of polarisability oscillates about the α and β axes without change of form. In the third sub-class on the other hand, the ellipsoid deforms but without any change in the position of its axes. In the first sub-class, both types of movements occur, the polarisability along the optic axis however remaining constant.

In an earlier paper, the author (1940) has shown how the selection rules for the Raman effect may be deduced and interpreted geometrically. The discussion in that paper showed that in systems in which the optic axis is one of threefold symmetry but not also one of twofold symmetry and has no plane of symmetry perpendicular to it, the degenerate vibrations are represented by one or another of the three types of tensor referred to above of which only the first was given by Placzek. The selection rules for the infra-red shown in the last column of the character table can also be derived from simple geometric considerations. Let M_α, M_β, M_γ be the electric dipole moments along the α, β and γ-axes, due to a particular vibration. γ is the optic axis and the direction of α is so chosen that it is an axis of twofold symmetry. If a vibration is symmetric to the γ-axis, then obviously M_α and M_β both vanish. If in addition, the vibration is symmetric to the α-axis, M_γ also vanishes. Such a vibration which belongs to class A is therefore inactive in the infra-red. Considering now a vibration which is antisymmetric to the α-axis, it is clear that M_α vanishes, and if, in addition, the vibration is symmetric to the γ-axis, $M\beta$ also vanishes. In such a vibration which belongs to class B, the dipole moment is therefore parallel to the optic axis, and the infra-red absorption appears only in the extraordinary ray. The vibrations in class E are doubly degenerate, *i.e.*, there are two normal co-ordinates having the same frequency but differing from each other in the directions of vibrations which can be obtained one from the other by a rotation about the optic axis of the crystal. These vibrations may be divided into three classes according as the motions of the atoms are in a

direction perpendicular to the optic axis or along the optic axis or along both simultaneously. It is evident that in the first case there would be no change of dipole moment along the optic axis. In the second case, the oscillations have the character of a tilt or rotation about a line perpendicular to the optic axis. In consequence, the amplitude of some of the atoms will be positive and of the others negative, and their magnitudes would be so related that there is no change of moment along the optic axis. The same result would be obtained when both types of vibration are combined.

8. *Intensity and Polarisation of Raman Lines*

The behaviour of the polarisability tensors given in the character table in transverse light scattering can be easily worked out. Let OX be the direction of illumination, OY the direction of observation, OZ being perpendicular to both, E_x, E_y and E_z the components of the incident electric vector in these directions and Δm_x and Δm_z the induced moments in x and z directions. Then we have

$$\Delta m_x = \epsilon_{xx} \cdot E_x + \epsilon_{xy} \cdot E_y + \epsilon_{xz} \cdot E_z$$

$$\Delta m_z = \epsilon_{zx} \cdot E_x + \epsilon_{zy} \cdot E_y + \epsilon_{zz} \cdot E_z$$

where ϵ_{xx}, ϵ_{yy}, ϵ_{zz}, ϵ_{xy}, ϵ_{yz}, ϵ_{zx} are the six components of the change of polarisability tensor such that $\epsilon_{xy} = \epsilon_{yx}$.

The components of the electric vector in the incident light are in the y and z directions. Hence if the incident light vector is along OY, the depolarisation is given by

$$\rho = \frac{(\Delta m_x)^2}{(\Delta m_z)^2} = \frac{\epsilon_{xy}^2}{\epsilon_{yz}^2}$$

and if the electric vector is along OZ, $\rho = \dfrac{\epsilon_{xz}^2}{\epsilon_{zz}^2}$.

If we denote the optic axis of the crystal by γ and the other two perpendicular axes of the crystal by α and β we can get the results for ρ for different orientations of the optic axis by simply denoting γ by z, y, x in turn and changing α and β accordingly. This is done in Table IV.

We can now find the behaviour in transverse scattering of the various tensor components given in the character table.

The behaviour of these tensors in longitudinal scattering has been worked out by the author in an earlier paper (1940).

9. *Symmetry Co-ordinates*

The character table shows that all the vibrations fall under three different classes of the point group, each class representing a type of symmetry which alone is allowed for the vibrations falling in that class. Any vibration Q_k may be stated in terms of the displacements of the atoms from their equilibrium positions as origin, *i.e.*,

$$Q_k = \sum_i a_{ik} x_i + \sum_i b_{ik} y_i + \sum_i c_{ik} z_i = \sum_i l_{ik} q_i$$

where x_i, y_i and z_i are the co-ordinates of the i^{th} atom with the equilibrium position as origin and a_{ik} is the amplitude of the i^{th} atom in the x_i direction for the co-ordinate Q_k. The various l_{ik}'s have therefore to satisfy certain symmetry conditions which give certain relations between them. But these conditions are not sufficient to give us the absolute values of l_{ik}'s for any particular vibration, because these depend also upon the binding forces in the vibrating system and have to be obtained by solving the secular equation. However, the geometry of the system gives us the required number of modes of vibration which possess the symmetry characters of the class to which they belong. These modes are called symmetry co-ordinates, and they differ from the normal co-ordinates in that the latter is a particular linear combination of them. The various symmetry co-ordinates are mutually orthogonal like the normal co-ordinates, *i.e.*, the coefficients l_{ik} of two symmetry co-ordinates (Q_k', Q_j') satisfy the relation

$$\sum_i l_{ik} \cdot l_{ij} = \begin{cases} 0 \text{ if } k \neq j \\ 1 \text{ if } k = j \end{cases}.$$

The symmetry co-ordinates are generally written as Q', but when a symmetry co-ordinate occurs singly in a class it becomes a normal co-ordinate and is written as Q.

The symmetry co-ordinates for the non-degenerate modes can be written down easily from the character table, and the symmetry co-ordinates for the three translations can be written directly. This enables us to write the symmetry co-ordinates for the degenerate class by using the orthogonality relations between the various co-ordinates and by the help of the character table. The degenerate symmetry co-ordinates are written with suffixes *a* and *b* (Q_a', Q_b').

TABLE V

Intensity and Depolarisation

Illumination along OX; Observation along OY

Class	Tensor component	Direction of optic axis	Depolarisation			Total intensities		
			Electric vector along OY	Electric vector along OZ	Electric vector along OY and OZ	Electric vector along OY	Electric vector along OZ	Electric vector along OY and OZ
A	$\epsilon_{\alpha\alpha} = \epsilon_{\beta\beta} \mp \epsilon_{\gamma\gamma}$ $\epsilon_{\alpha\beta} = \epsilon_{\beta\gamma} = \epsilon_{\alpha\gamma} = 0$ $\epsilon_{\alpha\alpha} = a$; $\epsilon_{\gamma\gamma} = c$	OZ OY OX	f f f	0 0 0	0 0 0	0 0 0	c^2 a^2 a^2	c^2 a^2 a^2
E_1	$\epsilon_{\alpha\alpha} = -\epsilon_{\beta\beta} = \epsilon_{\alpha\beta} = a$ $\epsilon_{\alpha\gamma} = \epsilon_{\beta\gamma} = b$ $\epsilon_{\gamma\gamma} = 0$	OZ OY OX	$\frac{a^2}{b^2}$ 1 $\frac{b^2}{a^2}$	∞ 1 $\frac{b^2}{a^2}$	$\frac{a^2+b^2}{b^2}$ 1 $\frac{b^2}{a^2}$	a^2+b^2 $2b^2$ b^2+a^2	b^2 $2a^2$ b^2+a^2	a^2+2b^2 $2(a^2+b^2)$ $2(b^2+a^2)$
E_2	$\epsilon_{\alpha\alpha} = -\epsilon_{\beta\beta} = \epsilon_{\alpha\beta} = 0$ $\epsilon_{\alpha\gamma} = \epsilon_{\beta\gamma} = b$ $\epsilon_{\gamma\gamma} = 0$	OZ OY OX	0 1 ∞	∞ f ∞	1 1 ∞	b^2 $2b^2$ b^2	b^2 0 b^2	$2b^2$ $2b^2$ $2b^2$
E_3	$\epsilon_{\alpha\alpha} = -\epsilon_{\beta\beta} = \epsilon_{\alpha\beta} = a$ $\epsilon_{\alpha\gamma} = \epsilon_{\beta\gamma} = 0$ $\epsilon_{\gamma\gamma} = 0$	OZ OY OX	∞ f 0	f 1 0	∞ 1 0	a^2 0 a^2	0 $2a^2$ a^2	a^2 $2a^2$ $2a^2$

We may now illustrate the method of deriving the symmetry co-ordinates by obtaining them for the totally symmetric vibrations (belonging to class A) in quartz. The vibrating unit in quartz consists of nine atoms, 3 silicons (1, 2, 3) and 6 oxygens (4, 5, 6, 7, 8, 9). The general linear expression for Q is then

$$Q = \sum_1^9 a_i x_i + \sum_1^9 b_i y_i + \sum_1^9 c_i z_i$$

Here positive (+) x_i points towards a point in the basal plane containing the given atom where the three-fold axis meets it, z_i is perpendicular to this plane and y_i is at right angles to both and is positive in a direction which makes the motion right-handed. On account of the symmetry about the three-fold axis C_3 we have

$$a_1 = a_2 = a_3; \quad a_4 = a_6 = a_8; \quad a_5 = a_7 = a_9$$

and similar relations in b and c. On account of the symmetry about a two-fold axis C_2^1 (see the representation of 3 C_2 in terms of the positions of atoms) we have

$$\begin{aligned} a_2 &= a_3, & a_4 &= a_9, & a_5 &= a_8, & a_6 &= a_7. \\ b_2 &= -b_3, & b_4 &= -b_9, & b_5 &= -b_8, & b_6 &= -b_7. \\ c_2 &= -c_3, & c_4 &= -c_9 & c_5 &= -c_8, & c_6 &= -c_7. \end{aligned}$$

Combining these relations with those previously obtained we find:

$$\begin{aligned} &a_1 = a_2 = a_3; && a_4 = a_5 = a_6 = a_7 = a_8 = a_9 \\ &b_1 = b_2 = b_3 = 0; && b_4 = b_6 = b_8 = -b_5 = -b_7 = -b_9 \\ &c_1 = c_2 = c_3 = 0; && c_4 = c_6 = c_8 = -c_5 = -c_7 = -c_9. \end{aligned}$$

Hence the general expression for Q becomes

$$\begin{aligned} Q = {} & a_2 (x_1 + x_2 + x_3) + a_4 (x_4 + x_5 + x_6 + x_7 + x_8 + x_9) \\ & + b_4 (y_4 + y_6 + y_8 - y_5 - y_7 - y_9) + c_4 (z_4 + z_6 + z_8 - z_5 - z_7 - z_9). \end{aligned}$$

This gives the following four symmetry co-ordinates:

$$\left.\begin{aligned} Q_1' &\to x_1 + x_2 + x_3 \\ Q_2' &\to x_4 + x_5 + x_6 + x_7 + x_8 + x_9 \\ Q_3' &\to y_4 + y_6 + y_8 - y_5 - y_7 - y_9 \\ Q_4' &\to z_4 + z_6 + z_8 - z_5 - z_7 - z_9. \end{aligned}\right\} \quad \text{A (4)}$$

The symmetry co-ordinates for class B can be similarly obtained. They are:

$$\left.\begin{aligned} Q_z &\to m_1^{\frac{1}{2}} (z_1 + z_2 + z_3) + m_2^{\frac{1}{2}} (z_4 + z_5 + z_6 + z_7 + z_8 + z_9) \\ Q_6' &\to x_5 + x_7 + x_9 - x_4 - x_6 - x_8 \\ Q_7' &\to 2 m_2^{\frac{1}{2}} (z_1 + z_2 + z_3) - m_1^{\frac{1}{2}} (z_4 + z_5 + z_6 + z_7 + z_8 + z_9) \\ Q_8' &\to y_1 + y_2 + y_3 \\ Q_9' &\to y_4 + y_5 + y_6 + y_7 + y_8 + y_9 \end{aligned}\right\} \quad \text{B (5)}$$

for the degenerate class E we have

$$\begin{aligned}
Q_x \rightarrow\ & m_1^{\frac{1}{2}}(-x_1+x_2\cos 60+y_2\sin 60+x_3\cos 60-y_3\sin 60)\\
& +m_2^{\frac{1}{2}}\{-x_5\cos\alpha+y_5\sin\alpha+x_7\cos(\alpha-60)-y_7\sin\\
& (\alpha-60)-x_9\cos(120-\alpha)-y_9\sin(120-\alpha)-x_4\cos\\
& (120-\alpha)+y_4\sin(120-\alpha)+x_5\cos(\alpha-60)+y_6\sin\\
& (\alpha-60)-x_8\cos\alpha-y_8\sin\alpha\}
\end{aligned}$$

$$\begin{aligned}
Q_{11a}' \rightarrow\ & 2\,m_2^{\frac{1}{2}}(x_1-x_2\cos 60-y_2\sin 60-x_3\cos 60+y_3\sin 60)\\
& +m_1^{\frac{1}{2}}[-x_5\cos\alpha+y_5\sin\alpha+x_7\cos(\alpha-60)\\
& -y_7\sin(\alpha-60)-x_9\cos(120-\alpha)-y_9\sin(120-\alpha)\\
& -x_4\cos(120-\alpha)+y_4\sin(120-\alpha)+x_6\cos(\alpha-60)\\
& +y_6\sin(\alpha-60)-x_8\cos\alpha-y_8\sin\alpha]
\end{aligned}$$

$$Q_{12a}' \rightarrow (2\,y_3-y_1-y_2)+\sqrt{3}\,(x_2-x_1)$$

$$\begin{aligned}
Q_{13a}' \rightarrow\ & \{-x_5\cos\alpha+y_5\sin\alpha+x_7\cos(\alpha-60)-y_7\sin(\alpha-60)\\
& -x_9\cos(120-\alpha)-y_9\sin(120-\alpha)\}-\{-x_4\cos(120-\alpha)\\
& +y_4\sin(120-\alpha)+x_6\cos(\alpha-60)+y_6\sin(\alpha-60)\\
& -x_8\cos\alpha-y_8\sin\alpha\}
\end{aligned}$$

$$\begin{aligned}
Q_{14a}' \rightarrow\ & (y_5+x_9\cos 30-y_9\sin 30-x_7\cos 30-y_7\sin 30)\\
& +(y_4+x_8\cos 30-y_8\sin 30-x_6\cos 30-y_6\sin 30)
\end{aligned}$$

$$\begin{aligned}
Q_{15a}' \rightarrow\ & (y_5+x_9\cos 30-y_9\sin 30-x_7\cos 30-y_7\sin 30)\\
& -(y_4+x_8\cos 30-y_8\sin 30-x_6\cos 30-y_6\sin 30)
\end{aligned}$$

$$\begin{aligned}
Q_{16a}' \rightarrow\ & m_1^{\frac{1}{2}}\sqrt{3}\,d\,(z_2-z_3)+\\
& 2\,m_2^{\frac{1}{2}}f\,\{(z_4-z_9)\sin(120-\alpha)+(z_5-z_8)\sin\alpha+\\
& (z_6-z_7)\sin(\alpha-60)\}
\end{aligned}$$

$$\begin{aligned}
Q_{17a}' \rightarrow\ & (z_4-z_9)\cos(120-\alpha)-(z_5-z_8)\cos\alpha-(z_6-z_7)\\
& \cos(\alpha-60)
\end{aligned}$$

$$\begin{aligned}
Q_{18a}' \rightarrow\ & m_2^{\frac{1}{2}}\sqrt{3}\,f(z_2-z_3)-m_1^{\frac{1}{2}}\,d\,\{(z_4-z_9)\sin(120-\alpha)\\
& +(z_5-z_8)\sin\alpha+(z_6-z_7)\sin(\alpha-60)\}
\end{aligned}$$

$$\begin{aligned}
Q_y \rightarrow\ & m_1^{\frac{1}{2}}\{-y_1-x_2\cos 30+y_2\sin 30+x_3\cos 30+y_3\sin 30\}\\
& +m_2^{\frac{1}{2}}\{-x_4\sin(120-\alpha)-y_4\cos(120-\alpha)-x_5\sin\alpha\\
& -y_5\cos\alpha-x_6\sin(\alpha-60)+y_6\cos(\alpha-60)\\
& +x_7\sin(\alpha-60)+y_7\cos(\alpha-60)+x_8\sin\alpha-y_8\cos\alpha\\
& +x_9\sin(120-\alpha)-y_9\cos(120-\alpha)\}.
\end{aligned}$$

$$Q_{11b}' \rightarrow 2\,m_2^{\frac{1}{2}}\{y_1 + x_2\cos 30 - y_2\sin 30 - x_3\cos 30 - y_3\sin 30\}$$
$$+ m_1^{\frac{1}{2}}\{-x_4\sin(120-\alpha) - y_4\cos(120-\alpha) - x_5\sin\alpha$$
$$- y_5\cos\alpha - x_6\sin(\alpha-60) + y_6\cos(\alpha-60)$$
$$+ x_7\sin(\alpha-60) + y_7\cos(\alpha-60) + x_8\sin\alpha - y_8\cos\alpha$$
$$+ x_9\sin(120-\alpha) - y_9\cos(120-\alpha)\}.$$

$$Q_{12b}' \rightarrow (2x_3 - x_2 - x_1) - \sqrt{3}\,(y_2 - y_1)$$

$$Q_{13b}' \rightarrow \{-x_5\sin\alpha - y_5\cos\alpha + x_7\sin(\alpha-60) + y_7\cos(\alpha-60)$$
$$+ x_9\sin(120-\alpha) - y_9\cos(120-\alpha)\} - \{-x_4\sin(120-\alpha)$$
$$- y_4\cos(120-\alpha) - x_6\sin(\alpha-60) + y_6\cos(\alpha-60) + x_8\sin\alpha$$
$$- y_8\cos\alpha\}.$$

$$Q_{14b}' \rightarrow (x_5 - x_9\cos 60 - y_9\sin 60 - x_7\cos 60 + y_7\sin 60)$$
$$+ (-x_4 + x_8\cos 60 + y_8\sin 60 + x_6\cos 60 - y_6\sin 60)$$

$$Q_{15b}' \rightarrow (x_5 - x_9\cos 60 - y_9\cos 60 - x_7\cos 60 + y_7\sin 60)$$
$$- (-x_4 + x_8\cos 60 + y_8\sin 60 - x_6\cos 60 - y_6\sin 60)$$

$$Q_{16b}' \rightarrow m_1^{\frac{1}{2}}\,d\,(2z_1 - z_2 - z_3) + 2\,m_2^{\frac{1}{2}}\,f\{(z_4 + z_9)\cos(120-\alpha)$$
$$+ (z_5 + z_8)\cos\alpha - (z_6 + z_7)\cos(\alpha-60)\}$$

$$Q_{17b}' \rightarrow (z_4 + z_9)\sin(120^\circ - \alpha) - (z_5 + z_8)\sin\alpha + (z_6 + z_7)$$
$$\sin(\alpha - 60)$$

$$Q_{18b}' \rightarrow m_2^{\frac{1}{2}}\,f\,(2z_1 - z_2 - z_3) - m_1^{\frac{1}{2}}\,d\{(z_4 + z_9)\cos(120-\alpha)$$
$$+ (z_5 + z_8)\cos\alpha - (z_6 + z_7)\cos(\alpha-60)\}.$$

In the above d and f are respectively the distances of the silicon atoms (1, 2 and 3) and of the oxygen atoms (4, 5, 6, 7, 8 and 9) projected on the basal plane and measured from its intersection with the three-fold axis, α, $(\alpha - 60°)$ and $(120° - \alpha)$ are the angles which d and f make with each other; and m_1 and m_2 are the masses of the silicon and oxygen atoms respectively.

10. Symmetry Modes

The types of displacement associated with the symmetry co-ordinates are diagrammatically represented in Fig. 2. In the degenerate class only those with suffix ' a ' are shown in the figure. All the observed frequencies belonging to any particular class of symmetry can be assigned to some combinations of the various symmetry modes belonging to that class.

These modes of vibration refer to an individual cell in the crystal lattice, but when we are considering the lattice as a whole, all the equivalent points of the lattice must have the same motion at a given instant. This leads to some interesting consequences in a crystal (like quartz) where the

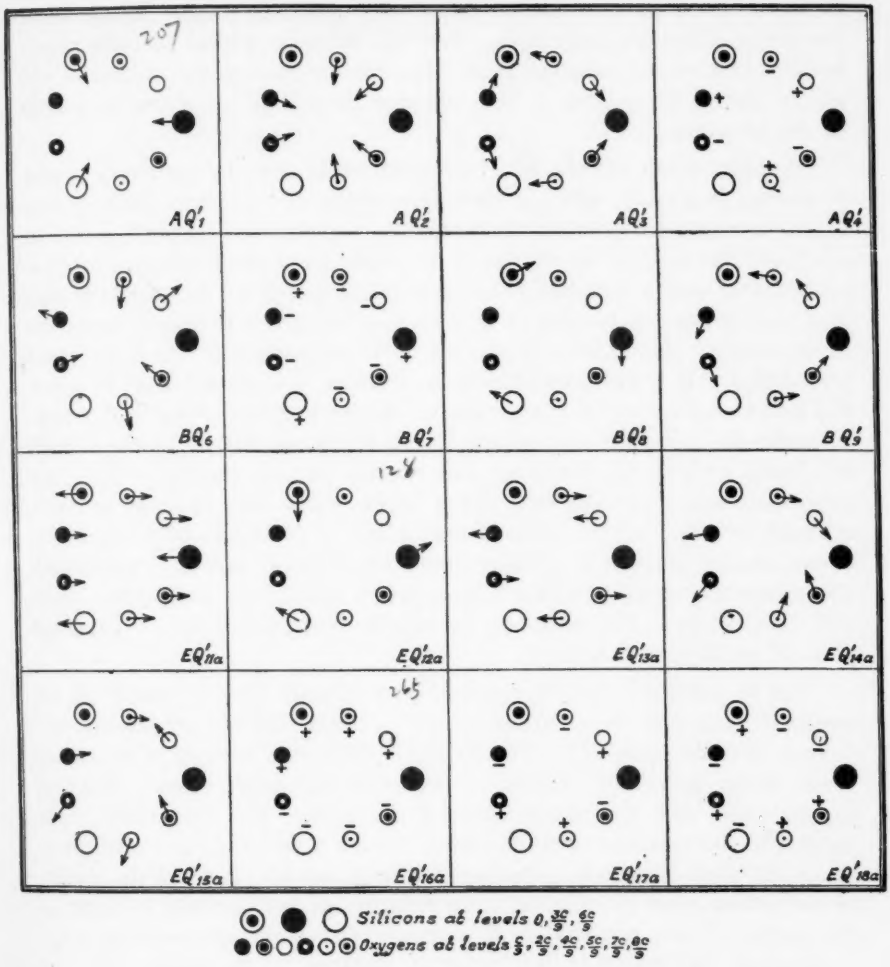

FIG. 2

Symmetry Modes of the Quartz Lattice

atoms are continuously linked together. Let us suppose that a vibration having the symmetry co-ordinate Q_1' is present in the different cells (see Fig. 1). In this vibration the three silicon atoms (1, 2, 3) move in the horizontal plane all away from or all towards the three-fold axis. It may now be seen that the motions of intermediate silicon atoms (1′, 2′, 3′) are always opposite in phase to those of (1, 2, 3). Thus the figure formed by the atoms

(1, 2, 3, 1′, 2′, 3′) alternately approaches towards or further recedes from the shape of a regular hexagon. We may therefore expect that the neighbouring cells would influence each other notably through the motion of the silicon atoms, the extent of this influence depending upon the amplitude of the vibration.

Another result evident from the diagrams is that the symmetry modes in quartz, in general, differ in form from those of an isolated SiO_4 group. If, for instance, we consider the breathing oscillation of the SiO_4 group in which the four oxygens move towards the silicon atom along the bond lengths, we find that such a vibration is not possible in quartz for the simple reason that each oxygen is bonded to two silicons, so that if it moves along the Si–O bond for one atom it is moving at an inclination to the Si–O bond for another. It is however possible to visualise two special cases in which the lattice oscillations in quartz may be similar to those of an SiO_4 group. Consider the symmetry co-ordinate Q_2' in which the oxygen atoms in each cell move towards the three-fold axis passing through that cell. The four oxygen atoms surrounding each silicon atoms would then be found to move symmetrically with regard to the *diad*-axis (axis of two-fold symmetry) of the crystal passing through it. This movement is therefore similar to the doubly degenerate vibration $\nu_{2,3}$ of the SiO_4 group in which only the oxygens move and transversally. The mode now belongs, however, to the totally symmetric class of oscillations in quartz.

Let us consider next the symmetry co-ordinate Q_{11a}' in which all the atoms in each cell move parallel to the 'x' axis [the line joining the projections of silicon atoms (1, 1′) on the basal plane], the motions of the silicon atoms being oppositely directed to those of the oxygen atoms. The four oxygen atoms and the silicon atom of the group SiO_4 therefore move parallel to the x-axis in opposite phases. Such a vibration is equivalent to one of the triply degenerate vibrations of the group AX_4 in which the motion of the central atom A is in the same direction as but opposite in phase to the motion of four surrounding X atoms. The symmetry co-ordinate Q_7' is similarly analogous to this mode of vibration of the group AX_4, the movements of the silicon and oxygen atoms being now parallel to the optic axis. We shall see later that this similarity between the symmetry co-ordinates Q_{11}' and Q_7' is very significant in relation to the infra-red absorption data.

11. Classification of the Observed Frequencies

The analysis of the possible vibrations set out in the character table immediately explains the general features revealed by a scrutiny of the available experimental data (Section 2). These are:

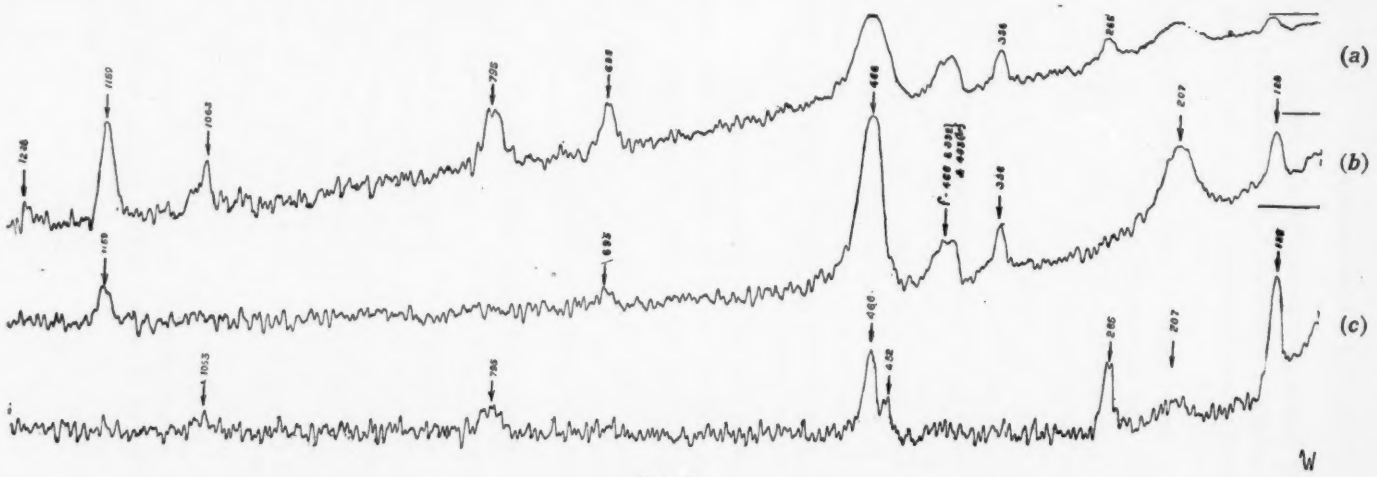

FIG. 3

Raman spectra of quartz with optic axis along the direction of observation and with
(*a*) incident light unpolarised
(*b*) incident light polarised with electric vector perpendicular to the directions of illumination and observation
(*c*) incident light polarised with electric vector along the direction of observation.

(1) the dichroism of quartz in the infra-red absorption;

(2) the fact that certain frequencies are Raman-active but are not allowed in the infra-red absorption either in the ordinary or extra-ordinary ray;

(3) the frequencies which appear in the infra-red absorption in the ordinary ray are also Raman-active; and

(4) the frequencies which appear in the infra-red absorption in the extra-ordinary ray are Raman-inactive.

The number of Raman-active frequencies according to the analysis is 12. Actually, 16 frequencies are observed and we have to discover which of these are fundamentals and which are combinations and to place the former in the three classes A, B and E. In doing this we may be guided by the following lines of evidence: (*a*) the intensity of the Raman lines; (*b*) their appearance in infra-red absorption in the ordinary ray; (*c*) their disappearance in the extraordinary infra-red absorption. On the basis of the observed facts, we may *provisionally* identify the following as fundamentals and place them in the classes indicated:

Class A: 207, 356 and 466 and one other frequency.

Class B: Reflection Maxima at $27{\cdot}5\mu$, $19{\cdot}7\mu$, $12{\cdot}87\mu$ and $8{\cdot}7\mu$.

Class E: 128, 265, 392, 695, 795 and three other frequencies.

To complete the classification it is necessary to ascertain the polarisation characters of the Raman lines and also their behaviour in excitation by polarised light for different orientations of the crystal.

12. *Results with Polarised Excitation*

In studying the Raman spectrum of a single crystal, we may vary its orientation relatively to the directions of the incident and scattered beams and in addition vary the state of polarisation of the incident light. Denoting the direction of the illuminating pencil by OX, the transverse direction of observation by OY and the direction perpendicular to both by OZ, the optic axis may be along either OX, OY or OZ and the incident light may be either unpolarised, or polarised with its electric vector either along OY or OZ. The optical activity of quartz and the consequent rotation of the plane of polarisation of a light beam passing along the optic axis, is a disturbing factor when we wish to study the effect of polarising an incident beam travelling along the optic axis or of analysing a scattered beam when it is observed along the optic axis. Table VI shows the various cases in which this complication does not arise.

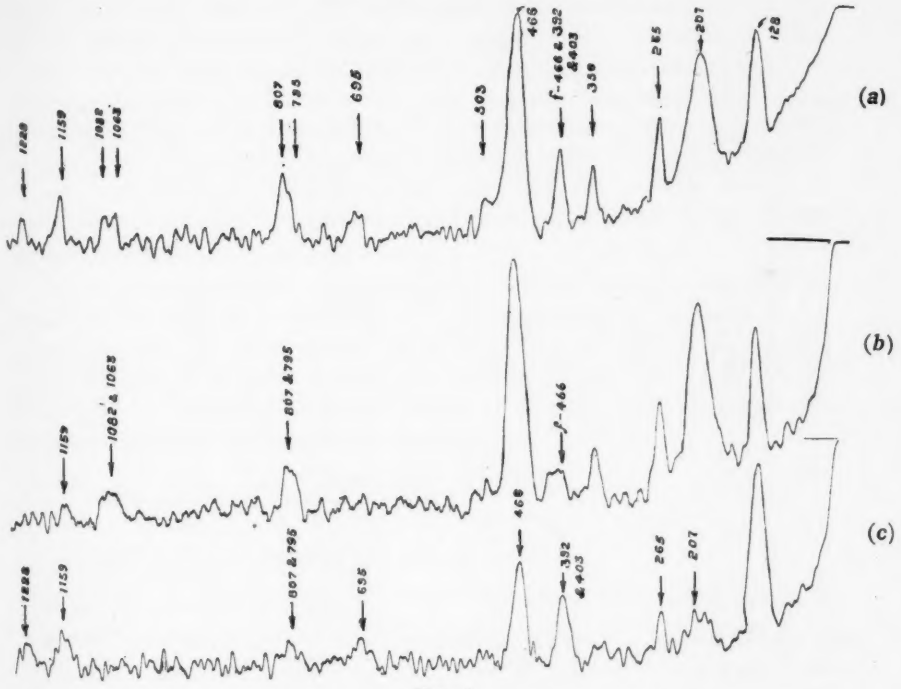

FIG. 4

Raman spectra of quartz with optic axis perpendicular to the directions of observation and illumination and with

(*a*) incident light unpolarised
(*b*) incident light polarised with electric vector along the optic axis
(*c*) incident light polarised with electric vector along the direction of observation.

The orientation of the crystal, the direction of the electric vector in the incident light (I. L.) and in the scattered light (S. L.) are indicated by appropriate symbols against the respective spectrograms to which references are given in this table. A scrutiny of these spectrograms which are reproduced in Plate III, Figs. 5 and 6 and in Plate IV, Figs. 7 and 8 enables us to appreciate the general nature of the experimental results at a glance.

In agreement with the results of the character table and the selection rules, there are four Raman lines which are fully polarised and are therefore due to the symmetric vibrations of class A. These are the lines with frequency shifts 207, 356, 466 and 1082. This is seen from the spectrograms reproduced in Fig. 8 which show the analysis of the scattered light. When the incident light is unpolarised, and the scattered light is analysed, these

TABLE VI

Index of Spectra

Incident Beam along	Optic axis along	Observation along	Incident vector light along	Nature of the Study	Reference to Spectrograms in the Plates
					FIG.
OX	OX	OY	OY and OZ	Total intensity	6 (h)
				State of polarisation	8 (p) and 8 (q)
OX	OY	OY	OY	Total intensity	5 (*a*)
OX	OY	OY	OZ	,,	5 (*c*)
OX	OY	OY	OY and OZ	,,	5 (*b*), 6 (*d*) and 6 (*g*)
OX	OZ	OY	OY	Total intensity	7 (*i*)
				State of polarisation	(not reproduced)
OX	OZ	OY	OZ	Total intensity	7 (*k*)
				State of polarisation	8 (*l*) and 8 (*m*)
OX	OZ	OY	OY and OZ	Total intensity	7 (*j*)
				State of polarisation	8 (*n*) and 8 (*o*); 6 (*e*) and 6 (*f*)

lines appear strongly in the OZ component, and either very weakly or not at all in the OX component. When the incident light is polarised with the electric vector along OZ, they appear strongly, but when the incident light vector is along OY they either fail to appear or appear only very weakly [Fig. 5 (*a*) and (*c*) and Fig. 7 (*i*) and (*k*) and microphotometer records Fig. 3 (*b*), (*c*) and Fig. 4 (*b*) and (*c*)]. The line 1082 is the weakest of the four and is of sensible intensity only when the optic axis of the crystal is perpendicular to the direction of observation and parallel to the incident light vector [Fig. 6 (*d*), (*e*), (*f*), (*g*), (*h*) and Fig. 8 (*p*) and (*q*)].

The remaining lines, namely, 128, 265, 392, 403, 479, 503, 695, 795, 807, 1063, 1159 and 1228 behave very differently from the lines in class A. They all have certain features in common which characterise the degenerate vibrations of class E. One of these is that the tensor $\epsilon_{\gamma\gamma}$ vanishes. Accordingly, as has already been remarked, all lines in class E should fail to appear in the component parallel to the optic axis when the vibrations in the incident light are also in that direction, whereas the lines in class A would appear strongly in the same circumstances. This result has been confirmed experimentally in the present investigation, and the contrasted behaviour of the A and E classes in this respect is strikingly illustrated in Fig. 8 (*lm*). Then,

again, as already remarked, the two directions perpendicular to the optic axis are exactly equivalent for vibrations of the E class. Accordingly, if the scattered light is observed in the direction of the optic axis, the lines in this class should all exhibit a depolarisation exactly equal to one irrespective of the direction or the state of polarisation of the incident light, whereas the lines in class A would in general be strongly polarised in the same circumstances. As we are dealing with monochromatic radiations, the optical activity of quartz should obviously not stand in the way of this result being experimentally confirmed.

Apart from the common features set out above, however, the lines in class E do not all behave similarly when the orientation of the crystal or the state of polarisation of the incident light is varied. A study of the spectrograms shows that they fall into three sub-classes which correspond to the three types of polarisability tensor shown in the character table and discussed in Section 7 above. These sub-classes are:

Sub-class E (1): 128, 452, 479, 503 and 1228;

Sub-class E (2): 265, 795, 807 and 1063; and

Sub-class E (3): 392, 403, 695 and 1159.

The differences between these classes become evident when we study their excitation using incident polarised light. The lines in sub-class E (2) vanish when the incident light vector is perpendicular to the optic axis and the scattered light is observed along the optic axis. It will be seen from Fig. 5 (*c*) and microphotometer record 3 (*b*) that the four lines under sub-class E (2) have vanished. These lines also vanish when the crystal is illuminated along the optic axis and the component of the scattered light with its electric vector perpendicular to the optic axis is observed [see Plate IV, Fig. 8 (*p*)]. The lines in sub-class E (3) should vanish when the electric vector in the incident light is parallel to the optic axis. It will be seen from Fig. 5 (*a*) and 7 (*k*) and microphotometer record Fig. 3 (*c*) and Fig. 4 (*b*) that the four lines in question vanish or become very weak in these circumstances. The lines belonging to sub-class E (1) continue to be observable strongly when the lines in sub-class (*a*) or (*b*) vanish or become very weak in the circumstances stated above [Fig. 5 (*a*), (*c*) and Fig. 7 (*i*), (*k*) and microphotometer records 3 and 4 (*b*) and (*c*)]. As explained in Section 7, the three sub-classes into which the E group of lines has been divided correspond to the three possible types of polarisability tensor entered under the column headed " Selection rules in Raman effect " in the character table. These three types of tensor indicate that the corresponding modes of vibration possess certain specific features to which we shall return later.

It is appropriate that we here refer to the earlier attempts made to classify the frequency shifts observed with quartz. Of the four lines now placed in the A class, three, namely, 207, 356 and 466 have been shown by earlier authors Menzies (1929), Cabannes (1929, 1937) and Michalke (1938) to be fully or strongly polarised, thus agreeing with the present classification. The addition of the 1082 now made to this list of symmetric vibrations has been possible by the fact that in the present investigation, it has been fully resolved from the 1063 line which belongs to the degenerate class and behaves in a wholly different manner, whereas the earlier authors studied the behaviour of the unresolved doublet. Bouhet (1937) and Cabannes and Bouhet (1937) attempted to classify the stronger lines by illuminating the crystal with a circularly polarised beam along its optic axis and observing the light scattered longitudinally backwards along the optic axis. They found that the lines 207, 356 and 466 (which, as we have seen, correspond to symmetric vibrations) appeared with direct circular polarisation, the lines 265 and the unresolved doublet 795–807 vanished, while the lines 128, 392, 695 and 1159 appeared with reversed circular polarisation. Nedungadi (1940) showed that in similar observations with unpolarised light, the lines 265 and the doublet at 800 vanished. The disappearance of the lines in these circumstances is equivalent to the behaviour characteristic of the present sub-class E (2) in which the weak line at 1063 has now been included. The sub-division of the remaining lines of the E class into the sub-classes E (1) and E (3) and the recognition of the features which characterise these sub-classes can only be made with the use of plane-polarised incident light which has not been done by the earlier workers.

13. The Fundamental Frequencies

In Section 7, we had provisionally identified some of the observed frequencies as fundamentals and had assigned them to the three classes A, B and E mentioned in the character table. The frequencies 207, 356 and 466 were assigned to class A. The polarisation results now enable us to confirm this and add the fourth frequency 1082 as required by theory. Four infra-red reflexion maxima observed only in the extraordinary ray at $27{\cdot}5\,\mu$, $19{\cdot}7\,\mu$, $12{\cdot}87\,\mu$ and $8{\cdot}7\,\mu$ were placed in class B. The theory requires only four frequencies in this class, and as no more of this type are observed it may be assumed that these are fundamental frequencies. Theory requires eight frequencies in class E, and these have to be selected from amongst the thirteen frequencies 128, 265, 392, 403, 452, 479, 503, 795, 807, 1063, 1159 and 1228. The polarisation results show definitely that all these frequencies are degenerate and are therefore either fundamentals in class E or combinations of a fundamental in that class with other fundamentals. The Raman

lines with frequency shifts 128, 265, 695, 1063 and 1159 appear with considerable intensity and are therefore undoubtedly fundamentals. The two lines at 392 and 403 behave analogously in the polarised excitation of the spectra and have been both placed in sub-class E (3). The pair of lines at 795 and 807 also behave rather similarly and have been placed in sub-class E (2). These lines appear with fair intensity and it is probably correct to take the pairs as fundamentals which have suffered a Fermi splitting as the result of accidental degeneracy. Thus:

$$128 + 265 = 393$$

which falls in the region of the doublet 392–403, and

$$2 \times 403 = 806$$

which falls in the region of the doublet 795–807.

The four remaining lines, namely, 452, 479, 503 and 1228 are all weak. Amongst these, 479 is probably the weakest. It, however, coincides with an extremely strong infra-red reflection maximum in the ordinary ray and we are therefore obliged to include it as a fundamental in the E class. The two weak lines at 452 and 479 and the very intense line at 466 form a close and equally spaced triplet (see Fig. 9). We may reasonably regard the 452

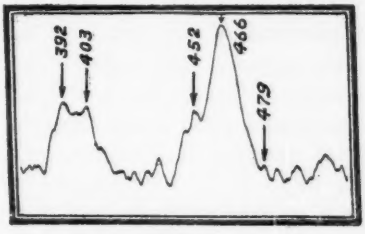

FIG. 9
Microphotometer Record

frequency as a combination due to the two fundamentals at 466 and 479 on the following scheme:

$$A + E \rightarrow E$$

$$2 \times 466 - 479 = 452$$

The weak line at 503 is probably also a combination on the scheme $B + E \rightarrow E$, of the fundamental frequency corresponding to the strong extraordinary reflection maximum at $27 \cdot 5\,\mu$ with the frequency 128 cm.$^{-1}$ which appears strongly in light scattering. The frequency 1228 may be explained as a combination on the scheme:

$$777\ B\ (= 12 \cdot 87\,\mu) + 452\ E \rightarrow 1229\ E$$

The result of the discussion is summed up in Table VII.

TABLE VII

Fundamental Frequencies

Frequency	Class	Selection rules	
		Raman	Infra-red
207, 356, 466, 1082	A	Permitted	Forbidden
364, 508, 777, 1149 (approximate) ..	B	Forbidden	$M_{\perp} = 0$
128, 479	E (1)	Permitted	$M_{\parallel} = 0$
265, 795–807, 1063	E (2)		
392–403, 695, 1159	E (3)		

$M_{\perp}$ and $M_{\parallel}$ signify respectively the electric moments perpendicular and parallel to the optic axis.

14. Correlation of Modes and Frequencies

As has already been stated, the symmetry modes illustrated in Fig. 2 are not actually the normal modes of vibration. The latter are obtained by suitable linear combinations of the symmetry modes falling within the particular class, and these cannot, in strict theory, be ascertained except by writing out the expression for the potential and kinetic energies for the general type of vibration in each class and finding the solution of the determinational equation which results. If, however, we are content with a less rigorous procedure and wish only to obtain an approximate idea of the nature of the vibration associated with each of the observed fundamental frequencies, this may be done partly by theoretical reasoning and partly from experimental evidence. We may, in fact, proceed to associate each of the 16 normal modes of vibration with that particular symmetry mode amongst the 16 illustrated in Fig. 2 which it resembles most nearly.

In the first place, the mass of a silicon atom is 28 while that of oxygen is 16. It is also known that the potential energies of deformation are greater for those displacements which involve extensions of the valence bonds than for those which involve a change of the angles between them. Accordingly, amongst the vibrations of any particular class, it may be expected that the lower frequencies would involve principally a motion of the silicon atoms, the higher frequencies principally a motion of the oxygen atoms and the intermediate frequencies a motion of both. Then again, the modes of vibration involving a stretching of the SiO bonds would be of higher

frequency than those involving only a change of the valence angles, while the modes which involve both would be of intermediate frequency. These principles may be the more readily applied to obtain a qualitative idea of the mode of vibration corresponding to a particular frequency when the number of independent modes is not too large and their frequencies differ widely. This is the case in respect of classes A and B, and we may, without fear of serious error, associate the observed frequencies with the symmetry modes pictured in Fig. 2 in the manner shown below in Table VIII.

TABLE VIII

Correlation of Modes and Frequencies : Classes A and B

Class	Frequency	Symmetry Mode	Description of Symmetry Mode
A	207	Q_1'	Radial motion of silicon atoms
total symmetric class	356	Q_4'	Motion of oxygen atoms along optic axis
	466	Q_2'	Radial motion of oxygen atoms
	1082	Q_3'	Valence oscillation of oxygen atoms
B	364	Q_8'	Transverse motion of silicon atoms
	508	Q_7'	Translational oscillation of silicon and oxygen atoms against each other along optic axis
	777	Q_6'	Radial motion of oxygen atoms
	1149	Q_9'	Valence oscillation of oxygen atoms

The assignments made in Table VIII on the grounds already stated are supported by other experimental evidence. The table assigns the lowest frequency of 207 in class A to the only symmetry mode in this class which involves a motion of the silicon atoms, this being radial and directed towards the trigonal axis. The intensity of the 207 line and its extraordinary behaviour with rise of temperature which distinguishes it sharply from the other lines of this class, both indicate that it involves principally a motion of this type. That the mode of highest frequency in the class (1082) involves an oscillation of the oxygen atoms in the direction of the valence bonds is *prima facie* clear, and this is further confirmed by the remarkable behaviour of the 1082 line which appears with sensible intensity only when the electric vector in the incident light is parallel to the optic axis. In the particular mode under consideration, two of the oxygen atoms attached to a silicon atom approach the latter in the basal plane while the two others recede to

an equal extent. The change of polarisability would therefore be zero in the basal plane and small but finite along the optic axis, in agreement with the observed feeble intensity of the line. The very great intensity of the 466 line as compared with 356, and the fact that the former broadens appreciably with rise of temperature while the latter does not, indicate quite clearly that the former must be assigned to a radial motion of the oxygen atoms and the latter to one involving their movement parallel to the optic axis.

The correlation of the modes and frequencies in class B is closely analogous to that for class A, as will be seen at once if the modes in the two classes as shown in Table VIII are arranged in the order of increasing frequency. The assignments made are further confirmed by the evidence of the infra-red absorption intensities. The vibrations in class B produce an electric moment parallel to the optic axis, and it is obvious that the most intense absorption would therefore correspond to the mode Q_7' in which all the oxygens and all the silicons move against each other parallel to the optic axis. The frequency assigned to this mode actually corresponds to the strongest infra-red reflection in the extraordinary ray at $19{\cdot}7\,\mu$. The three other modes in the class involve only movements of the atoms perpendicular to the optic axis, and it might seem at first sight that the resulting electric moment parallel to the optic axis should vanish. A closer consideration shows, however, that as the valence bonds within the cell spiral upwards, the movements of the oxygen atoms, though parallel to the basal plane, would involve a transport of charge perpendicular to it, thus giving rise to a strong electric moment along the optic axis. The magnitude of the electric moment thus produced would evidently be largest for the mode Q_9' in which six oxygens move parallel to the valence bonds, less for the mode Q_8' in which only the three silicon atoms move parallel to the valence bonds and least for the mode Q_6' in which three oxygens move in and three oxygens move out radially. These conclusions are in accord with the experimental facts, namely, that the infra-red reflexion maxima at $8{\cdot}7\,\mu$, $27{\cdot}5\,\mu$ and at $12{\cdot}87\,\mu$ follow each other in the order stated in respect of intensity.

Table IX indicates in respect of the eight doubly degenerate normal modes in class E, the symmetry modes which they most nearly resemble. The assignments have been made on the basis of the general principles already indicated and considering also the observed intensities of the infra-red maxima in the ordinary ray and the behaviour of the Raman lines in respect of intensity and polarisation. We shall now proceed to justify the assignments in detail.

TABLE IX

Correlation of Modes and Frequencies: Class E

Class	Frequency	Symmetry Mode	Description of Symmetry Mode
E (1)	128	Q_{12}'	Deformational oscillation of silicon atoms in the basal planes
	479	Q_{11}'	Translational oscillation of oxygen and silicon atoms against each other in basal planes
E (2)	265	Q_{16}'	Group movements of silicon and oxygen atoms along optic axis
	795 } 807 }	Q_{17}'	Oscillation of oxygen atoms along optic axis
	1063	Q_{18}'	Oscillation of oxygen and silicon atoms along optic axis
E (3)	392 } 403 }	Q_{14}'	Deformational oscillation of oxygen atoms in the basal planes
	695	Q_{13}'	Translational oscillation of oxygen atoms against each other in the basal planes
	1159	Q_{15}'	Deformational oscillation of oxygen atoms in the basal planes

As remarked earlier in the paper, the symmetry mode Q_{11}' represents the translatory motion of the silicon atoms against the oxygen atoms in the basal plane and closely resembles the mode Q_7' where such motion is along the optic axis. It has already been remarked that Q_7' should give the most intense absorption in the extraordinary ray and for the same reason therefore Q_{11}' should give the most intense absorption in the ordinary ray. It will be noticed that the frequencies assigned to Q_{11}' and Q_7' are nearly equal, being 479 and 508 respectively; while these frequencies are respectively weak and absent in light scattering, they actually correspond to the most pronounced reflection maxima in the ordinary and extraordinary rays respectively, these maxima being of nearly equal intensity.

In the mode Q_{13}', three oxygen atoms symmetrically disposed with respect to the optic axis move perpendicularly to that axis in one way, against the three other oxygen atoms which move the opposite way, while the silicons remain at rest. In this mode, therefore, the resulting electric moment in the basal plane should be quite small. The frequency of this

mode should also not differ greatly from that of the mode Q_6' which it somewhat resembles and to which we have assigned the frequency 777. The frequency 695 actually corresponds to a fairly strong Raman line, and to a very weak infra-red reflexion, thus justifying its assignment to the mode Q_{13}'.

The modes Q_{14}' and Q_{15}' are deformational oscillations of the oxygen atoms parallel to the basal plane and should therefore appear with moderate intensity both in light scattering and in infra-red absorption, Q_{15}' having the higher frequency and the greater intensity in light scattering of the two. This is in agreement with the observed facts.

It will be noticed that the vibrations assigned to the sub-class E(2) represent modes in which the atoms move parallel to the optic axis, there being actually only three such symmetry modes and three frequencies in this subclass. The peculiar behaviour of the corresponding lines in light scattering, namely, that they vanish when the directions of illumination and of observation are both along the optic axis is evidently the result of the special geometric character of these vibrations, namely, that they involve rotational oscillations about an axis in the basal plane, the ellipsoid of polarisability oscillating about that axis without any deformation.

It will be noticed that the modes Q_6' in the B class and Q_{17}' in the E class have been assigned nearly equal frequencies (777 for the former and 795–807 for the latter). They both correspond to oscillations of the oxygen atoms in which neighbours move with opposite phases transversely to the valence bonds, in one case parallel to the basal plane, and in the other case parallel to the optic axis. We should therefore expect the infra-red absorption intensities in the extraordinary and ordinary rays respectively, in the two cases to be nearly the same. This agrees with the experimental facts.

The assignments made in Tables VIII and IX are further supported by a comparative study of the thermal behaviour of the Raman lines. According to Nedungadi, the three frequencies which broaden most with rise of temperature are in order, the 207, 466 and 128 lines, whereas in respect of the shift towards lower frequency at higher temperatures, the order is 207, 128 and 466. He remarks also that the lines 265, 356, 392–403 are sufficiently sharp and strong even at 530° C. to be conspicuously visible, though 265 shifts to 252 at that temperature. The doublet 795–807 becomes a band covering the region 784–805. The doublet 1062–1083 also becomes a band retaining a sharp maximum at 1061. The line 1158 becomes weaker with rise of temperature, while 695 shifts to 682. On comparing these results with the chart of the symmetry modes (Fig. 2) and the assignments of frequency mode in Tables VIII and IX, it will be noticed that the modes Q_4'

Q_{16}', Q_{17}' and Q_{18}' to which the frequencies 356, 265, 795–807 and 1063 have been respectively assigned possess a common feature, namely, that the movements of the atoms are parallel to the optic axis which appears to be responsible for the fact that these lines remain tolerably sharp and strong even at high temperatures. On the other hand, the lines that broaden most correspond to modes in which there is a radial movement of the silicon or oxygen atoms, namely, the modes Q_1', Q_2' and Q_{12}' which correspond to the frequencies 207, 466 and 128. This result may be interpreted as a consequence of the fact that these vibrations tend (in alternate phases) to transform the trigonal symmetry of the crystal to hexagonal symmetry, in other words, to favour the α-β transformation of quartz which actually takes place at 575° C. Considering the four other modes Q_3', Q_{13}', Q_{14}' and Q'_{15} involving only movements of the oxygen atoms in the basal plane to which the frequencies 1082, 695, 392–403 and 1159 have been assigned, the nature of these vibrations is different in character from those previously discussed. *Prima facie*, therefore, it is not surprising that these lines display the influence of temperature to a lesser extent than the modes Q_1', Q_2' and Q_{12}' and to a greater extent than Q_4', Q_{16}', Q_{17}' and Q_{18}'. It would be premature, however, in the present stage of the investigation to endeavour to explain the individual behaviour of the lines in detail.

15. Intensity Measurements and Comparison with Theory

In a previous section we grouped the degenerate Raman lines into three sub-classes on the consideration that they vanish or become very weak in certain orientations of the crystal with polarised excitation. For the second and third sub-classes, this disappearance is sufficient to indicate their behaviour in other orientations with polarised or unpolarised excitation, but for the lines in the first sub-class, a more detailed investigation is necessary. Even for the second and third sub-classes, such an investigation is useful as furnishing a further confirmation of the theory.

Before describing the results, a few words may be added regarding the experimental arrangements used. Clear natural crystals of quartz having the illumination and observation surfaces ground and polished were used for the purposes of investigation. A sphere of quartz was also employed in certain cases. Light from a mercury arc was condensed on the crystal with a lens of 6 inches diameter, the maximum semi-convergence angle introduced by the lens being about 12°. The scattered light was passed through a brass tube 10 cm. long and 5 mm. bore for correctly fixing the direction of observation and was focussed on the slit of a Zeiss three-prism glass spectrograph having two camera attachments $f = 27$ cm. and $f = 12$ cm. A polaroid

disc, whose efficiency in the 4358 region was about 90%, was used for polarising the incident light. The intensities of Raman lines and their state of polarisation were obtained by running the plates through a microphotometer and reading the intensity from the density-log-intensity curves. For analysing the scattered light a double-image prism was used and care was taken to illuminate only a small region at the centre of the crystal. For polarisation work the intensities were corrected for instrumental errors arising from oblique refraction and reflection from the surfaces of the prism which strengthen the horizontal component. Most of the exposures had to run for ten days continuously to bring out the weak lines.

The results are given in Tables X and XI. Table XII gives a comparison of the author's results with those of previous workers obtained with unpolarised incident light.

The results of the author are in good agreement with those of previous workers except in certain cases where their results do not appear to be correct. These authors have not been able to resolve the lines 392 and 403, 795 and 807, and 1063 and 1082. However as the pairs 392 and 403 and 795 and 807 show nearly similar behaviour, the results of these workers are in agreement with those of the author. This is, however, not the case for the lines 1063 and 1082. Further the value for the depolarisation obtained by Cabannes for the line 128 and by Michalke for the line 404 are definitely not correct [*vide* Plate IV, Fig. 8 (*n*) and 8 (*o*)].

We shall now interpret these results in the light of theory as indicated in Table V, Section 8. The results regarding the vanishing of the lines in specific orientations have already been explained in an earlier section and will not be repeated here. The following points, however, arise from a consideration of the intensities of the lines.

(1) In quartz the atoms are arranged in a spiral form round the threefold axis and we cannot therefore expect a large anisotropy of scattering, *i.e.*, even in those totally symmetric modes where the motions of atoms are radial, the spiral arrangement will give a tensor component $\epsilon_{\gamma\gamma}$. For these vibrations the anisotropy will not be marked, *i.e.*, $\epsilon_{\alpha\alpha} \gtrapprox \epsilon_{\gamma\gamma}$. However, in the case of totally symmetric vibrations involving a motion along the optic axis, the change of polarisability will be greater along the optic axis than in the perpendicular directions. It is noticed that the ratio of intensities of 466 and 356 lines is less when the optic axis is along OZ than in the two perpendicular directions, which shows that the line 356 is the more anisotropic in respect of intensity, as is to be expected theoretically.

TABLE X

Intensities of Raman Lines for Various Orientations. Illuminating Beam along OX ; Observation along OY

Direction of optic axis	Incident electric vector along	128	207	265	356	392	403	453	466	502	695	795	807	1063	1082	1159	1228	Remarks
OZ	OY & OZ Unpolarised	37	30	16	10	12 (not resolved)		100 (not resolved)		2	5	6	9	3	4	11	2	Short focal length camera was used
OZ	OZ	23	40	12	9	4 (not resolved)		100 (not resolved)		1	0	5	8	2	4	1	—	
OZ	OY	100	11	12	0	20 (not resolved)		30 (not resolved)		2	7	7 – (diffuse and broad)		0	0	15	4	
OY	OY & OZ Unpolarised	50	25	7	6	6 (broad)			100		3	6 (broad)		2	0	8	1	Long focal length camera was used
OY	OZ	26	22	0	7	5 (broad)			100		3	0	0	½	0	6	—	
OY	OY	100	12	38	0	6 (broad)		10	35		0	20 (diffuse and broad)		6	0	1	..	
OX	OY & OZ Unpolarised	55	25	16	7	7 (broad)		3	100		4	11 (broad)		3	0	6	—	

FOOTNOTE : The strongest line in each spectrogram was assigned an intensity 100.

TABLE XI

Polarisation of Raman Lines for Various Orientations
(Long-Focal Length Camera was used)

Optic axis along→	OZ						OX	
Direction of incident electric vector along→	(OY & OZ) Unpolarised light		OZ		OY		(OY & OZ) Unpolarised light	
Components of scattered radiation along→	OX	OZ	OX	OZ	OX	OZ	OX	OZ
128	24	9	10	0	20	8	16	33
207	3	33	2	33	0	0	3	36
265	7	7	4	0	—	—	9	0
356	1	10	—	—	—	—	1	9
392	4	0	—	—	4	0	1	7
403	4	0			(not resolved)		(not resolved)	
452	2	—	—	—	—	—	3	
466	10	100	6	100	6	0	9	100
479	½				(not resolved from 452)			
503	1	0						
695	3	0	—	—			1	4
795	2	> 1	—	—	—	—	7	0
807	3	3	—	—	—	—	(the line is broad)	
1063	2	0	—	—	—	—	3	0
1082	0	3	—	—	—	—	0	0
1159	8	0	—	—	2	0	1	8
1227	1	0			1	—	< 1	0

TABLE XII

Comparison with Earlier Results
Depolarisations with Incident Unpolarised Light

Author		Frequencies	Menzies (1929)		Cabannes (1929, 1937)		Michalke (1938)			Cabannes and Bouhet (1937)
ρ_x	ρ_z		ρ_x	ρ_z	ρ_x	ρ_z	ρ_x	ρ_y	ρ_z	Circular polarisation
—	—	85	1	1	—	—	~1	—	~1	—
·5	2·9	128	1	∞	1 0	⩾1 ∞	·6	~1	~4	reverse
0	0	207	0	0	0 0	0 0	·05	⩽1	< ·05	direct
∞	1	265	∞	∞	⩾1 ∞	⩾1 1	~3	⩾1	1·5	vanishes
0	0	356	0	0	0 0	0 0	·1	⩽1	·1	direct
⩽1 (~·07)	∞	392			0	∞	·1	⩽1	2	reverse
	∞	403	0	1						
⩾1	⩾1	452	—	—	∞	—	—	—	—	—
0	0	466	0	0	0 0	0 0	·05	·06	·05	direct
—	> 1	479	—	—	—	—	—	—	—	—
—	> 1	503	—	—	0	—	—	—	—	—
—	—	526	∞	0	—	—	—	—	—	—
⩽1 (·16)	∞	695	0	∞	0	∞	< 1	—	> 1	reverse
∞	⩾1	795	∞	∞	∞	1	~3	—	1·3	vanishes
	1	807								
∞	> 1	1063	∞	0	∞	0	> 1		< 1	—
absent	0	1082								
⩽1 (·04)	∞	1159	0	∞	0	∞	< 1		3·4	reverse
< 1	> 1	1228	(0)	(∞)	(0)	(∞)	(< 1)		(> 1)	—

ρ_x and ρ_z are the polarisation ratios when the optic axis is along OX and OZ respectively.
Brackets [indicate the two different observations of Cabannes.
Brackets { indicate that the lines have not been separated.
Brackets ( ) indicate that the results are uncertain.

(2) Another interesting result is that for all the degenerate lines, the depolarisation ρ_{ox}^{unpol} (incident light unpolarised, optic axis along OZ) is never less than one in accordance with theory, (*vide* Table V). [See also spectrograms 6 (*e*), 6 (*f*), 8 (*n*) and 8 (*o*).]

(3) The measurements show very clearly that the line 128 falls under the first sub-class for which the tensor components are of the most general type permissible for class E. Taking empirically $a^2/b^2 = 2$ where $\epsilon_{\alpha\beta} = \epsilon_{\alpha\alpha} = a$; $\epsilon_{\alpha\gamma} = \epsilon_{\beta\gamma} = b$, we find from Table V that ρ_{oz}^{unpol} should be 3, $\rho_{ox}^{unpol} = \cdot 5$, $\rho_{oz}^{oz} = \infty$, $\rho_{oz}^{oy} = 2$, in fair agreement with the observed depolarisations. Table V also explains the observed result that the line 128 becomes much weaker than the line 207 when the optic axis and the incident electric vector are both along OZ, for it is in this case that the intensity of the 128 line is a minimum.

The line 452 also belongs to the sub-class E because $\rho\,(1)_{ox}^{unpol}$ and ρ_{oz}^{unpol} are both greater than 1 ($b^2 > a^2$). For the lines 479, 502 and 1228, $\rho_{ox}^{unpol} > 1$ and ρ_{oz}^{unpol} cannot be stated because the lines become too weak to be observed.

(4) The lines 265, 795, 807 and 1063 have been placed in the sub-class E (2). Polarisation results support this classification. As seen from Table V the lines of this sub-class will have $\rho_{oz}^{unpol} = 1$, $\rho_{ox}^{unpol} = \infty$, $\rho_{oz}^{oz} = \infty$. The frequency 265 fulfils these requirements. 795 and 1063 show $\rho_{ox}^{unpol} = \infty$ but ρ_{ox}^{unpol} is slightly greater than 1.

(5) The lines 392, 403, 695 and 1159 have been placed in sub-class E (3). For these vibrations, Table V shows that ρ_{ox}^{unpol} should be zero and ρ_{ox}^{unpol} should be infinity. Experimentally the value observed for ρ_{oz}^{unpol} is ∞ but for ρ_{ox}^{unpol} is slightly greater than zero.

We may finally draw attention to some curious features which must here remain unexplained.

(*a*) The lines 795 and 807 are sharp and well separated when the optic axis is along OZ [*vide* Fig. 6 (*f*) and 8 (*o*)], but, they appear as a broad band of width 13 cm.$^{-1}$ with a mean shift of 795 when the optic axis is in the other two directions [see Fig. 8 (*q*), 6 (*h*), 6 (*g*)].

(*b*) The very weak combination line 1228 becomes comparable in intensity to the much stronger lines 695 and 800 in the particular case when the optic axis is along OZ and the electric vector along OY [see Fig. 7 (*i*)].

16. Specific Heat of α-Quartz

The identification of the fundamental frequencies of the quartz crystal enables us to make a theoretical computation of its heat capacity which can be compared with the experimental data already available. The energy

taken up by the crystal when heated at constant pressure is utilised in three ways: (1) in exciting the acoustic oscillations of the crystal lattices, (2) in exciting the oscillations of the interpenetrating lattices in the crystal with respect to one another and (3) in the work of expanding the lattices. The sum of these energies gives us the heat content of the crystal at constant pressure. The unit cell in quartz contains three silicon and six oxygen atoms These give twenty-seven degrees of freedom. The analysis contained in the character table shows that of these the translations of the unit cell account for three degrees of freedom, while the internal oscillations account for 24 degrees of freedom in the following manner. The frequencies 207, 356, 466 and 1082 belonging to class A and the frequencies 364 (R 27·5 μ), 508 (R 19·7 μ), 777 (R 12·87 μ) and 1149 (R 8·7 μ) belonging to class B together represent eight degrees of freedom, while the eight frequencies 128, 265, 397 (392–403), 479, 695, 798 (795–807), 1063, 1159 belonging to class E represent 16 degrees of freedom, each frequency having a weight two due to the double degeneracy. The complete expression for the specific heat at constant pressure is accordingly

$$C_p = 3\,R\,D\left(\frac{\theta}{T}\right) + \sum_{i=1}^{i=24} R\,E\left(\frac{h\,\nu_i}{k\,T}\right) + 2{\cdot}39 \times 10^{-8}\,\frac{\alpha^2\,T}{\chi\,d}.$$

In this expression, R is the gas constant, T the absolute temperature, $D\left(\frac{\theta}{T}\right)$ is the Debye function, $E\left(\frac{h\,\nu_i}{k\,T}\right)$ is the Einstein function corresponding to the characteristic frequency ν_i, α is the coefficient of thermal expansion (cubical), χ is the coefficient of compressibility and d the density. To valuate the first item in this expression, we require to know the temperature θ appearing in the Debye function. Actually, the contribution due to the Einstein functions is far larger than that given by the Debye function except at the lowest temperatures. Moreover, the use of the Debye function with a sharp limiting frequency to represent the acoustic energy is itself only in the nature of a rough approximation to the truth. Accordingly, we may, without any real sacrifice in completeness, first evaluate the second and third terms in the expression for the specific heat, and then assume such a value for θ as would give the best fit with the observations at very low temperatures at which the second and third terms become unimportant.

The value of θ found in the manner indicated is 204. The thermal dilatation and the density of quartz at different temperatures are tabulated in Sosman's book on the properties of silica (pp. 361–62). The cubical compressibility χ is according to Voigt (1887) given by the relation

$$\chi = 2\,S_{11} + S_{33} + 2\,S_{12} + 4\,S_{13},$$

where $S_{11} = 1/E_{\parallel}$ and $S_{33} = 1/E_{\perp}$; $E_{\parallel}$ and $E_{\perp}$ being the elasticity modulus parallel and perpendicular to the optic axis whose values are known from the work of Perrier and Mandrot (1923). According to Bechmann (1934) the temperature variation of S_{12} and S_{13} is given by

$$S_{12} = -1 \cdot 69 \times 10^{-13} (1 - 1125 \times 10^{-6} t)$$

$$S_{13} = -1 \cdot 54 \times 10^{-13} (1 - 148 \times 10^{-6} t).$$

The values of the constants α, χ, d for various temperatures are given in Table XIII.

TABLE XIII

Data for Quartz

T°	$\alpha \times 10^6$	$\chi \times 10^{13}$	d
273	33·6	25	2·651
316·5	36·5	25·5	2·647
381·1	40·5	26·05	2·640
428·8	44·0	26·5	2·634
475·8	47·0	27·0	2·629
565·3	54·5	28·0	2·617
670	69	30·5	2·601
777·3	103	34·25	2·589
808·6	126	36·75	2·571

The calculated and the observed values of C_p are given in Table XIV. The values of C_p given under the heading observed values have been taken from Sosman's book (p. 314) for temperatures between 23° K. and 273° K. and from the work of Moser between temperatures 316·5° K. to 808·6° K. At lower temperatures a continuous series of observations have not been made by a single worker. The values given by Sosman have been obtained from an extrapolated curve between heat capacity and temperature drawn from the observations recorded by several workers. Between 123° and 273° K. the data are very scanty and the course of the curve is not quite certain. There are only two observations of Koref for the mean heat capacity between − 193° C. to − 79° C. and between − 77° C. to 0° C.

It may be seen from the table that there is a good fit between the observed and calculated values of C_p for all temperatures; the greatest measure of disagreement of about ·004 units between the observed and

TABLE XIV

Calculation of the Specific Heat of α-Quartz

	A	B	C	D	E	F	G	H
	Absolute Temp. T°	Debye term Contribution = $3RD\left(\frac{204}{T}\right)$	Einstein term contribution = $\sum_{1}^{24} RE\left(\frac{h\nu_i}{kT}\right)$	Total = B + C	(Calc.) $C_v \times 10^3$ = $\frac{D}{180}$	(Calc.) $(C_p - C_v) \times 10^3$ = $\frac{\alpha^2 T}{\chi d} \times \frac{1}{J}$	(Calc.) $C_p \times 10^3$ = E + F	Observed $C_p \times 10^3$
1	23	0·63	0·09	0·72	4·0	..	4·0	5·4
2	30	1·21	0·34	1·55	8·6	..	8·6	9·4
3	40	2·13	0·97	3·10	17·2	..	17·2	16·1
4	50	2·93	1·73	4·66	25·9	..	25·9	23·5
5	73	4·16	3·92	8·08	44·9	..	44·9	41·0
6	92·6	4·74	5·99	10·73	59·6	..	59·6	56·9
7	123	5·21	9·41	14·62	81·2	..	81·2	77·4
8	173	5·56	14·92	20·48	113·8	..	113·8	111·4
9	223	5·70	19·71	25·41	141·2	..	141·2	141·2
10	273	5·79	23·89	29·68	164·9	1·1	166·0	166·4
11	316·5	5·83	27·11	32·94	183·0	1·5	184·5	187·2
12	381·1	5·87	30·85	36·72	204·0	2·2	206·2	205·7
13	428·8	5·89	33·18	39·07	217·0	2·8	219·8	219·2
14	475·8	5·90	35·04	40·94	227·4	3·5	230·9	231·4
15	565·3	5·92	37·86	43·78	243·2	5·5	248·7	251·6
16	670	5·93	40·26	46·19	256·6	9·6	266·2	268·3
17	777·3	5·93	41·84	47·77	265·4	22·3	287·7	291·2
18	808·6	5·93	42·21	48·15	267·5	32·5	300·0	303·6

calculated values lies in the region 73° K. to 123° K. The discrepancy may be due in part to the uncertainty in the specific heat curve in this region. The close agreement between the observed and calculated values of C_p shows that the assignment of fundamental frequencies is correct. The characteristic frequencies have been assumed in the calculation to be those observed at the room temperature. This has been done for the sake of simplicity. The change in the characteristic frequencies observed would, at the lower temperatures, not sensibly influence the results of the calculation, while at the higher temperatures, though the shifts are in some cases of appreciable importance, they are accompanied by a broadening of the observed band of frequencies which cannot be taken into account without making the calculation unduly complicated and laborious.

17. Summary

The paper is partly theoretical and partly experimental. On the basis of the known crystal structure of quartz and the character table for the relevant point group, the symmetry modes of vibration of the atoms in the unit cell are derived and geometrically represented, and their appearance in the Raman effect and in infra-red absorption is discussed in detail. The paper also presents a detailed experimental study of the Raman spectrum of quartz using incident light unpolarised and also polarised in different azimuths and for the different orientations of the crystal. The experimental results obtained as well as those already known regarding the infra-red reflexion and absorption have been satisfactorily correlated with the deductions from theory. The following are the principal results of the investigation: (1) Quartz has sixteen fundamental vibration frequencies. Of these, four, namely—207, 356, 466 and 1082 cm.$^{-1}$, are Raman-active and infra-red inactive. Four others, namely—364, 508, 777, 1149—are Raman-inactive and infra-red active but only in the extraordinary ray. Eight doubly degenerate frequencies are both Raman-active and infra-red active but only in the ordinary ray. These are 128, 265, 479, 695, 1063, 1159 and the doublets (due to Fermi splitting) at 392–403 and 795–807. The weak lines at 452, 503 and 1228 are combinations appearing in the degenerate class. (2) The symmetry modes which these fundamental vibrations most nearly resemble have been identified from theoretical considerations, the assignments being confirmed from the observed behaviour of the lines in infra-red absorption and in light scattering. (3) The thermal behaviour of the Raman lines is correlated with the modes of vibration concerned. The extraordinary broadening and shift of the 207 line which occurs when the quartz is heated towards the α–β transformation temperature is shown to be connected with the tendency of

this mode of vibration to change the symmetry of quartz from trigonal to hexagonal. (4) The specific heat of quartz between 23° K. to 808° K. has been calculated theoretically on the basis of the analysis and is in excellent agreement with the experimental results. Numerous spectrograms and microphotometer records illustrate the paper.

In conclusion, the author wishes to express his gratitude to Sir C. V. Raman for the facilities afforded for carrying out this investigation and his constant encouragement and interest during its progress.

REFERENCES

1. Introductory

Rutherford .. *Proc. Roy. Soc.*, (A), 1931, **130,** 259.
Brester, C. J. .. *Zeit. f. Phy.*, 1924, **24,** 324.
Placzek, G. .. *Leipziger Vörtrage*, 1930; *Handbuch der Radiology*, 2 Auflage, Bd. 6, Teil II (1934).
Wigner .. *Göttinger Nachrichten*, 1930, 133.

2. Infra-red

Rubens, H. .. *Wied Ann.*, 1892, **45,** 238.
Merritt, E. .. *Ibid.*, 1895, **55,** 49.
Nichols, E. F. .. *Ibid.*, 1897, **60,** 401.
Rosenthal, H. .. *Ibid.*, 1899, **68,** 783.
Coblentz, W. W. .. *Phy. Rev.*, 1906, **32,** 125.
Reinkober, O. .. *Ann. der Phy.*, 1911, **34,** 343.
Liebisch, Th., and Rubens, H. *Berl. Ber.*, 1919, 199.
Dreisch, Th. .. *Zeit. f. Phy.*, 1927, **42,** 426.
Plyler, E. K. .. *Phy. Rev.*, 1929, **33,** 48.
Parlin, W. A. .. *Ibid.*, 1929, **34,** 81.
Czerny, M. .. *Zeit. f. Phy.*, 1929, **53,** 317.
Havelock .. *Proc. Roy. Soc., London*, 1912, **86,** 1.

3. Raman Spectrum

Landsberg and Mandelstam .. *Naturwissenchaften*, 1928, **16,** 1557.
Rao, I. R. .. *Ind. J. Phy.*, 1928, **3,** 123.
Krishnan, K. S. .. *Ibid.*, 1929, **4,** 131.
Pringsheim and Rosen .. *Zeit. f. Phy.*, 1928, **50,** 741.
Daure .. *Ann. Physik*, 1929, **12,** 375.
Gross and Romanova .. *Zeit. f. Phy.*, 1929, **55,** 744.
Nisi .. *Pro. Imp. Acad. (Tokyo)*, 1929, **5,** 127; *Proc. phy. math. soc. Japan*, 1932, Ser. 3, **14,** 214.
Hollaender and Williams .. *Phy. Rev.*, 1931, **9,** 72.
Rasetti .. *Nuovo Cimento*, 1932, **9,** 72.

Weiler .. *Helv. Phy. Acta*, 1932, **5**, 302.
Kujumzelis .. *Zeit. f. Phy.*, 1936, **100**, 221.
Nedungadi, T. M. K. .. *Proc. Ind. Acad. Sci.*, (A), 1940, **11**, 86.

4. Thermal Behaviour of Quartz

Rubens, H., and Hertz, G. .. *Berl. Ber.*, 1912, 256.
Reinkober, O., and Kipcke, H. *Zeit. f. Phy.*, 1928, **48**, 205.
Landsberg and Leontowitch .. *Ibid.*, 1929, **53**, 439.
Brickwedde and Peters .. *Phy. Rev.*, 1929, **33**, 116.
Landsberg and Mandelstam .. *Zeit. f. Phy.*, 1929, **58**, 250.
———— .. *Ibid.*, 1931, **68**, 554.
Ney .. *Ibid.*, 1931, **68**, 554.
Ornstein and Went .. *Physica*, 1935, **2**, 503.
Nedungadi, T. M. K. .. *Proc. Ind. Acad. Sci.*, (A), 1940, **11**, 87.
Raman and Nedungadi .. *Nature*, 1940, **144**, 147.
Nernst, W. .. *Ann. d. Phy.*, 1911, (4), **36**, 395.
Koref, F. .. *Ibid.*, 1911, (4), **(36)**, **49**.
Moser, H. .. *Phy. Zeit.*, 1936, **37**, 737.
Regnault, V. .. *Ann. Chim. et Phy.*, 1841, (3), **1**, 148.
Weber, R. .. *R. Bull. Soc. Sci. Nat. Neuchatel*, 1895, **23**, 17.
White, W. P. .. *Amer. J. Sci.*, 1919, (4), **47**, 1.
Wietzel .. *Zeit. Anorg. Allg. Chem.*, 1921, **116**, 71.
Cohn, W. M. .. *Amer. Ceram. Soc.*, 1924, **7**, 359, 475, 548.
Perrier, A., and Roux, H. .. *Mem. de la Soc. Vaud.*, 1923, **1**, 109.

5. Structure of α-Quartz

Wyckoff .. *Zeit. f. Kristallographie*, 1926, **63**, 512.
Gibbs, R. E. .. *Proc. Roy. Soc., Lond.*, 1926, **110**, 443.
Bragg, W., and Gibbs, R. E. .. *Ibid.*, 1925, **109**, 405.

6. Optical Excitation of Lattice Vibrations

Tamm, Ig. .. *Zeit. f. Phys.*, 1930, **60**, 345.
Raman, C. V. .. *Proc. Ind. Acad. Sci.*, (A), 1940, **11**, 379.

7. Character Table

Weiler .. *Zeit. f. Phy.*, 1933, **80**, 617.
Tisza .. *Ibid.*, 1933, **82**, 48.

8. Selection Rules

Saksena, B. D. .. *Proc. Ind. Acad. Sci.*, (A), 1940, **11**, 229.

9. Results with Polarised Excitation

Cabannes .. *Compt. Rendus*, 1929, **188**, 249.
Menzies .. *Phil. Mag.*, 1929, **8**, 504.

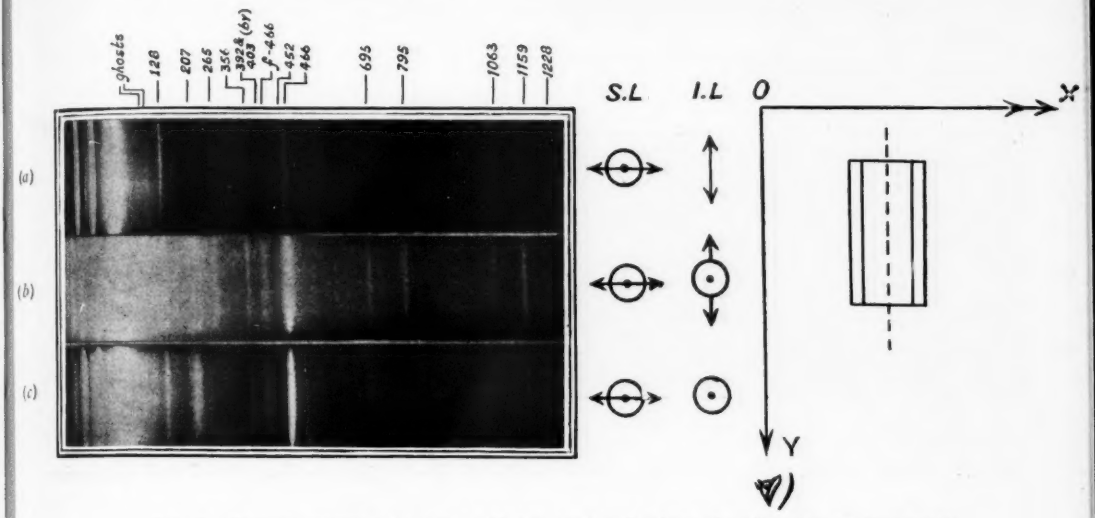

FIG. 5. Raman spectra of quartz with the optic axis along the direction of observation.

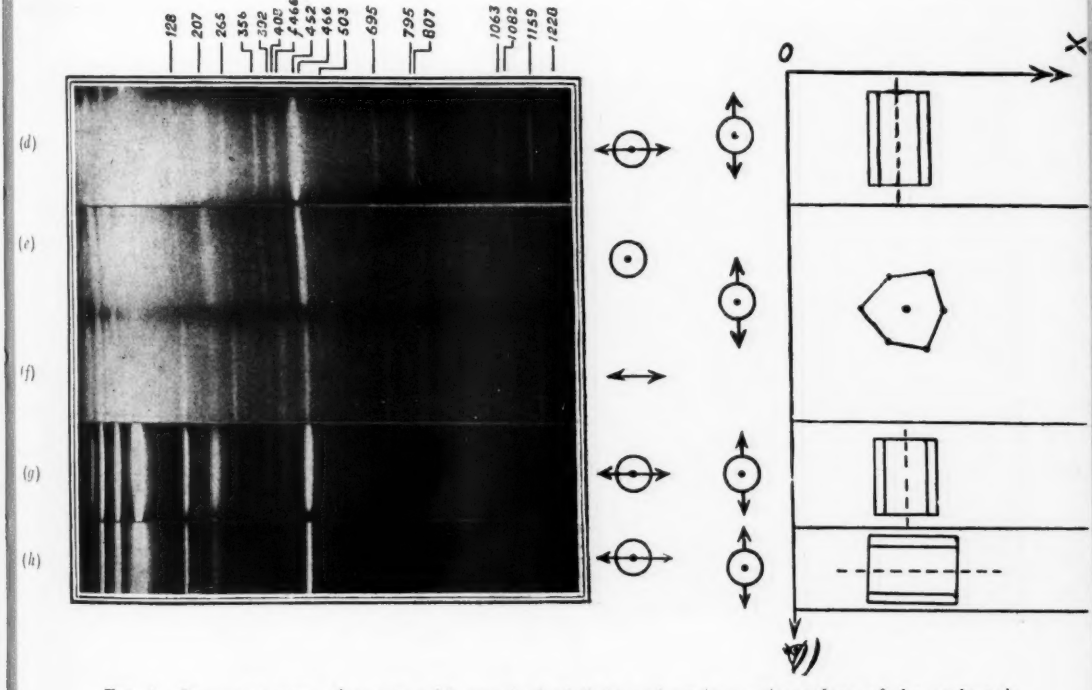

FIG. 6. Raman spectra of quartz with unpolarised light and various orientations of the optic axis.

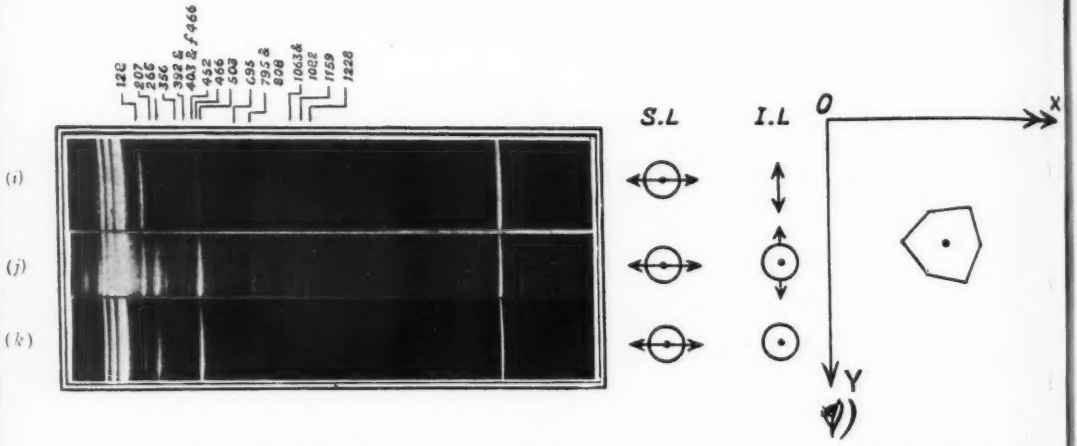

FIG. 7. Raman spectra with the optic axis perpendicular to the directions of illumination and observation.

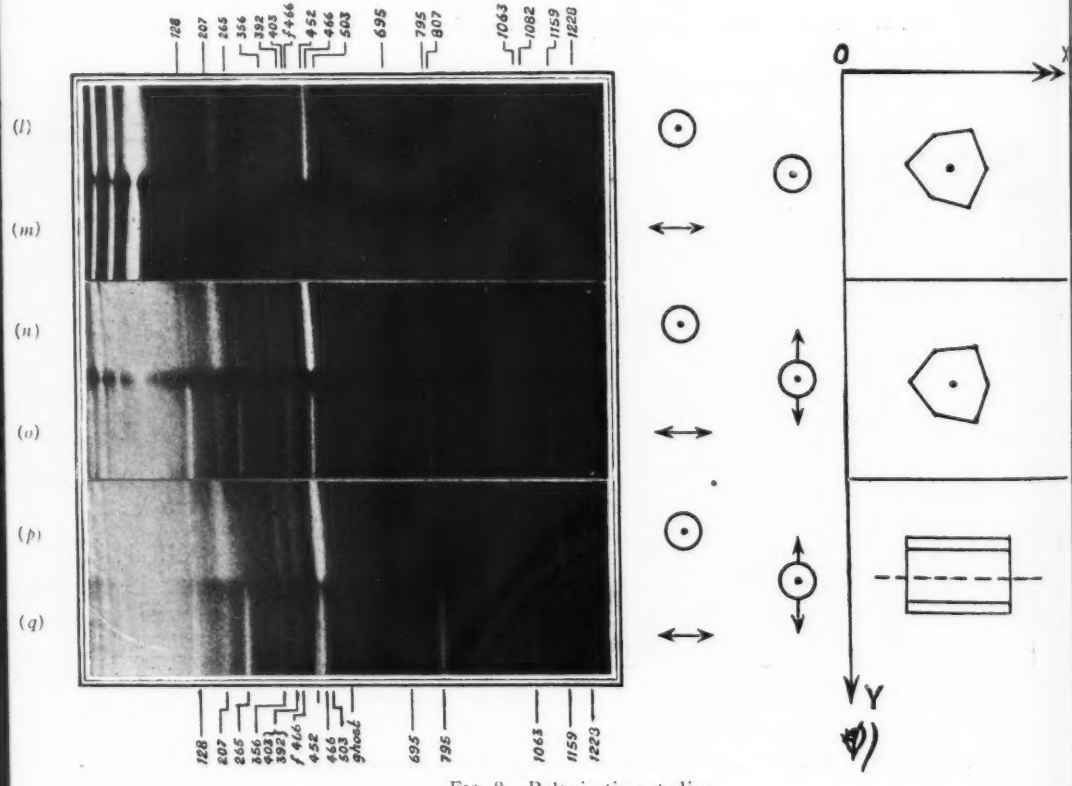

FIG. 8. Polarisation studies.

Bouhet .. *Compt. Rend.*, 1937, **204**, 1661.
Cabannes and Bouhet .. *Ibid.*, 1937, **205**, 768.
Michalke, H. .. *Zeit. f. Phy.*, 1938, **108**, 748.

10. Specific Heat of α-Quartz

Voigt, W. .. *Wied. Ann. d. Phy. und Chem.*, 1887, **31**, 507.
Perrier and Mandrot .. *Mem. de la Soc. Vaud.*, 1923, **1**, 337.
Bechmann .. *Hochfrequenztechnik und Elektroakustik*, 1934, **44**, 145.

1013-40 Printed at The Bangalore Press, Bangalore City, by G. Srinivasa Rao, Superintendent,
and Published by The Idian Academy of Sciences, Bangalore